

*Simon*

# RCA REVIEW

*a technical journal*

RADIO AND ELECTRONICS  
RESEARCH • ENGINEERING

VOLUME X

MARCH 1949

NO. 1

# RCA REVIEW

GEORGE M. K. BAKER  
*Manager*

CHAS. C. FOSTER, JR.  
*Business Manager*

---

## SUBSCRIPTIONS:

United States, Canada, and Postal Union: One Year \$2.00, Two Years \$3.50, Three Years \$4.50  
Other Countries: One Year \$2.40, Two Years \$4.30, Three Years \$5.70

## SINGLE COPIES:

United States: \$.75 each. Other Countries: \$.85 each

*Copyright, 1949, by Radio Corporation of America, RCA Laboratories Division*

Published quarterly in March, June, September, and December by Radio Corporation of America, RCA Laboratories Division, 30 Rockefeller Plaza, New York 20, N. Y.

Editorial and General Offices: RCA Review, Radio Corporation of America,  
RCA Laboratories Division, Princeton, New Jersey

Entered as second class matter April 3, 1946, at the Post  
Office at New York, New York, under the act of March 3, 1879

## RADIO CORPORATION OF AMERICA

DAVID SARNOFF, *Chairman of the Board*

FRANK M. FOLSOM, *President*

LEWIS MACCONNACH, *Secretary*

ARTHUR B. TUTTLE, *Treasurer*

PRINTED IN U.S.A.

## RCA REVIEW

CLAUDE M. E. BROWN  
Manager

CHAS. C. FORTNA, JR.  
Business Manager

---

### SUBSCRIPTIONS

United States, Canada, and Postal Union: One Year \$1.00, Two Years \$1.80, Three Years \$2.50  
Other Countries: One Year \$1.40, Two Years \$2.50, Three Years \$3.70

### SINGLE COPIES

United States: 17¢ each. Other Countries: 1.80 each

Copyright, 1943, by Radio Corporation of America, RCA Laboratories Division

Published quarterly in March, June, September, and December by Radio Corporation of America, RCA Laboratories Division, 10 East 42nd Street, New York 17, N. Y.

Editorial and General Office: RCA Review, Radio Corporation of America,  
RCA Laboratories Division, Princeton, New Jersey

Entered as second class matter April 1, 1942, at the Post  
Office at New York, New York, under the act of March 3, 1907

### RADIO CORPORATION OF AMERICA

DAVID SARGENT, Chairman of the Board

FRANK M. FORTNA, President

LEWIS MACGREGOR, Secretary

ARTHUR S. TAYLOR, Treasurer

PRINTED IN U.S.A.

# RCA REVIEW

GEORGE M. K. BAKER  
*Manager*

CHAS. C. FOSTER, JR.  
*Business Manager*

---

## SUBSCRIPTIONS:

United States, Canada, and Postal Union: One Year \$2.00, Two Years \$3.50, Three Years \$4.50  
Other Countries: One Year \$2.40, Two Years \$4.30, Three Years \$5.70

## SINGLE COPIES:

United States: \$.75 each. Other Countries: \$.85 each

*Copyright, 1949, by Radio Corporation of America, RCA Laboratories Division*

Published quarterly in March, June, September, and December by Radio Corporation of America, RCA Laboratories Division, 30 Rockefeller Plaza, New York 20, N. Y.

Editorial and General Offices: RCA Review, Radio Corporation of America,  
RCA Laboratories Division, Princeton, New Jersey

Entered as second class matter April 3, 1946, at the Post  
Office at New York, New York, under the act of March 3, 1879

## RADIO CORPORATION OF AMERICA

DAVID SARNOFF, *Chairman of the Board*

FRANK M. FOLSOM, *President*

LEWIS MACCONNACH, *Secretary*

ARTHUR B. TUTTLE, *Treasurer*

PRINTED IN U.S.A.

# RCA REVIEW

*a technical journal*

RADIO AND ELECTRONICS  
RESEARCH • ENGINEERING

*Published quarterly by*

RADIO CORPORATION OF AMERICA  
RCA LABORATORIES DIVISION

*in cooperation with*

RCA VICTOR DIVISION  
RADIOMARINE CORPORATION OF AMERICA  
RCA INTERNATIONAL DIVISION

RCA COMMUNICATIONS, INC.  
NATIONAL BROADCASTING COMPANY, INC.  
RCA INSTITUTES, INC.

---

VOLUME X

MARCH 1949

NUMBER 1

---

## CONTENTS

	PAGE
FOREWORD .....	<i>The Manager</i> , RCA Review 3
Some Novel Circuits for the Three-Terminal Semiconductor Amplifier W. M. WEBSTER, E. EBERHARD, AND L. E. BARTON	5
Standardization of the Transient Response of Television Transmitters R. D. KELL AND G. L. FREDENDALL	17
Phase and Amplitude Equalizer for Television Use..... E. DUDLEY GOODALE AND RALPH C. KENNEDY	35
Development of a Large Metal Kinescope for Television..... H. P. STEIER, J. KELAR, C. T. LATTIMER AND R. D. FAULKNER	43
The Graphechon—A Picture Storage Tube..... L. PENSAK	59
Certain Aspects of Triode Reactance-Tube Performance for Frequency Modulation at Ultra-High Frequencies .....	74
C. L. Cuccia	
Ultrafax .....	99
DONALD S. BOND AND VERNON J. DUKE	
Thyratrons in Radar Modulator Service .....	116
HUBERT H. WITTENBERG	
Some Characteristics of Diodes with Oxide-Coated Cathodes.....	134
W. R. FERRIS	
RCA TECHNICAL PAPERS .....	150
AUTHORS .....	153

---

*RCA Review* is regularly abstracted and indexed by *Industrial Arts Index*, *Science Abstracts* (I.E.E.-Brit.), *Engineering Index*, *Electronic Engineering Master Index*, *Abstracts and References* (*Wireless Engineer*-Brit. and *Proc. I.R.E.*) and *Digest-Index Bulletin*.

# RCA REVIEW

*a technical journal*

RADIO AND ELECTRONICS  
RESEARCH • ENGINEERING

*Published quarterly by*

Radio Corporation of America  
RCA Laboratories Division

*in cooperation with*

RCA Video Division

Electronic Corporation of America

RCA Laboratories Division

RCA Communications, Inc.

National Broadcasting Company, Inc.

RCA Institute, Inc.

VOLUME X

MARCH 1961

NUMBER 1

## CONTENTS

	PAGE
FOREWORD .....	1
<i>The Manager, RCA Review</i>	
Some Novel Circuits for the Three-Terminal Semiconductor Amplifier .....	2
W. M. WILSON, E. EDWARDS, AND L. E. RAYSON	
Standardization of the Transient Response of Television Transmitters .....	17
R. D. KELL AND G. L. FURBERGALL	
Phase and Amplitude Equalizers for Television Use .....	25
E. DUNLAP GOSNOLD AND RALPH C. KERRICK	
Development of a Large Metal Kinoscope for Television .....	43
H. P. FISHER, J. KILIAN, C. T. LITTON, AND R. D. FULFORD	
The Graphicon—A Picture Storage Tube .....	59
L. PUNAR	
Certain Aspects of Triode Resistor-Tube Performance for Frequency Modulation at Ultra-High Frequencies .....	74
C. L. CHEW	
Ultrafax .....	90
DONALD S. BIRD AND VIRGINIA J. TROTT	
Thyratrons in Radar Modulator Service .....	116
HENRY H. WITVENBERG	
Some Characteristics of Diodes with Oxide-Coated Cathodes .....	134
W. R. FORBES	
RCA TECHNICAL PAPERS .....	180
AUTHORS .....	183

RCA Review is regularly abstracted and indexed by Industrial Arts Index, Science Abstracts (I.R.E. Div.), Engineering Index, Electronic Engineering Master Index, Abstracts and Reports (Working Engineer-EE), and Proc. I.R.E. and Digital-Data Bulletin.



# RCA REVIEW

---

## BOARD OF EDITORS

*Chairman*

**C. B. JOLLIFFE**

*RCA Laboratories Division*

**M. C. BATSEL**  
*RCA Victor Division*

**G. L. BEERS**  
*RCA Victor Division*

**H. H. BEVERAGE**  
*RCA Laboratories Division*

**I. F. BYRNES**  
*Radiomarine Corporation of America*

**D. D. COLE**  
*RCA Victor Division*

**O. E. DUNLAP, JR.**  
*Radio Corporation of America*

**E. W. ENGSTROM**  
*RCA Laboratories Division*

**A. N. GOLDSMITH**  
*Consulting Engineer, RCA*

**O. B. HANSON**  
*National Broadcasting Company, Inc.*

**E. A. LAPORT**  
*RCA International Division*

**C. W. LATIMER**  
*RCA Communications, Inc.*

**H. B. MARTIN**  
*Radiomarine Corporation of America*

**H. F. OLSON**  
*RCA Laboratories Division*

**D. F. SCHMIT**  
*RCA Victor Division*

**S. W. SEELEY**  
*RCA Laboratories Division*

**G. R. SHAW**  
*RCA Victor Division*

**R. E. SHELBY**  
*National Broadcasting Company, Inc.*

**S. M. THOMAS**  
*RCA Communications, Inc.*

**G. L. VAN DEUSEN**  
*RCA Institutes, Inc.*

**A. F. VAN DYCK**  
*RCA Laboratories Division*

**I. WOLFF**  
*RCA Laboratories Division*

**V. K. ZWORYKIN**  
*RCA Laboratories Division*

*Secretary*

**GEORGE M. K. BAKER**

*RCA Laboratories Division*

---

## REPUBLICATION AND TRANSLATION

Original papers published herein may be referenced or abstracted without further authorization provided proper notation concerning authors and source is included. All rights of republication, including translation into foreign languages, are reserved by RCA Review. Requests for republication and translation privileges should be addressed to *The Manager*.

# RCA REVIEW

## BOARD OF EDITORS

Chairman

C. S. Jacobs  
RCA Laboratories Division

W. C. Cline  
RCA Victor Division

H. L. Berry  
RCA Victor Division

H. W. Benson  
RCA Laboratories Division

I. F. Brown  
Radioactive Corporation of America

W. H. Chen  
RCA Victor Division

H. E. Dwyer, Jr.  
Radio Corporation of America

R. W. Eastman  
RCA Laboratories Division

A. R. Gussow  
Consulting Engineer, RCA

G. S. Hahn  
National Broadcasting Company, Inc.

E. A. Lohr  
RCA International Division

C. W. Lottum  
RCA Communications, Inc.

W. R. Moore  
Radioactive Corporation of America

H. P. Olson  
RCA Laboratories Division

H. F. Ostrin  
RCA Victor Division

A. W. Sauer  
RCA Laboratories Division

G. S. Saxe  
RCA Victor Division

R. E. Sencer  
National Broadcasting Company, Inc.

A. M. Terman  
RCA Communications, Inc.

G. L. Van Dusen  
RCA Institute, Inc.

A. F. Van Dine  
RCA Laboratories Division

I. Weiss  
RCA Laboratories Division

V. E. Woodard  
RCA Laboratories Division

Secretary

James M. E. Swan  
RCA Laboratories Division

## REPLICATIONS AND TRANSLATIONS

Original papers published herein may be reprinted or abstracted without further authorization provided proper notation concerning authors and source is included. All rights of replication, including translation into foreign languages, are reserved by RCA Review. Requests for replication and translation privileges should be addressed to The Manager.

# RCA REVIEW

---

## BOARD OF EDITORS

*Chairman*

**C. B. JOLLIFFE**

*RCA Laboratories Division*

**M. C. BATSEL**

*RCA Victor Division*

**G. L. BEERS**

*RCA Victor Division*

**H. H. BEVERAGE**

*RCA Laboratories Division*

**I. F. BYRNES**

*Radiomarine Corporation of America*

**D. D. COLE**

*RCA Victor Division*

**O. E. DUNLAP, JR.**

*Radio Corporation of America*

**E. W. ENGSTROM**

*RCA Laboratories Division*

**A. N. GOLDSMITH**

*Consulting Engineer, RCA*

**O. B. HANSON**

*National Broadcasting Company, Inc.*

**E. A. LAFORT**

*RCA International Division*

**C. W. LATIMER**

*RCA Communications, Inc.*

**H. B. MARTIN**

*Radiomarine Corporation of America*

**H. F. OLSON**

*RCA Laboratories Division*

**D. F. SCHMIT**

*RCA Victor Division*

**S. W. SEELEY**

*RCA Laboratories Division*

**G. R. SHAW**

*RCA Victor Division*

**R. E. SHELBY**

*National Broadcasting Company, Inc.*

**S. M. THOMAS**

*RCA Communications, Inc.*

**G. L. VAN DEUSEN**

*RCA Institutes, Inc.*

**A. F. VAN DYCK**

*RCA Laboratories Division*

**I. WOLFF**

*RCA Laboratories Division*

**V. K. ZWORYKIN**

*RCA Laboratories Division*

*Secretary*

**GEORGE M. K. BAKER**

*RCA Laboratories Division*

---

## REPUBLICATION AND TRANSLATION

Original papers published herein may be referenced or abstracted without further authorization provided proper notation concerning authors and source is included. All rights of republication, including translation into foreign languages, are reserved by RCA Review. Requests for republication and translation privileges should be addressed to *The Manager*.

## FOREWORD

**T**HE EIGHTH volume in the RCA Technical Book Series was published by RCA Review in August 1948. This book—**RADIO AT ULTRA-HIGH FREQUENCIES, Volume II**—includes technical papers on various aspects of the higher radio frequencies (the VHF and UHF bands and microwaves) written by RCA scientists and engineers and originally published during the years 1940-1947. In addition to the papers published in full, a number are also included in summary form. Two appendixes provide reference material in the form of a UHF bibliography and summaries of all papers appearing in **RADIO AT ULTRA-HIGH FREQUENCIES, Volume I** (now out of print).

\* \* \*

The ninth and tenth volumes in the RCA Technical Book Series are being published in April, 1949. These two books—**ELECTRON TUBES, Volume I (1935-1941)** and **Volume II (1942-1948)** include technical papers concerning vacuum tubes, thermionics and related subjects written by RCA scientists and engineers and originally published during the years indicated. Summaries of various papers, a bibliography and a reference list are included in each volume in addition to the complete papers.

\* \* \*

The eleventh volume in the RCA Technical Book Series is scheduled for publication early this fall. This book extends the **television** series started in 1936 and is entitled **TELEVISION, Volume V (1947-1949)**. *Further information thereon will be circulated at the appropriate time.*

Volumes currently available in the RCA Technical Book Series include:

<i>Title</i>	<i>Year Published</i>
ELECTRON TUBES, Volume I (1935-1941)	—1949
ELECTRON TUBES, Volume II (1942-1948)	—1949
RADIO AT ULTRA-HIGH FREQUENCIES, Volume II (1940-1947)	—1948
FREQUENCY MODULATION, Volume I (1936-1947)	—1948
TELEVISION, Volume III (1938-1941)	—1947
TELEVISION, Volume IV (1942-1946)	—1947
RADIO FACSIMILE, Volume I	—1938

Earlier volumes in the **television** and **UHF** series are out of print.

\* \* \*

## FOREWORD

THE EIGHTH volume in the RCA Technical Book Series was published by RCA Review in August 1948. This book—**RADIO AT ULTRA-HIGH FREQUENCIES, Volume II**—includes technical papers on various aspects of the higher radio frequencies (the VHF and UHF bands and microwaves) written by RCA scientists and engineers and originally published during the years 1946-1947. In addition to the papers published in full, a number are also included in summary form. Two appendices provide reference material in the form of a UHF bibliography and summaries of all papers appearing in **RADIO AT ULTRA-HIGH FREQUENCIES, Volume I** (now out of print).

The sixth and seventh volumes in the RCA Technical Book Series are being published in April, 1949. These two books—**ELECTRON TUBES, Volume I (1935-1941)** and **Volume II (1942-1948)** include technical papers concerning vacuum tubes, thermionics and related subjects written by RCA scientists and engineers and originally published during the years indicated. Summaries of various papers, a bibliography and a reference list are included in each volume in addition to the complete papers.

The eleventh volume in the RCA Technical Book Series is scheduled for publication early this fall. This book extends the television series started in 1938 and is entitled **TELEVISION, Volume V (1947-1949)**. *Further information thereon will be circulated at the appropriate time.*

Volumes currently available in the RCA Technical Book Series include:

Title	Year Published
ELECTRON TUBES, Volume I (1935-1941)	--1949
ELECTRON TUBES, Volume II (1942-1948)	--1949
RADIO AT ULTRA-HIGH FREQUENCIES, Volume II (1946-1947)	--1948
FREQUENCY MODULATION, Volume I (1936-1947)	--1948
TELEVISION, Volume III (1938-1941)	--1947
TELEVISION, Volume IV (1942-1946)	--1947
RADIO FACSIMILE, Volume I	--1938

Earlier volumes in the television and UHF series are out of print.

Volumes in the RCA Engineering Book Series are under consideration for future publication. *Information thereon will be circulated as the books are published.* One volume is now available:

PATENT NOTES FOR ENGINEERS

—1947

\* \* \*

RCA TECHNICAL PAPERS—INDEX, Volume II(c) (1948) is being published this month and will be distributed early in April, 1949. Indexes now available include:

Volume I (1919-1945); Volume II(a) (1946); Volume II(b) (1947); Volume II(c) (1948).

\* \* \*

A few of the seven-color RCA Radio Frequency Allocation Charts are still available.

\* \* \*

Information concerning any of the above material may be obtained by writing to:

RCA Review  
Radio Corporation of America  
RCA Laboratories Division  
Princeton, N. J.

*The Manager, RCA Review*

March 21, 1949

Volumes in the RCA Engineering Book Series are under consideration for future publication. Information thereon will be circulated as the books are published. One volume is now available:

PATENT NOTES FOR ENGINEERS

—1947—

\* \* \*

RCA TECHNICAL PAPERS—INDEX, Volume II(c) (1948) is being published this month and will be distributed early in April, 1949. Indices now available include:

Volume I (1915-1945); Volume II(a) (1946); Volume II(b) (1947); Volume II(c) (1948).

\* \* \*

A few of the respective RCA Radio Frequency Allocation Charts are still available.

\* \* \*

Information concerning any of the above material may be obtained by writing to:

RCA Review  
Radio Corporation of America  
RCA Laboratories Division  
Princeton, N. J.

*The Messager, RCA Review*

March 21, 1949

# SOME NOVEL CIRCUITS FOR THE THREE-TERMINAL SEMICONDUCTOR AMPLIFIER\*

BY

W. M. WEBSTER†, E. EBERHARD‡ AND L. E. BARTON†

*Summary*—This paper is concerned with circuits for the semiconductor amplifier which consists of two small-area probes, known as emitter and collector, placed on a block of semiconducting material to which is made a third, large-area contact called the base connection.

When such a device was announced, an amplifier circuit was suggested in which the input signal is applied to the emitter and the output taken from the collector, the base being the common electrode. The input impedance of the device when connected in this fashion is low and the output impedance is relatively high, a disadvantageous situation for most applications. In this paper two other amplifier connections are described. The base electrode is used as the input terminal in both of these circuits. In the first case, output is taken from the collector and the input impedance is of the order of the output impedance. In the second circuit, output is taken from the emitter and the input impedance is much higher than the output impedance. Equivalent circuits, both direct current and alternating current, which are adequate representations of the semiconductor amplifier are shown. Algebraic expressions and experimental values of impedance and gain for each of the basic amplifiers are presented. The empirically derived relationships which link the elements of the equivalent circuit to the applied voltages are also given.

The paper discusses two novel oscillator circuits. The first is a two-terminal sine wave generator making use of a very interesting property of negative resistance in the base lead. The second is a simple relaxation oscillator which will furnish either pulse or sawtooth wave form. It makes use of negative resistance effects in the collector circuit when a resistance is placed in the base lead.

## INTRODUCTION

THE discovery of a three-terminal semiconductor (crystal) amplifier called the transistor was made known by the Bell Telephone Laboratories about July 1, 1948. A more complete description appeared in a series of three letters published in the July 15, 1948 issue of the *Physical Review*.<sup>1</sup> Since then little information has been published which pertains either to the fundamental nature of the transistor

\* Decimal Classification: R363.

† Research Department, RCA Laboratories Division, Princeton, N. J.

‡ Engineering Products Department, RCA Victor Division, Camden, N. J.

<sup>1</sup> J. Bardeen and W. H. Brattain, "The Transistor, A Semi-Conductor Triode," W. H. Brattain and J. Bardeen, "Nature of the Forward Current in Germanium Point Contacts," W. Shockley and G. L. Pearson, "Modulation of Conductance of Thin Films of Semi-Conductors by Surface Charges," *Phys. Rev.*, Vol. 74, No. 2, pp. 230-233, July 15, 1948.

# SOME NOVEL CIRCUITS FOR THE THREE-TERMINAL SEMICONDUCTOR AMPLIFIER\*

By

W. M. WENGER,<sup>†</sup> E. EDEGARD<sup>‡</sup> AND L. E. BARTON<sup>§</sup>

**Summary**—This paper is concerned with circuits for the semiconductor amplifier which consists of two small-area probes, known as emitter and collector, placed on a block of semiconducting material to which is made a third, large-area contact called the base connection.

When such a device was encountered, an amplifier circuit was suggested in which the input signal is applied to the emitter and the output taken from the collector, the base being the common electrode. The input impedance of the device when connected in this fashion is low and the output impedance is relatively high, a disadvantageous situation for most applications. In this paper two other amplifier connections are described. The base electrode is used as the input terminal in both of these circuits. In the first case, output is taken from the collector and the input impedance is of the order of the output impedance. In the second circuit, output is taken from the emitter and the input impedance is much higher than the output impedance. Equivalent circuits, both direct current and alternating current, which are adequate representations of the semiconductor amplifier are shown. Algebraic expressions and experimental values of impedance and gain for each of the basic amplifiers are presented. The empirically derived relationships which link the elements of the equivalent circuit to the applied voltages are also given.

The paper discusses two novel oscillator circuits. The first is a two-terminal sine wave generator making use of a very interesting property of negative resistance in the base lead. The second is a simple relaxation oscillator which will furnish either pulse or sawtooth wave form. It makes use of negative resistance effects in the collector circuit when a resistance is placed in the base lead.

## INTRODUCTION

THE discovery of a three-terminal semiconductor (crystal) amplifier called the transistor was made known by the Bell Telephone Laboratories about July 1, 1948. A more complete description appeared in a series of three letters published in the July 13, 1948 issue of the *Physical Review*.<sup>1</sup> Since then little information has been published which pertains either to the fundamental nature of the transistor

\* Derivat Classification: R342.

<sup>†</sup> Research Department, RCA Laboratories Division, Princeton, N. J.

<sup>‡</sup> Engineering Products Department, RCA Victor Division, Camden, N. J.

<sup>§</sup> J. Barton and W. H. Brattain, "The Transistor, A Semi-Conductor Triode," W. H. Brattain and J. Barton, "Nature of the Forward Current in Germanium Point Contacts," W. Shockley and G. L. Pearson, "Measurement of Conductance of Thin Films of Semi-Conductors by Surface Charges," *Phys. Rev.*, Vol. 74, No. 2, pp. 226-233, July 15, 1948.

or to circuits involving the transistor. It therefore seems desirable to report some of the observations which have been made while evaluating this type of device as a circuit element. The discussion which follows begins with the evolution of a direct-current equivalent circuit with which the static characteristics of the crystal amplifier may be duplicated. From this, an alternating current equivalent circuit (for small signals and low frequencies) and the dependence upon bias conditions of the elements which make up this equivalent circuit are derived. A discussion of the various basic amplifier connections will follow and the description of two novel oscillator circuits concludes the paper.

The semiconductor amplifier has not yet been established on a commercial basis. As a result, it is difficult to find two units with substantially identical characteristics. The differences, however, are generally quantitative rather than qualitative and the circuits which are to be described are operable with a majority of the not obviously defective units made in our laboratory.

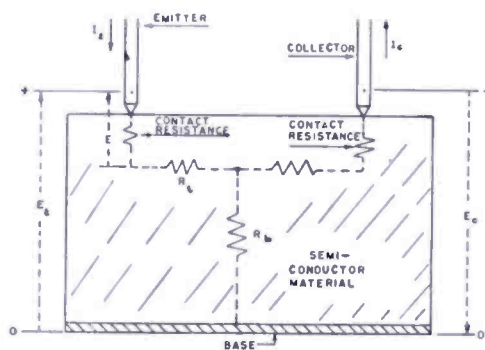


Fig. 1—The semiconductor amplifier with contact and bulk resistances represented schematically.

The results discussed in this paper are confined to those obtained using amplifiers made with germanium, the bulk of which is of "N" or "excess" type. This type of semiconductor is characterized by impurity centers (or lattice defects) which furnish the electrons essential to conduction. When a crystal rectifier is constructed using "N" type material, its resistance will be lowest when the point contact is made positive with respect to the

crystal.

In this paper, reference is made to the three elements of the device, as they are shown in Figure 1, in the following sense: The "emitter" electrode is that contact of relatively small area which is normally maintained at a positive potential with respect to the bulk of the semiconductor. The "collector" electrode is generally similar to the emitter electrode but is maintained at a negative potential with respect to the semiconductor. The "base" electrode makes contact to the material over a large area; consequently, the contact resistance between the base and the bulk of the semiconductor is very low.

#### EQUIVALENT CIRCUITS

By analogy to the theory of crystal rectifiers, particularly those

or to circuits involving the transistor. It therefore seems desirable to report some of the observations which have been made while evaluating this type of device as a circuit element. The discussion which follows begins with the evolution of a direct-current equivalent circuit with which the static characteristics of the crystal amplifier may be duplicated. From this, an alternating current equivalent circuit (for small signals and low frequencies) and the dependence upon bias conditions of the elements which make up this equivalent circuit are derived. A discussion of the various basic amplifier connections will follow and the description of two novel oscillator circuits concludes the paper.

The semiconductor amplifier has not yet been established on a commercial basis. As a result, it is difficult to find two units with substantially identical characteristics. The differences, however, are generally quantitative rather than qualitative and the circuits which are to be described are operable with a majority of the not obviously defective units made in our laboratory.



Fig. 1.—The semiconductor amplifier with contact and bulk resistances represented schematically.

The results discussed in this paper are confined to those obtained using amplifiers made with germanium, the bulk of which is of "N" or "n-type" type. This type of semiconductor is characterized by impurity centers (or lattice defects) which furnish the electrons essential to conduction. When a crystal rectifier is constructed using "N" type material, its resistance will be lowest when the point contact is made positive with respect to the

crystal.

In this paper, reference is made to the three elements of the device, as they are shown in Figure 1, in the following sense: The "emitter" electrode is that contact of relatively small area which is normally maintained at a positive potential with respect to the bulk of the semiconductor. The "collector" electrode is generally similar to the emitter electrode but is maintained at a negative potential with respect to the semiconductor. The "base" electrode makes contact to the material over a large area; consequently, the contact resistance between the base and the bulk of the semiconductor is very low.

#### EQUIVALENT CIRCUITS

By analogy to the theory of crystal rectifiers, particularly those

made with germanium, it might be expected that the current flowing from the emitter into the semiconductor (i.e. in the "forward" direction) would be an exponential function of some potential difference,  $E$ . Moreover,  $E$  might be expected to be the applied voltage,  $E_c$ , less the potential drop due to currents flowing in the bulk of the material. Consider Figure 1. The bulk resistance is represented by a  $T$  section of resistors. If  $E$  is assigned to be the potential difference appearing across the contact resistance at the emitter, it is equal to

$$E = E_c + R_b (I_c - I_e) - R_e I_e \quad (1)$$

where  $E_c$ ,  $R_b$ ,  $R_e$ ,  $I_c$  and  $I_e$  are as defined in Figure 1. The relationship between  $I_e$  and  $E$  as suggested above is:<sup>2</sup>

$$I_e = k (e^{\alpha E} - 1) \quad (2)$$

where  $k$  and  $\alpha$  are constants. If  $R_b$  and  $R_e$  are assumed to be constants and values for  $I_c = f(E_c, E_c)$  are obtained from experimental data,  $I_e$  may be calculated as a function of  $E_e$  and  $E_c$ . Such calculations show good agreement with measurements.

All that remains is to determine the relationship between  $I_c$  and the applied voltages. Unfortunately, there is no simple analogue by which to be guided in considering this relationship as there was in the case of the emitter. An analysis of the observed variation of  $I_c$  with respect to  $E_e$  and  $E_c$  has been carried out using the static characteristics of several different units. This analysis has shown that a variable resistance of magnitude  $R_c = a - bE$  may be used to replace the contact resistance at the collector plus the unlabeled branch of the  $T$  section in Figure 1.

In other words, the equation

$$I_c = \frac{E_c + R_b I_e}{R_b + a - bE} \quad (3)$$

where  $E$  is as described above and  $E_c$  is the voltage applied between the collector and the base, expresses the variation of  $I_c$  with the applied voltages to a sufficient degree of approximation.

Figure 2 is a direct-current equivalent circuit based on the above conclusions. The contact resistance at the emitter is represented as

<sup>2</sup> Torrey and Whitmer, CRYSTAL RECTIFIERS, p. 21, 1st Edition, McGraw-Hill Book Company, New York, N. Y., 1948.



$$d I_{\epsilon} = k \alpha e^{\alpha E} d E \tag{4}$$

$$d E_o + R_b d I_{\epsilon} = (R_b + a - b E) d I_c - b I_c d E \tag{5}$$

$$d E = d E_{\epsilon} + R_b d I_c - (R_b + R_{\epsilon}) d I_{\epsilon}. \tag{6}$$

Then let us define:

$$\begin{aligned} d I_{\epsilon} &= i_{\epsilon} & d E &= e_1 \\ d I_c &= i_c & d E_{\epsilon} &= e_{\epsilon} \\ d E_o &= -e_o. \end{aligned}$$

Equation (4) becomes:

$$i_{\epsilon} = \alpha I_{\epsilon} e_1 \quad \text{or} \quad \frac{e_1}{i_{\epsilon}} = \frac{1}{\alpha I_{\epsilon}} \text{ ohms,}$$

equation (5):  $-e_o + b I_c e_1 = -R_b i_{\epsilon} + (R_b + a - b E) i_o$

and equation (6):  $e_1 = e_{\epsilon} + R_b (i_c - i_{\epsilon}) - R_{\epsilon} i_{\epsilon}.$

Figure 4 illustrates an alternating-current equivalent circuit<sup>3</sup> which satisfies these three equations providing:

$$\begin{aligned} r_{\epsilon} &= \frac{1}{\alpha I_{\epsilon}} + R_{\epsilon} & r_b &= R_b \\ r_o &= a - b E & \mu &= \frac{b I_c}{\alpha I_{\epsilon} R_{\epsilon} + 1} \end{aligned}$$

where  $I_{\epsilon}$ ,  $I_c$  and  $E$  are direct-current values of current and voltage as described above.

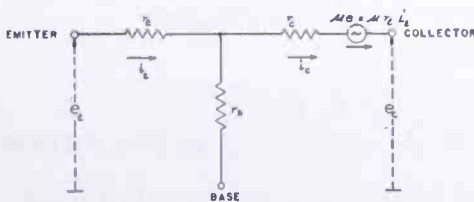


Fig. 4—An alternating current equivalent circuit.

Since this small-signal equivalent circuit was derived from direct-current characteristics, no reactive elements are included and its use must be restricted to low frequencies. Experiments indicate that a phase angle should be associated

<sup>3</sup> This alternating-current equivalent circuit, one of many which have been found satisfactory, is similar to that presented at various technical meetings by the authors of the letters referred to in footnote 1.

with the dimensionless parameter  $\mu$ . The effects of this phase displacement have been observed at frequencies as low as five kilocycles.

Using this equivalent circuit, expressions for input impedance, output impedance and gain may be obtained for any connection of the crystal amplifier. To simplify the algebra, the following approximations, valid over the operating range, have been made:

$$r_c \pm r_b \approx r_c$$

$$r_c \pm r_e \approx r_c$$

$$\mu \pm 1 \approx \mu$$

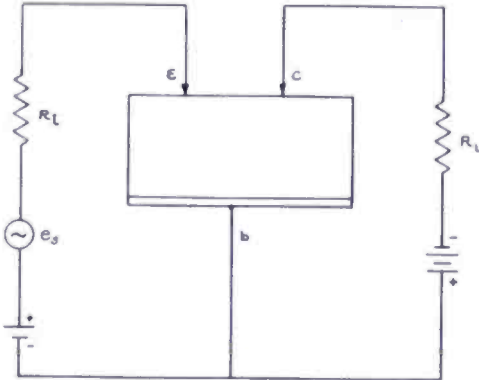


Fig. 5—The emitter input amplifier connection.

### AMPLIFIER CIRCUITS

The circuit illustrated in Figure 5 was described by Bardeen and Brattain.<sup>1</sup> This connection will be referred to as the "emitter input" connection. Expressions for input and output impedance, and power gain for this amplifier have been derived from the equivalent circuit:

$$\text{input impedance} = r_e + r_b \left( 1 - \frac{\mu r_e}{R_L + r_c} \right)$$

$$\text{output impedance} \cdot r_c \left[ 1 - \frac{\mu r_e r_b}{r_c (R_i + r_e + r_b)} \right]$$

$$\text{maximum available power gain} = \frac{\mu^2 r_e^2}{r_c (r_e + r_b) (1 + \beta)^2}$$

where

$$\beta = \sqrt{1 - \frac{\mu r_e r_b}{r_c (r_e + r_b)}}$$

The available power gain is defined as  $4 \frac{i_L^2 R_L R_i}{e_s^2}$ ,  $i_L$  is the current flowing in the load,  $R_L$ , and the above equation is for matched conditions. Near match,  $R_L$  is of the order of  $r_c$  and  $R_i$  approaches  $r_e$ .

The term  $\beta$  in the expression for power gain is generally less than unity but always positive in the region under consideration. The stability of an emitter input amplifier is usually quite good.

Experimental measurements yield the following numerical results for a typical unit connected in this fashion.

$$\begin{aligned} \text{input impedance} &= 700 \text{ ohms} & \text{power gain} &= 16 \text{ decibels} \\ \text{output impedance} &= 30,000 \text{ ohms.} \end{aligned}$$

These values, and the numerical results of other analyses which follow, were obtained experimentally by adjusting the emitter bias, load and input matching device until the point of maximum stable gain was reached. All such measurements were made at a frequency of five kilocycles. No attempt was made to tune out any reactive components that might exist.

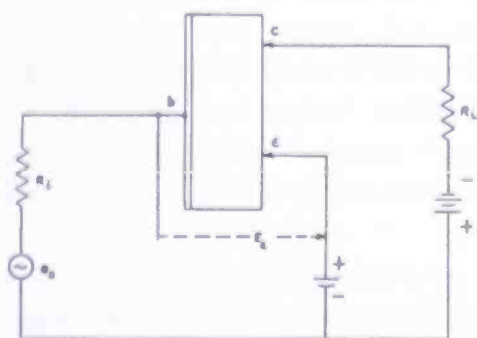


Fig. 6—The base input amplifier connection.

The low input impedance of the emitter input amplifier is generally considered a disadvantage since a matching device is required for most applications. The description of two other amplifier circuits, both of which are more satisfactory in this sense, will follow.

The circuit shown in Figure 6 is called the "base input" amplifier<sup>4</sup>. An analysis of this circuit shows:

$$\text{input impedance} = r_b + \frac{r_e}{1 - \frac{\mu r_e}{R_L + r_c}}$$

$$\text{output impedance} = r_o \left[ 1 - \frac{\mu r_e}{r_o} \left[ \frac{R_L + r_b}{R_L + r_b + r_e} \right] \right]$$

$$\text{maximum available power gain} = \frac{\mu^2 r_e^2 \beta^2}{r_o (r_e + r_b) (1 + \beta' \beta)^2}$$

where, as before, 
$$\beta = \sqrt{1 - \frac{\mu r_e r_b}{r_o (r_e + r_b)}}$$

and 
$$\beta' = \sqrt{1 - \frac{\mu r_e}{r_o}}$$

<sup>4</sup> This circuit was suggested by E. W. Herold of RCA Laboratories.

Note that  $\beta'$  will be less than  $\beta$  since  $\frac{r_b}{r_e + r_b}$  is less than unity. In practice,  $(\beta')^2$  may be equal to or less than zero while  $\beta$  is positive as pointed out above.

Figure 7 shows graphically the dependence on emitter bias of the input impedance. Two worth-while observations may be made while inspecting these curves. 1) The negative resistance appearing between

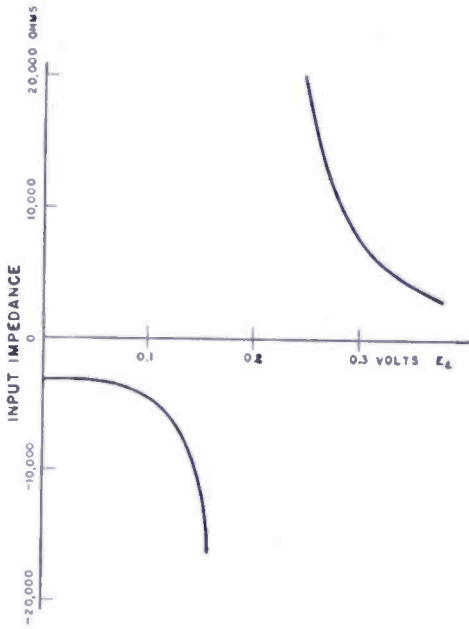


Fig. 7—The low frequency input impedance of the base input amplifier as a function of emitter bias.  $R_L = 10,000$  ohms, collector supply voltage = 10 volts.

the base and ground at low bias voltages may be used to supply the losses of a resonant circuit, and 2) the very high input impedance in the neighborhood of  $E_e = 0.2$  volts (for this unit) is most attractive when the device is to be used as an amplifier. A two-terminal oscillator which operates in the negative resistance region will be described later.

It has been noted that  $\beta'$  in the algebraic expression for power gain may be zero or imaginary. This indicates that the circuit is generally regenerative and high gain may be obtained. Some care, however, must be taken to avoid unwanted oscillations. Practical values of impedance and gain obtained under stable amplifier conditions are as follows:

$$\text{input impedance} = 5,000 \text{ ohms}$$

$$\text{power gain} = 23 \text{ decibels}$$

$$\text{output impedance} = 10,000 \text{ ohms.}$$

With careful adjustment of bias, a much higher input impedance may be measured at low frequencies. However, it is generally not practical to operate with matched impedances at this point because of instability. At higher frequencies the situation is complicated by the phase shift in  $\mu$ .

A third basic amplifier circuit is termed "emitter output" amplifier and is illustrated in Figure 8. An analysis yields the following alge-

braic expressions. Practical values obtained experimentally are also listed.

$$\text{input impedance} = r_b + \frac{(r_c + R_L) r_c}{R_L + r_c - \mu r_e} = 20,000 \text{ ohms}$$

$$\text{output impedance} = \left[ \frac{(R_i + r_b) (r_c - \mu r_e) + r_c r_e}{R_i + r_c} \right] = 500 \text{ ohms}$$

$$\text{maximum available power gain} = \frac{r_c}{[\sqrt{r_e} + \sqrt{r_c - \mu r_e}]^2} = 16 \text{ decibels.}$$

Near match,  $R_i$  will be of the order of  $r_c$  and  $R_L$  the order of  $r_e$ .

The emitter output amplifier may be used as a matching device between stages of base input or emitter input amplifiers. As such, it will furnish power gain to the system. The major disadvantage of this circuit is that the power output which may be obtained is comparatively low. Operation is best in the region where  $r_c - \mu r_e$  is of the order of  $r_c$ . The adjustment of the direct-current biases to obtain this condition is quite critical.

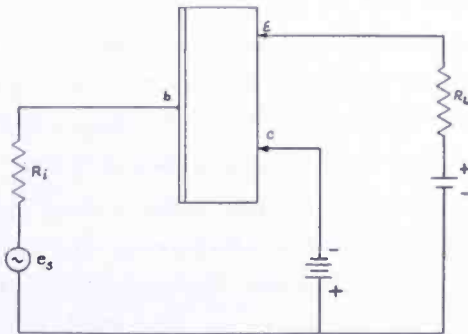


Fig. 8—The emitter output amplifier connection.

The following table is included in order that the three amplifier connections may be compared. The results are those obtained experimentally with an average unit. Because of the large variation in crystal amplifiers, these results should not be considered typical of all units.

	Emitter Input	Base Input	Emitter Output
Input impedance . . .	700 ohms	5,000 ohms	20,000 ohms
Output impedance . .	30,000 ohms	10,000 ohms	500 ohms
Power gain . . . . .	16 decibels	23 decibels	16 decibels
Voltage gain . . . . .	40:1	20:1	less than 1:1
Current gain . . . . .	about 1:1	10:1	40:1
Maximum power output with tolerable distortion . . . . .	$2 \times 10^{-2}$ watt	$2 \times 10^{-2}$ watt	$10^{-4}$ watt

With the foregoing in mind, it is possible to design direct-coupled amplifiers of two or more stages which fulfill certain conditions of gain and impedance. One such combination is illustrated in Figure 9. Using two average units in this circuit, stable gain of 36 decibels was obtained. The input and output impedances were equal to 10,000 ohms, at 5,000 cycles per second.

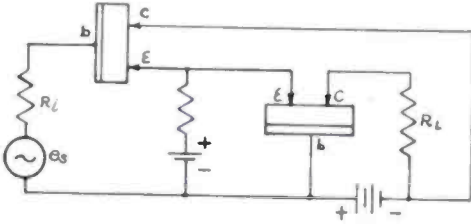


Fig. 9—A two-stage direct-coupled amplifier.

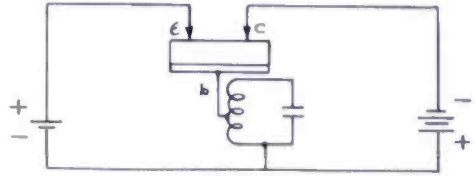


Fig. 10—A two-terminal sine-wave oscillator.

### OSCILLATOR CIRCUITS

As indicated in Figure 7 and the associated discussion, the input impedance of the base input amplifier will be a "voltage controlled" negative resistance under certain conditions, and a two-terminal sine wave oscillator may be constructed which operates in this region. This negative resistance is not associated with the "current controlled" negative resistance observed in a crystal rectifier near breakdown.

Figure 10 illustrates such an oscillator. Signal output may be obtained by coupling to the resonant circuit, the emitter or the collector, loading at any of these points will decrease the amplitude of oscillation. The circuit shown in Figure 10 may be operated with about 40 per cent efficiency and is capable of delivering 50 to 100 milliwatts at a frequency of one megacycle. Experimental data indicate that frequency variations with changing bias conditions are fairly severe. There also exists a small frequency fluctuation that is apparently due to the inherent noise of the device. This type of oscillator may be easily pulse-modulated by the application of a pulse to the emitter.

### RELAXATION OSCILLATORS

A negative resistance of the "current-controlled" type appears between the collector and ground when a resistance is placed in the base lead and the bias and supply voltages are properly adjusted. This can be seen from the expression for the output impedance of a base input amplifier. The presence of this negative resistance permits the construction of the simple relaxation oscillator, illustrated in Figure

11. The operation of this circuit is further explained in a qualitative fashion as follows.

We have seen that both emitter and collector currents are increased as the base is made negative with respect to the emitter. In this case, the potential of the base is equal to  $R_d (i_e - i_c)$  (the base is negative if  $i_c$  is greater than  $i_e$ ). With the correct biases, the circuit becomes regenerative with respect to the collector current. Connection of the condenser,  $C$ , between the collector and ground, and the series resistor,  $R_a$ , between the collector and its power supply is all that is needed to make a relaxation oscillator.

The factors responsible for the alternate charge and discharge of condenser,  $C$ , will be investigated with the aid of Figure 12. This is a plot of the collector voltage,  $E_c$ , with respect to time. From time  $t_0$  to time  $t_1$  the condenser is charged through  $R_a$  by the power supply. When the collector voltage reaches level  $A$ , the condenser is discharged through the crystal amplifier by the regenerative effect

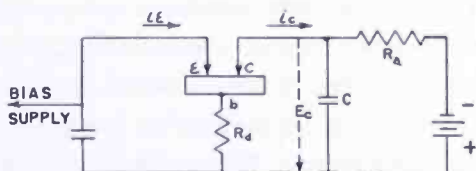


Fig. 11—A simple relaxation oscillator.

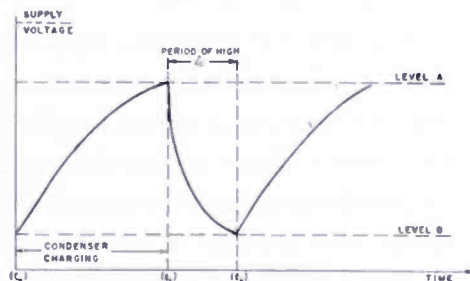


Fig. 12—The voltage across condenser,  $C$ , as a function of time.

described above. The cycle then repeats itself. A sawtooth wave form appears across condenser,  $C$ , and pulses may be obtained between the base and ground.

Free-running operation at frequencies up to 100 kilocycles is possible with most units. A ratio of discharge time to charge time of nearly unity may be obtained although performance will generally be more satisfactory if the ratio is about 1:5. One microsecond pulses with rise times of the order of 0.2 microseconds are obtainable. Output voltage is available at the collector, the base or across an impedance in the emitter lead. The latter coupling exhibits the lowest impedance and, generally, the sharpest pulses.

If the circuit constants and biases are such that level  $A$  in Figure 12 is more negative than the collector supply voltage, the condenser will not be automatically discharged and the circuit will operate as a single cycle relaxation oscillator when an external trigger pulse is applied.

Figure 13 shows the circuit of such an oscillator which is triggered by a positive pulse on the emitter.

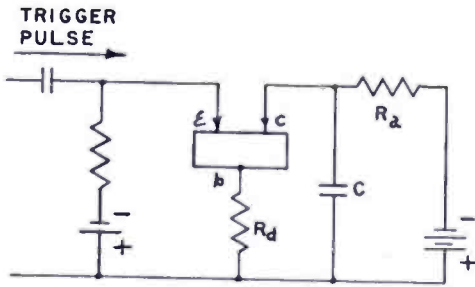


Fig. 13—A single cycle relaxation oscillator.

Measurements on both types indicate a dependence of pulse-width on supply voltage. A variation as great as 6 per cent in pulse-width may result from a 10 per cent change in voltage. The high noise power generated in most crystal amplifiers may be troublesome if the circuit is operating in such a way that the collector voltage approaches either operating limit

slowly. In this case, there will be a variation in repetition rate and pulse width of 5 per cent or more.

#### CONCLUSION

The crystal amplifier is a highly versatile circuit element. It has been shown that it is possible to draw direct-current and alternating-current equivalent circuits which are satisfactory representations of the device. With a knowledge of certain constants, characteristic of the semiconductor material and the geometry of the device, the behavior of a crystal amplifier of the transistor type may be predicted for any connection and any set of bias conditions. The various amplifier connections differ appreciably in input and output impedance. Internal feedback in the device makes operable two novel oscillator circuits.

# STANDARDIZATION OF THE TRANSIENT RESPONSE OF TELEVISION TRANSMITTERS\*

BY

R. D. KELL AND G. L. FREDENDALL

Research Department, RCA Laboratories Division,  
Princeton, N. J.

*Summary*—Standardization of the square-wave response of a television transmitter is suggested on the basis of a comparison of the response of a standard monitor to square-wave signals generated by the transmitter and the calibrated response of the monitor to a double-sideband television signal modulated by a square-wave.

Standardization of picture monitors also appears to be imperative because uniform quality of transmission is desirable from all broadcasters.

## INTRODUCTION

WHEN the standards of the present television system were agreed upon by the engineers of the industry, it was realized that additional standards relating to the amplitude and phase or some equivalent characteristics of the transmitter would have to be adopted later in order to fully specify the picture quality or fidelity. At that time there was insufficient technical data and operating experience with the complete television system to specify the additional standards and tolerances. There was, however, sufficient experience with vestigial sideband transmission and reception for standardization of the radio-frequency amplitude characteristics of the transmitter and receiver, which are shown in idealized form in Figure 1. It is specified that the carrier position in the receiver shall be at the point of 50 per cent amplitude response and that the lower sideband spectrum and part of the upper sideband spectrum shall be attenuated as shown. It is standard that the amplitude response in the transmitter shall substantially cover the receiver characteristic since the basic premise of the entire arrangement is that receiver operation shall be essentially the same whether the receiver is supplied with signal from a double-sideband signal generator or from a transmitter in which the lower sideband is suppressed beyond the frequency at which the receiver has no response. It was assumed that eventually the phase characteristic of the vestigial sideband transmitter would be specified. Adherence to standards is required of broadcasters. The observance by manufacturers of receivers can only be advised.

---

\* Decimal Classification: R140.

During the seven years since the adoption of the standards shown in Figure 1, considerable knowledge concerning the fidelity of transmitters and receivers has been accumulated. In this paper a basis is proposed for additional standards equivalent to a specification of amplitude and phase but logically superior. The suggested standards will include phase compensation networks for installation in the video section of the transmitter that will make possible the attainment of the fidelity of which the present system is capable.

Sole dependence on the amplitude and phase characteristics of various parts of the system as the criterion of fidelity of picture transmission has proven to be illusive because these quantities are not directly observable in a television picture, and therefore are difficult to specify with logical tolerances. In a television picture of high fidelity the transitions in half-tones corresponding to abrupt changes in the subject are sharp and there is a minimum of spurious halftone variations, such as leading whites or blacks, ringing, long black or white smears, and so forth. Possible tolerances or permissible deviations

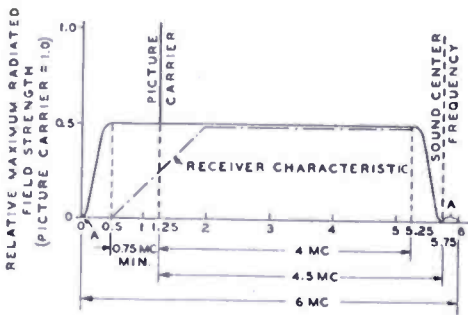


Fig. 1—RMA idealized amplitude characteristics of transmitter and receiver.

of phase and amplitude from the distortionless state within the channel would have to be tried in connection with the transmission of critical waveforms which permit observation of abrupt transitions and spurious signals. Such a critical waveform that has received general recognition by engineers is the unit function or its practical equivalent, the square wave. The abrupt transition in a square wave

represents an abrupt transition in picture halftone value that involves the transmission of video frequencies ranging from a few hundred kilocycles to 4 megacycles per second. The flat part of a square wave permits testing for long black or white smears and involves the lower frequencies of the video spectrum beginning with 60 cycles per second. It is reasonable, therefore, to use the square-wave response as the primary measure of the overall performance of the television system. In brief, the standard of Figure 1, which defines the type of transmission, may be supplemented by standards which prescribe certain significant characteristics of the wave shape of the output of a standard monitoring receiver in response to a square wave applied as modulation to the input of the transmitter.

## SQUARE-WAVE RESPONSE OF A TELEVISION RECEIVER

The concept of a standard receiver appears to be necessary in the discussion of transmission and reception in a vestigial sideband system. The sidebands of the radiated signal are not in proper balance until the signal is passed through a selective receiving circuit having an appropriate amplitude response such as the standard response of Figure 1. It is obvious that all broadcasters should monitor with a standardized receiver so the transmission characteristics of various transmitters will not vary. A chaotic condition is likely to occur if monitors are non-standard. At this point it is sufficient to observe that a monitor should be a good receiver, the performance of which could be duplicated in a high-grade commercial television receiver. The combined radio-frequency and intermediate-frequency amplitude response should approximate that shown in Figure 1. Before a basis for the specification of standard monitor is given, a preliminary study of the square-wave response of actual television receivers is helpful.

The response of a certain commercial receiver to a square-wave transition generated by a double-sideband laboratory signal generator is shown by curve 4, in Figure 2. This simulates the ideal functioning of the transmitting portion of the television system and permits analysis of the receiver alone<sup>1</sup>. The ultimate criterion by which the real receiver may be judged is curve 3, the response of an idealized receiver having the RMA amplitude characteristic of Figure 1 and a linear phase characteristic. The real response (curve 4) departs from the idealized response in two respects. First, the time of rise of the real transition (0.13 microseconds) as measured between the points of 10 per cent and 90 per cent response is greater than that of the idealized transition (0.1 microseconds), and second, the transition itself is dissymmetrical. The time of rise  $T$ , is a measure of capability of the receiver for the reproduction of sharp edges or transitions in picture halftones. Symmetry or dissymmetry of the transition as relates principally to the damped oscillatory component, commonly termed a "cutoff transient", occurs before and after the main transition of curve 3, but only after the transition of curve 4. Cutoff transients appear visually as striated patterns near the transition and are seen more clearly when the amplitude is large and the frequency of repetition is low. The question which naturally arises concerning the desira-

<sup>1</sup> In all observations cited, the depth of modulation of the radio-frequency carrier was moderate so that the peculiarities of vestigial sideband transmission near 100 per cent modulation were avoided. For a discussion of these effects see R. D. Kell and G. L. Fredendall, "Selective Sideband Transmission in Television", *RCA Review*, Vol. 4, pp. 425-440, April, 1940.

bility of a symmetrical cutoff transient is answered in the following section.

In practice, means must be provided at the transmitter for the attenuation of one sideband in accordance with Figure 1. This attenuation is provided in the output of the laboratory signal generator by the use of a commercial vestigial sideband filter identical in design to those currently used in the field<sup>2</sup>. In some transmitters sideband attenuation is accomplished in several cascade stages of band-pass amplification at the radio-frequency level<sup>3</sup>. Ideally, the square-wave response measured at the output of the receiver should remain

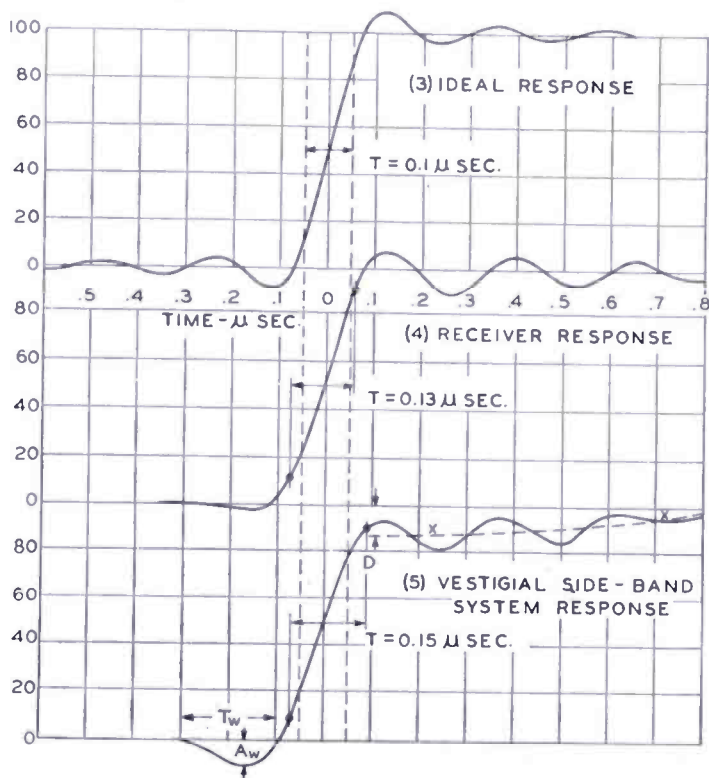


Fig. 2—Square-wave response of ideal receiver and an actual receiver.

unchanged when the vestigial sideband transmission is substituted for a double-sideband transmission. However, there is additional waveform distortion introduced into the response due principally to phase distortion associated with the attenuation of the sideband spectrum. This is shown in curve 5 of Figure 2. A leading spurious signal  $T_w$  which is barely evident in double sideband operation, curve 4, is prominently displayed in curve 5. If the transition is from white to black the spurious signal appears as a leading white; if the transition is from black to white the spurious signal is a leading black. The

<sup>2</sup> RCA vestigial sideband filter, type M19104-4 for channel 4.

<sup>3</sup> "Design Trends in Television Transmitters", *Electronics*, Vol. 21, p. 76, January 1948.

time interval occupied by this signal, as well as its amplitude, is of considerable importance. Usually the interval  $T_w$  is about equal to a complete cycle of the cutoff transient, and therefore represents a visible halftone variation when the viewing distance is such that the eye tends to average the variation of a cycle of the cutoff transient without responding to the halftone variation over the cycle. The axis  $XX$  of the cutoff transient represents the general trend in halftone variation as the transition attains the final level of 100 per cent. If the axis does not coincide with the final level a smear component is thereby introduced following the abrupt transition. A measure of the smear component is the deviation  $D$  of the axis from the reference level of 100 per cent and the length of time required for the axis to attain this level. The slope may be either positive or negative, depending in part upon the position of the carrier on the receiver characteristic. Operation below the point of 50 per cent response tends to result in a negative slope.

Recourse to the steady-state characteristics of amplitude and phase is helpful in explaining the various aspects of the square-wave response. Fortunately, the square-wave response contains all of the information necessary for derivation of the effective or overall amplitude and phase distortion of the receiver<sup>4</sup>. The term "overall video distortion" is especially appropriate

since the picture signal enters the signal generator as a video signal and reappears at the terminals of the picture tube as a video signal. Distortion originating in the radio-frequency, intermediate-frequency, or the video sections of the receiver are conveniently lumped as an equivalent video distortion. Figure 3 shows the steady-state characteristics for double-sideband operation of the receiver. A more convenient term, the relative time delay, equal to  $\phi/2\pi f$  is substituted for the phase angle,  $\phi$ . The amplitude and delay characteristics of an ideal receiver would be independent of frequency out to a limit imposed by the width of the television channel. However, in practice both the amplitude and delay characteristics fall short. The delay distortion in Figure 3 exhibits a sharp up-turn at the end of the video band in

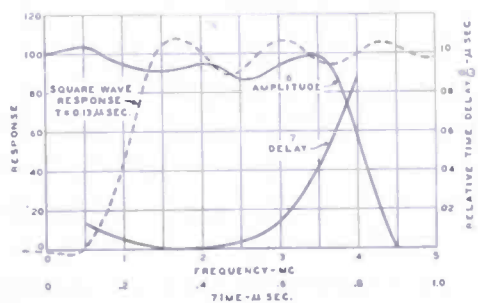


Fig. 3—Receiver (A) DSB transmission.

<sup>4</sup> A. V. Bedford and G. L. Fredendall, "Analysis, Synthesis, and Evaluation of the Transient Response of Television Apparatus", *Proc. I.R.E.*, Vol. 30, pp. 440-457, October, 1942.

the range 3 to 4 megacycles as a consequence of the cutoff of the intermediate-frequency and video-frequency amplifiers of the receiver. A more gradual increase in delay occurs as the frequency becomes lower over the range below 1.5 megacycles. If the delay distortion in the lower frequency interval and the delay distortion above 3 megacycles are removed, the magnitude of the following cutoff transients of curve 4, Figure 2 is approximately halved and a similar transient is added before the advent of the transition. That is, when the delay distortion in curve 4, Figure 2, is arbitrarily removed, the resulting response closely resembles curve 3, Figure 2, which is the ideal response. The remaining discrepancy in the compensated response is a slower time of rise caused by deficiencies in amplitude response, as revealed in Figure 3.

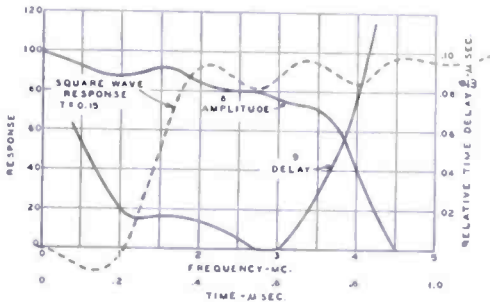


Fig. 4—Receiver (A) VSB transmission.

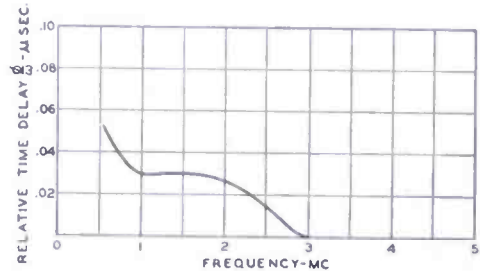


Fig. 5—Delay distortion introduced by VSB transmission.

A steady-state analysis corresponding to the square-wave response (curve 5) of the complete vestigial sideband system appears in Figure 4. It is seen here (curve 9) that the introduction of vestigial sideband transmission has acted chiefly to increase the delay distortion in the frequency range below 3 megacycles. The shape of the delay curve 9 above 3 megacycles is unaltered and is still controlled exclusively by the cutoff of the receiver. There is some modification of the amplitude characteristic. The effective delay distortion introduced by the filter as shown in Figure 5 is the difference between the overall delay characteristic measured with and without the filter.

The existence of this delay distortion due to the means for obtaining sideband attenuation prevents the reception of pictures with the full fidelity possible within the 4-megacycle video channel unless corrected. Fortunately, the delay distortion can be substantially removed by the use of phase compensating networks connected in the video input of the transmitter. For complete compensation, the delay of the correcting network is complementary to the overall time delay characteristic as calculated from the square-wave response of the receiver when supplied with signal from a vestigial sideband transmitter. A

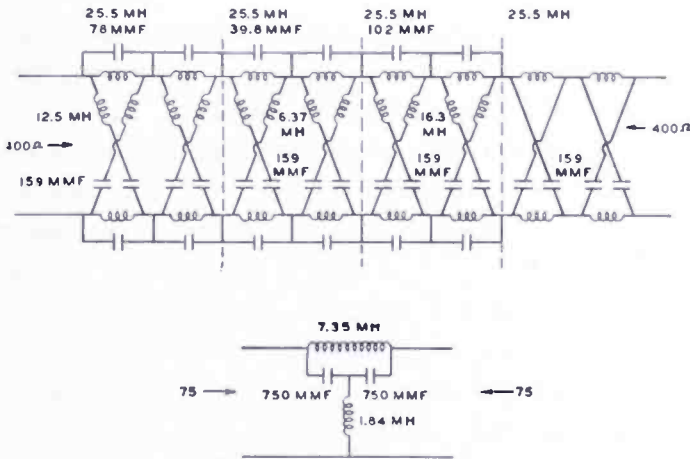


Fig. 6  
Equalizer for phase distortion due to cut-off in receiver.

Equalizer for phase distortion due to VSB transmission.

very considerable improvement in the square-wave response of the receiver resulted when delay networks shown in Figure 6 were connected in the video input of the laboratory signal generator. The total correction consisted of two parts, (1) a bridged-T all-pass section for correction of the delay distortion introduced by the vestigial sideband transmission and (2) an eight-section lattice type network for the correction of delay distortion due to cutoff in the receiver. Figure 7 illustrates the successive stages of the improvement. Curve 4 is the response of the receiver to a double sideband signal taken from Figure 2; curve 5 is the uncompensated response of the receiver to the vestigial sideband signal taken from Figure 2; curve 11 is the response after compensation of the delay distortion due to the sideband filter; curve 12 is the response involving compensation of the delay distortion due to cutoff in the receiver, as well as compensation for the filter.

Compensation of the effective delay distortion due to vestigial sideband operation by means of video networks is not absolutely independent of the amplitude and delay characteristics of the particular receiver over the range for which the upper and lower sidebands are present<sup>5</sup>. This dependence does not exist if the correction is made in the radio-frequency section of the transmitter, but the utilization of all-pass networks at television radio-frequencies is not feasible in general. However, since the present television system has been established on the basis of the receiver characteristic illustrated in Figure 1, it is not anticipated that the

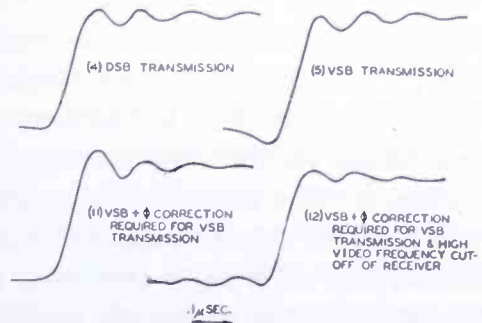


Fig. 7—Television receiver square-wave response.

<sup>5</sup> See appendix 1, Eqs. (8) and (9); appendix 2, Eq. (14).

designs of various commercial receivers will differ to such an extent that a network can not be found that yields a high measure of correction for all receivers. Figure 8 confirms this assumption. Here the effective delay characteristic of the filter has been calculated from square-wave measurements made on unselected television receivers of five different manufacturers. In this figure no curve deviates seriously from the arithmetic average of all curves. Curve  $\phi$  is the delay which is exactly compensated by the bridged-T network shown in Figure 6. It may be concluded, therefore, that this network connected in the video input of a transmitter will substantially compensate for the delay distortion due to vestigial sideband transmission. The means for attenuating one sideband of the transmitter in accordance with Figure 1 will differ depending upon the transmitter design of the various manufacturers. This means merely that the appropriate phase compensation networks for the transmitters of various types may differ slightly. Some amplitude compensation may also be required.

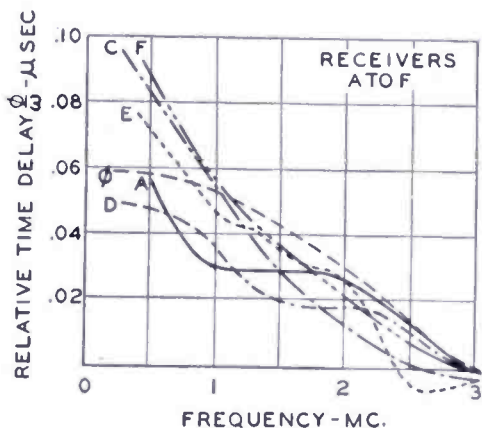


Fig. 8—Delay distortion introduced by VSB transmission.

The fidelity of receivers would be measurably improved if the delay distortion due to the high-frequency cutoff were compensated. Since involved networks such as the lattice structure in Figure 6 probably are required, their use would be justified only in receivers of the deluxe class. However, it is to be anticipated that the compensation required by the receivers of various manufacturers will be similar, since the amplitude response of all receivers must show high attenuation at the associated sound carrier. Similarity follows from application of the minimum phase shift law<sup>6</sup>. The possibility of including in the video section of the transmitter a delay correction for all receivers is convincingly demonstrated by the data taken on the receivers of various manufacturers as shown in Figure 9. The amplitude characteristics of this group of receivers ranged from substantially flat out to 4 megacycles to very low at 2 megacycles. The delay curves of this group of receivers are seen to be similar in the range 2.5 to 4 megacycles. Curve  $\phi$  in Figure 9 is

<sup>6</sup> H. W. Bode, NETWORK ANALYSIS AND FEEDBACK AMPLIFIER DESIGN, p. 276, D. Van Nostrand Company, Inc., New York, N. Y., 1945.

the delay characteristic which is exactly compensated by the all-pass lattice structure shown in Figure 6.

### COMPENSATION OF A TELEVISION TRANSMITTER

A working illustration of compensation is given in Figure 10, which shows the uncompensated and compensated response of a television receiver located in Princeton, New Jersey, to a signal radiated from television station WNBT in New York.

Figure 11 is a demonstration of the extent of phase compensation possible in television transmitter WNBT, Washington, D. C., when the networks shown in Figure 6 were inserted in the video frequency section of the transmitter without modification of this particular transmitter. In practice, adjustments would be made based on square-wave measurements of the transmitter.

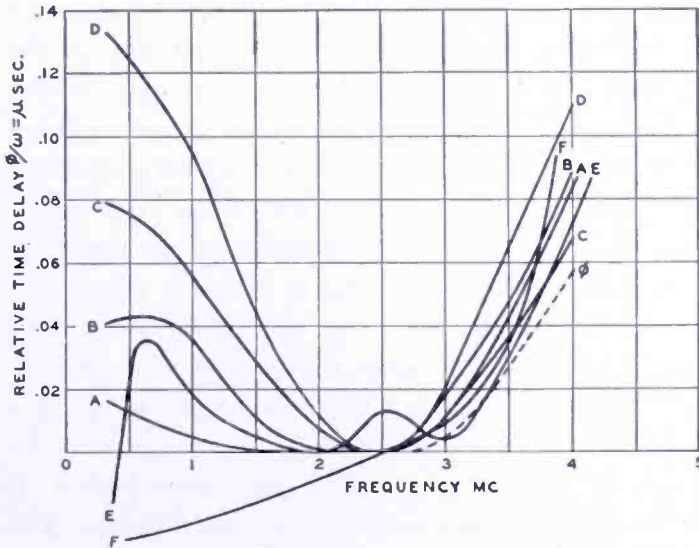


Fig. 9—Overall delay characteristics of receivers of 6 manufacturers.

### THE STATION PICTURE MONITORING RECEIVER

A standardized monitor is the first step in the direction of achieving uniform transmission characteristics among the television stations. Such a monitor should have the characteristics of a receiver of a high class that could be duplicated for domestic use if desired. The monitor would not include costly compensating circuits for the correction of delay distortion due to cutoff. There are various alternative approaches to the specification of a standard monitor. One alternative involves only steady-state amplitude and phase characteristics. It has been pointed out above, however, that this approach must depend finally upon transient response as a primary criterion. Hence, in devising the standards which are proposed here, reference is made only to

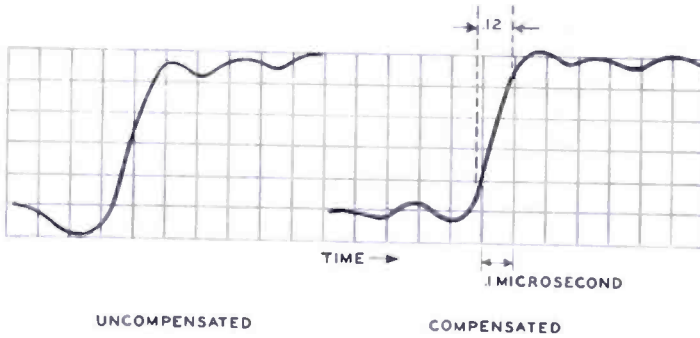


Fig. 10—Overall response of station WNBT + receiver at Princeton, N. J.

certain frequency intervals of the Radio Manufacturers Association (RMA) idealized receiver characteristics in Figure 1 that affect critically the performance of the monitor. One such interval is  $f_1$  to  $f_4$  (Figure 12) which contains the sloping portion of the amplitude characteristic. Tolerance in amplitude response of about  $\pm 5$  per cent are proposed from  $f_2$  to  $f_3$  as shown in Figure 12. This amounts to a definite restriction upon the position of the carrier between the points of 45 and 55 per cent response. Symmetry of the remainder of the sloping characteristic about the carrier position is desirable within limits as suggested in Figure 12. The amplitude of the wing response which occurs in the lower adjacent channel should not exceed a specified maximum of about 5 per cent. A restriction on this wing response is necessary in connection with the following specification of the transient response of the monitor. The portion of the RMA receiver characteristic between a frequency such as  $f_4$  and the frequency associated sound,  $f_5$ , does not require specification since the overall video amplitude and phase response corresponding to this region may be divided in any physically possible way between the carrier-frequency and the video-frequency portions of the monitor. The net contribution is implicitly contained in the square-wave response of the monitor. The wing response beyond the associated sound should be restricted to a maximum amplitude of about 30 per cent. The response of the monitor to a double-sideband signal which is modulated with a square wave should be subjected to the tolerances illustrated in Figure 13. Such

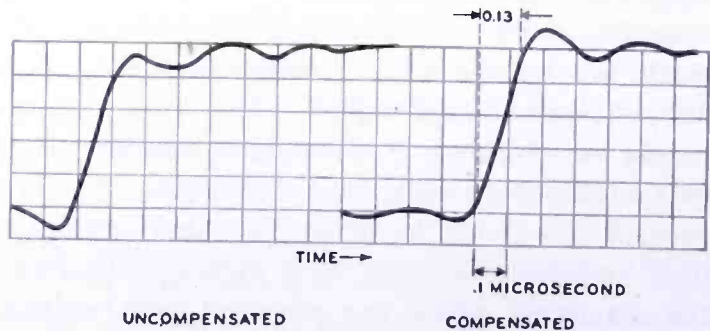
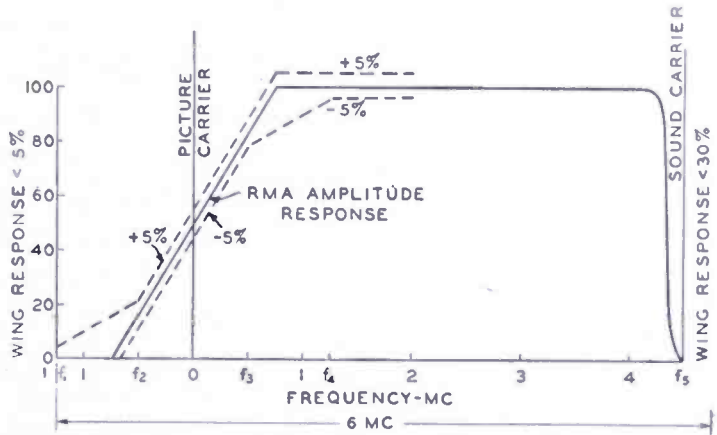


Fig. 11—Overall response of station WNBW + station monitor.

Fig. 12 — Standardization of amplitude characteristic of monitor.



tolerances pertain to the fidelity of a response to an abrupt transition, and therefore do not involve the low-frequency characteristics of the monitor. The time of rise as measured between the points of 10 and 90 per cent response shall not exceed a specified value, that is, the transition must lie within the region *ALG*. A time of rise at least as fast as 0.12 microseconds is attainable. The anticipatory signal shall be contained within the region *DEFLGHJ*. This limits the amplitude and length of the leading white and leading black signals. The cutoff transient shall be a damped sinusoid with a periodicity equal to or greater than 4 megacycles. Cutoff transients having a periodicity appreciably below the video cutoff frequency of 4½ megacycles are visible at normal viewing distances. The axis of the damped cutoff transient shall lie within *A, B, C, C', B', A'*. This sets limits on the smear signal component. The maxima and minima of the cutoff transient measured from the axis of the transient shall not exceed a specified amplitude of about 20 per cent. Provision for a minimum rate of damping can be imposed by stating for example that the fourth

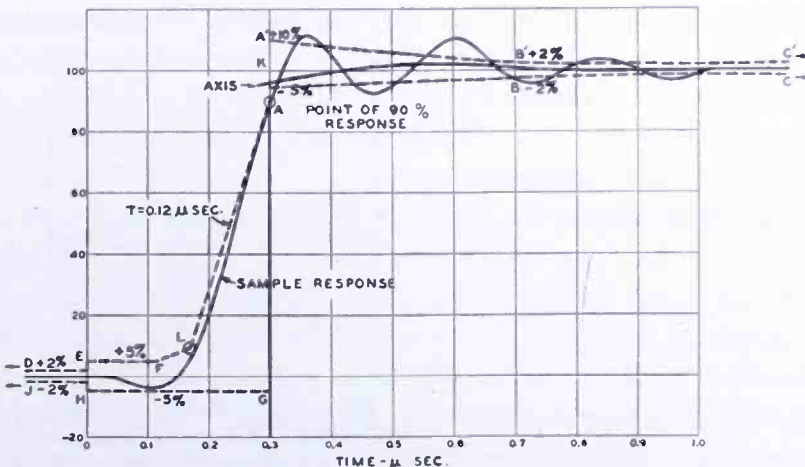


Fig. 13 — Standardization of square-wave response of monitor.

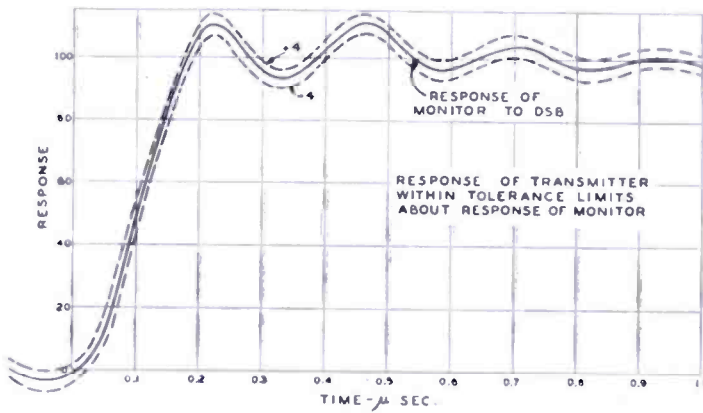


Fig. 14 — Standardization of square-wave response of transmitters.

and successive maxima and minima shall not exceed 2 per cent.

The response of the monitor corresponding to the rising and falling transitions of a square wave shall be subject to the same standard.

#### TRANSMISSION STANDARDS FOR TELEVISION TRANSMITTERS

A proposed standard for transmitters, including the means for sideband attenuation, involves essentially a substitution method wherein the monitoring receiver is the instrument for comparison of the transmitter with a double-sideband signal from a distortionless source such as a signal generator. Figure 14 illustrates one method for establishment of tolerances. The square-wave response of the monitor for a double sideband source is enclosed by two limiting curves, which represent the tolerable limits. The response of the monitor to an acceptable transmitter would lie within the area formed by these. Compensating networks such as those used for compensation of phase distortion introduced by the sideband attenuating means would be regarded as an integral part of the transmitter when the comparison with a double-sideband signal is made. The standardized phase compensation for distortion due to cutoff in the average receiver is conveniently specified on a basis of the steady-state delay and is not included when Figure 14 is considered. Figure 15 is the delay characteristic of the compensating network shown in Figure 6.

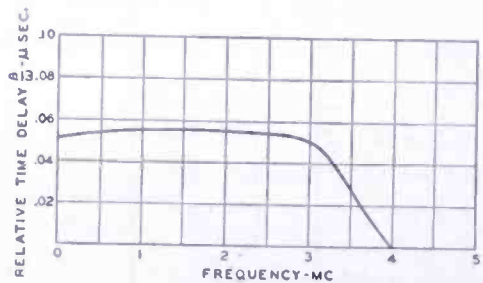


Fig. 15 — Delay characteristic of network for compensation of phase distortion associated with cut-off in receiver.

## STANDARDS FOR LOW-FREQUENCY RESPONSE

The effects of amplitude and phase distortion in the low-frequency video spectrum ranging from 60 cycles per second to about 100 kilocycles per second has been extensively studied by means of square-waves having a repetition rate of 60 cycles per second. The fidelity of television apparatus is judged by the extent of the deviation of the output over the constant portion of the square wave, as illustrated in Figure 16. A standard governing the low-frequency response of the monitoring receiver may be set up by assigning limits within which the flat top of the response must fit as shown in Figure 16A, and Figure 16B illustrates limits centered about the response of the monitor within which the response of the transmitter may fall. In a manner analogous to Figure 14, the low-frequency square-wave response of the transmitter may be assigned limits centered about the response of the monitor to a double sideband signal bearing 60 cycles square-wave modulation. Such tolerances are indicated in Figure 16B.

## CONCLUSIONS

A square-wave response is set forth as the logical criterion of fidelity for reproduction of television detail, involving frequencies above 100 kilocycles per second, and also subject matter involving the low frequencies between 60 cycles and about 100 kilocycles per second.

An experimental study of vestigial sideband transmission shows that the phase distortion introduced by the means of obtaining sideband attenuation in the transmitter and the phase distortion associated with high frequency cutoff in the receiver may be compensated by all-pass networks inserted in the video input of the transmitter. Definite indications resulting from an analysis of five receivers having different effective bandwidths are that a network designed for the compensation of the average delay distortion of these receivers in the range of  $2\frac{1}{2}$  to 4 megacycles improves the square-wave response of all receivers. It is proposed that correction for such an average delay distortion be incorporated in the transmitter. Standardization

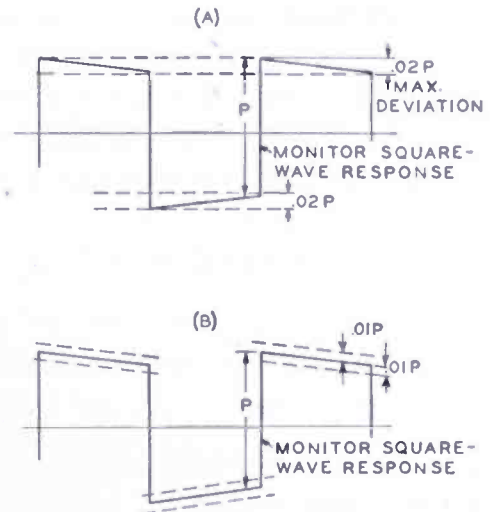


Fig. 16—Standardization of low-frequency square-wave response (A) Station monitor, (B) Transmitter.

of transmitters and station monitoring receivers is suggested through the medium of square-wave response. The tolerances to be applied in such standards involve engineering judgment as well as theoretical considerations, and therefore are matters for industry-wide agreement.

## APPENDIX 1

### OVERALL VIDEO AMPLITUDE AND PHASE CHARACTERISTICS OF A VESTIGIAL-SIDEBAND TRANSMISSION SYSTEM

As used here, a vestigial-sideband transmission system comprises the carrier-frequency portions of the transmitter and receiver. The input is a video signal applied as amplitude modulation of a carrier wave and the output is the envelope of the carrier signal after passage through the system. The overall video amplitude and phase characteristics of the system refer to the ratio of output to input amplitudes of a sine-wave of video modulation and the relative phase shift of the output and input wave as a function of frequency.

A carrier wave of frequency  $f_c$  modulated by a video sine-wave of frequency  $f_1$  has the well-known form:

$$e = E (1 + m \cos \omega_1 t) \cos \omega_c t$$

$$= E \cos \omega_c t + \frac{mE}{2} \cos (\omega_c + \omega_1) t + \frac{mE}{2} \cos (\omega_c - \omega_1) t. \quad (1)$$

The vestigial sideband system alters the relative amplitudes and phases of the signal so that (1) becomes:

$$v = E \left[ A_c \cos (\omega_c t + \phi_c) + \frac{mA_u}{2} \cos \{ (\omega_c + \omega_1) t + \phi_u \} \right. \\ \left. + \frac{mA_L}{2} \cos \{ (\omega_c - \omega_1) t + \phi_L \} \right] \quad (2)$$

in which the subscripts  $c$ ,  $u$ , and  $L$  refer to the carrier frequency, the upper sideband, and the lower sideband, respectively<sup>7</sup>. The way in which the alteration is divided between transmitter and receiver has no significance provided the system is linear.

Since the envelope of the carrier signal is sought, (2) is expressed

<sup>7</sup> D. W. Epstein and W. J. Poch, "Partial Suppression of One Sideband in Television Reception", *RCA Review*, Vol. 1, pp. 19-35, January, 1937.

in the form:

$$v = V_c \cos (\omega_c t + \alpha). \quad (3)$$

The envelope  $V_c$  is found to be a function of all of the amplitude and phase factors and the percentage of modulation, namely,

$$V_c = E \left[ A_c^2 + \frac{m^2}{4} \{A_u^2 + A_L^2 + 2A_u A_L \cos (2\omega_1 t + \phi_u - \phi_L)\} + mA_c \{A_u \cos (\omega_1 t + \phi_u - \phi_c) + A_L \cos (\omega_1 t + \phi_c - \phi_L)\} \right]^{\frac{1}{2}} \quad (4)$$

Although no use is made of  $\alpha$  in (3), it is interesting to note that  $\tan \alpha$  as given by

$$\tan \alpha = \frac{A_c \sin \phi_c + \frac{mA_u}{2} \sin (\omega_1 t + \phi_u) - \frac{mA_L}{2} \sin (\omega_1 t - \phi_L)}{A_c \cos \phi_c + \frac{mA_u}{2} \cos (\omega_1 t + \phi_u) + \frac{mA_L}{2} \cos (\omega_1 t - \phi_L)} \quad (5)$$

is in general a function of time and that therefore there is some phase modulation of the carrier in a vestigial sideband system.

In all of the following derivations the assumption is made that the percentage of modulation is sufficiently small that terms in  $m^2$  and higher orders can be neglected. That is,

$$v_c = E \left[ A_c + \frac{m}{2} \{A_u \cos (\omega_1 t + \phi_u - \phi_c) + A_L \cos (\omega_1 t + \phi_c - \phi_L)\} \right]. \quad (6)$$

The amplitude of the envelope is therefore proportional to

$$A_u \cos (\omega_1 t + \phi_u - \phi_c) + A_L \cos (\omega_1 t + \phi_c - \phi_L) = V(f_1) \cos \{\omega_1 t + \phi(f_1)\}. \quad (7)$$

Therefore, the overall video amplitude characteristic is given by

$$V(f_1) = [A_u^2 + A_L^2 + 2A_u A_L \cos (\phi_u + \phi_L - 2\phi_c)]^{\frac{1}{2}} \quad (8)$$

and the overall video phase characteristic by

$$\phi(f_1) = \tan^{-1} \frac{A_u \sin(\phi_u - \phi_c) + A_L \sin(\phi_c - \phi_L)}{A_u \cos(\phi_u - \phi_c) + A_L \cos(\phi_c - \phi_L)} \quad (9)$$

## APPENDIX 2

### EQUALIZATION OF OVERALL AMPLITUDE AND PHASE DISTORTION IN A VESTIGIAL SIDEBAND SYSTEM

Since, in general,  $V(f_1)$  is not independent of frequency and  $\phi(f_1)$  is not proportional to frequency within the video band, some amplitude and phase distortion will exist. It is possible to insert equalizers in the video input of the transmitter for the compensation of the output of the system at the receiver.

#### A. Phase equalization

If a phase angle  $\beta(f_1)$  is introduced into the video input of the transmitter by a phase equalizer, (1) modified

$$e = E [1 + m \cos(\omega_1 t + \beta)] \cos \omega_c t \quad (10)$$

and

$$\phi_c(f_1) = \tan^{-1} \frac{A_u \sin(\phi_u - \phi_c + \beta) + A_L \sin(\phi_c - \phi_L + \beta)}{A_u \cos(\phi_u - \phi_c + \beta) + A_L \cos(\phi_c - \phi_L + \beta)} \quad (11)$$

An equivalent form for (11) is

$$\tan \phi_e = \tan(\phi + \beta)$$

or

$$\phi_e = \phi + \beta \quad (12)$$

where  $\phi$  is the uncompensated phase characteristic. Hence, if  $\beta(f_1)$  is defined such that

$$\phi_e = \phi + \beta = af \quad (13)$$

where  $a$  is a constant, the overall phase is proportional to frequency and there is no phase distortion.

A different requirement may be that the overall phase characteristic of a given receiver and an imperfect vestigial-sideband transmitter with a suitable phase equalizer in the video input is the same as the response of the receiver and an ideal double sideband transmitted. That is, only the phase distortion due to the vestigial sideband transmitter is to be compensated. For this case

$$\beta = \omega_1 T - (\phi_{vs} - \phi_{ds}) \quad (14)$$

in which  $T$  is a constant time delay,  $\phi_{vs}$  is the phase shift in the uncorrected vestigial sideband system, and  $\phi_{ds}$  is the phase shift of the system when the transmitter is ideal double sideband. If the value of  $\beta$  in (14) is substituted in (11) or (12) there results

$$\phi_e = \phi_{vs} + \beta = \phi_{vs} + \omega_1 T - (\phi_{vs} - \phi_{ds}) = \omega_1 T + \phi_{ds}. \quad (13)$$

That is, the partially phase equalized vestigial sideband system has the same distortion  $\phi_{ds}$  as the receiver operating in a double sideband system. A formula for  $\beta$  may be developed as follows:

From (14):

$$\tan(\beta - \omega_1 T) = \tan(\phi_{ds} - \phi_{vs}) = \frac{\tan \phi_{ds} - \tan \phi_{vs}}{1 + \tan \phi_{ds} \tan \phi_{vs}}. \quad (14)$$

According to (9)

$$\tan \phi_{ds} = \frac{A_{u1} \sin v_1 + A_{L1} \sin \epsilon_1}{A_{u1} \cos v_1 + A_{L1} \cos \epsilon_1} \quad (15)$$

$$\tan \phi_{vs} = \frac{A_{u1} A_{u2} \sin(v_1 + v_2) + A_{L1} A_{L2} \sin(\epsilon_1 + \epsilon_2)}{A_{u1} A_{u2} \cos(v_1 + v_2) + A_{L1} A_{L2} \cos(\epsilon_1 + \epsilon_2)} \quad (16)$$

where

$$\begin{aligned} v_1 &= \phi_{u1} - \phi_{c1} & \epsilon_1 &= \phi_{c1} - \phi_{L1} \\ v_2 &= \phi_{u2} - \phi_{c2} & \epsilon_2 &= \phi_{d2} - \phi_{L2} \end{aligned}$$

The subscript 1 refers to the amplitude and phase response of the receiver alone to the sidebands, and the subscript 2 refers to the amplitudes and phases of the sidebands as radiated by the vestigial sideband transmitter.

*Case 1.*

$\beta$  in region of transmitted sideband for which  $A_{L1} = A_{L2} = 0$ . Setting  $A_{L1} = A_{L2} = 0$  in (15) and (16) and substituting the values of  $\tan \phi_{ds}$  and  $\tan \phi_{vs}$  in (14), there results

$$\beta = -v_2 + \omega_1 T = -\phi_{u2} + \phi_{c2} + \omega_1 T \quad (17)$$

*Case 2.*

$\beta$  in region in which both sidebands are transmitted.

$$\beta = \frac{\tan^{-1} A_{L1} A_{u1} A_{u2} \sin (\epsilon_1 - \nu_1 - \nu_2) + A_{u1} A_{L1} A_{L2} \sin (\nu_1 - \epsilon_1 - \epsilon_2) - A_{u1}^2 A_{u2} \sin \nu_2 - A_{L1}^2 A_{L2} \sin \epsilon_2}{A_{L1} A_{u1} A_{u2} \cos (\epsilon_1 - \nu_1 - \nu_2) + A_{u1} A_{L1} A_{L2} \cos (\nu_1 - \epsilon_1 - \epsilon_2) + A_{u1}^2 A_{u2} \cos \nu_2 + A_{L1}^2 A_{L2} \cos \epsilon_2} \quad (18)$$

+  $\omega_1 T$ .

**B. Amplitude equalization.**

Phase and amplitude equalization may be applied independently and without interaction. The amplitude characteristic  $V(f_1)$  given by (8) is the basis for design.

# PHASE AND AMPLITUDE EQUALIZER FOR TELEVISION USE\*

BY

E. DUDLEY GOODALE AND RALPH C. KENNEDY

National Broadcasting Company, Inc.,  
New York, N. Y.

*Summary*—A phase and amplitude equalizer is described which permits considerable improvement to be made in the performance of a transmission system whose overall response has been deteriorated by poor phase and amplitude characteristics. Specific examples are given in which it is shown that the picture quality is appreciably enhanced by the use of such a device. A brief discussion of the effects of phase and amplitude distortion on square waves is included.

## INTRODUCTION

AMPLITUDE equalizers for use on audio frequency systems have long been known to the art. Their use in conjunction with everyday transmission practice is as accepted as the use of an amplifier. Phase equalizers have not become so well known, probably because the effects of phase distortion are generally considered to be of secondary importance in the reproduction of sound and they may be made to occur at frequencies above the audio range by merely increasing the frequency response of the system. They are, however, employed on many long distance circuits to compensate for different times of transmission and to minimize the objectionable effects of echoes. In video systems<sup>1</sup> such is not the case. For the transmission of good television pictures the phase and amplitude characteristics of the system assume equal importance. As a matter of fact, in some instances the phase characteristic may be of greater significance than the amplitude characteristic in contributing to picture deterioration. This is particularly noticeable at the higher video frequencies when reproducing a sharp transition from white to black or black to white.

Considerable information is available on methods of measuring and calculating the phase and amplitude characteristics of a transmission

\* Decimal Classification: R246.2×R583.

<sup>1</sup> H. E. Kallmann, R. E. Spencer and C. P. Singer, "Transient Response," *Proc. I.R.E.*, Vol. 33, No. 3, p. 169, March, 1945.

system,<sup>2, 3</sup> but thus far the art does not include much useful information on how to apply corrections to result in an improved phase and amplitude characteristic. One method of approach is to design constant impedance lattice networks to produce the desired correction.<sup>4</sup> Then by a series of transformations they can usually be unbalanced and built in the Bridged-T configuration. This method is time consuming and difficult, and the networks are fixed allowing no adjustable correction to take care of normal variations in the many elements of the transmission system. With the equalizer described in this paper it is possible by simply turning knobs to effect not only amplitude correction in the response of a transmission system but also to effect phase correction within limits.<sup>5, 6</sup>

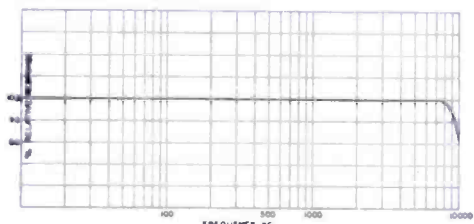


Fig. 1—Response curve of phase and amplitude equalizer when used as a video amplifier.

The amplitude corrections do cause some phase changes but the phase corrections do not cause amplitude variations. The equalizer may be used in camera chains, in transmitter feeds, at video relay points, or other locations where it is desired to effect some improvements in overall transmission.

### EQUALIZER CHARACTERISTICS

The equalizer, when all phase and amplitude equalizing controls are at zero, consists of an eight stage video amplifier whose response is flat to 8 megacycles (see Figure 1) and down about 16 per cent at 10 megacycles. It is intended to be fed from a 75-ohm source and to work into a 75-ohm load. The normal output level is 1 volt peak to peak. The overall amplifier gain is 4. There is an 18 decibel variable wide band attenuator located in the input circuit together with an additional 6 decibels of fixed attenuation which may be inserted if required. Thus an input signal level of 0.25 volts peak to peak minimum and 4 volts peak to peak maximum may be used to feed the equalizer to produce

<sup>2</sup> R. D. Kell, A. V. Bedford and H. H. Kozanowski, "A Portable High Frequency Square Wave Oscillograph for Television," *Proc. I.R.E.*, Vol. 30, No. 10, p. 458, October, 1942.

<sup>3</sup> A. V. Bedford and G. L. Fredendall, "Analysis, Synthesis, and Evaluation of the Transient Response of Television Apparatus," *Proc. I.R.E.*, Vol. 30, No. 10, p. 440, October, 1942.

<sup>4</sup> O. J. Zobel, "Distortion Correction in Electrical Networks with Constant Resistance Recurrent Networks," *Bell Sys. Tech. Jour.*, July, 1928.

<sup>5</sup> R. D. Kell and G. L. Fredendall, "Standardization of the Transient Response of Television Transmitters," pp. 17-34 of this issue.

<sup>6</sup> E. L. C. White, U. S. Patent No. 2,178,012.

1 volt peak to peak output. The equalizer capacitively couples to input and output circuits. The load may be coupled to either the plate or cathode of the output stage thereby making available either polarity of signal for utilization. This greatly increases the flexibility of the unit. Facilities are also provided to terminate the unused output in 75 ohms. The equalizer requires 6.3 volts at 4.9 amperes for the heaters and +285 volts regulated at 140 milliamperes for the plates and screens. All the tubes are self biased.

The amplitude equalization is accomplished by having adjustable shunt peaked compensation circuits act as variable plate loads. There are two such circuits, one preceding and one following the phase correction sections of the equalizer. One consists of a single coil shunted with a variable resistance. This circuit provides high frequency peaking at about 7 megacycles depending upon the value of the coil inductance. The other amplitude correction circuit consists of three coils any one of which may be connected across a variable resistance. The

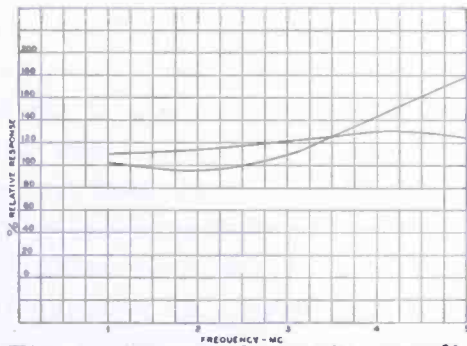


Fig. 2—Measured relative amplitude response of equalizer for two different settings of peaking controls.

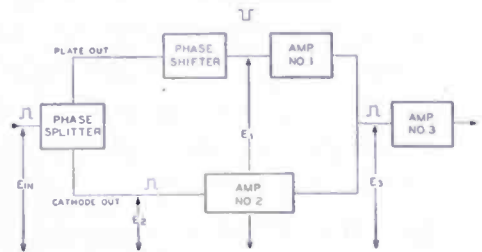


Fig. 3—Block diagram of phase compensating network.

three coils produce maximum peaking at approximately 4, 2.5, and 1.5 megacycles respectively. The maximum peaking ratio is in the order of 2 or 3 to 1. Figure 2 shows the measured amplitude peaking response curves for two different settings of the variable resistance across one of the coils.

The operation of the phase correcting portions of the equalizer may best be understood by referring to Figure 3. The signal  $E_{IN}$  to be corrected is fed to the grid of the phase splitting tube. The plate output of the phase splitter  $E_1$  is fed to Amplifier #1. A phase shifting network is included in the plate circuit of the phase splitting tube. The cathode output of the phase splitter  $E_2$  is fed to Amplifier #2. The output of amplifiers #1 and #2 are added vectorially in the grid circuit of amplifier #3. The voltage  $E_3$  applied to the grid of amplifier #3 is the vector sum of  $E_1$  and  $E_2$ .

It is possible to produce different degrees and types of phase shift by shunting the plate load resistor of the phase splitting tube with different variable reactances. In the schematic, Figure 4, there are shown two specific cases, one of which is a capacity across the load resistance, the other of which is a capacity in series with an inductance, the combination of which is across the load resistance. These two combinations permit the introduction of either leading or lagging phase throughout a limited range of frequencies.

Figure 5 shows the measured overall relative time delay characteristic of the unit for several typical settings of the phase knobs. Curve A is for resistance and capacitance only in the plate circuit of the phase splitter. Curves B, C, D, and E are for combinations of resistance, capacitance and inductance in the plate of the phase splitter.

Figure 6 shows the effect produced on a square wave by various values of inductance in the first "peaker" circuit. Likewise Figure 7 shows the effect on similar square waves of the second "peaker" circuit. It is obvious that the several coils operate throughout different frequency ranges. The purpose of these two compensating stages is, of course, to correct mainly for certain amplitude deficiencies in the incoming signal. As might be expected the rate of rise of the wave front is in general improved. Since the original signal used for test was not particularly deficient amplitudewise the effect produced on the signals exhibits itself as an overpeaking or an overshoot on the leading edge. This effect is characteristic of a high boost. By selecting the proper coil or combination of coils and an optimum amount of resistance across them it is possible to produce a large family of amplitude response curves. If the exact curve which is needed to compensate any given system is known, it is generally possible to design a two terminal network which could be inserted in place of the coil and resistor combination to serve as the plate load of one or both of the peaker stages in order to obtain the correct amplitude equalization.<sup>7, 8</sup>

#### OPERATION

Figure 8 shows the effect of varying the capacity across the load resistor of one of the phase shifting sections. The general effect of an RC combination in the plate of the phase shifting tube is to produce an overall phase angle versus frequency curve which is concave toward the frequency axis. The slope of such a curve decreases with

<sup>7</sup> T. E. Shea, TRANSMISSION NETWORKS AND WAVE FILTERS, D. Van Nostrand Company, Inc., New York, N. Y., 1929.

<sup>8</sup> K. S. Johnson, TRANSMISSION CIRCUITS FOR TELEPHONIC COMMUNICATION, D. Van Nostrand Company, Inc., New York, N. Y., 1925.

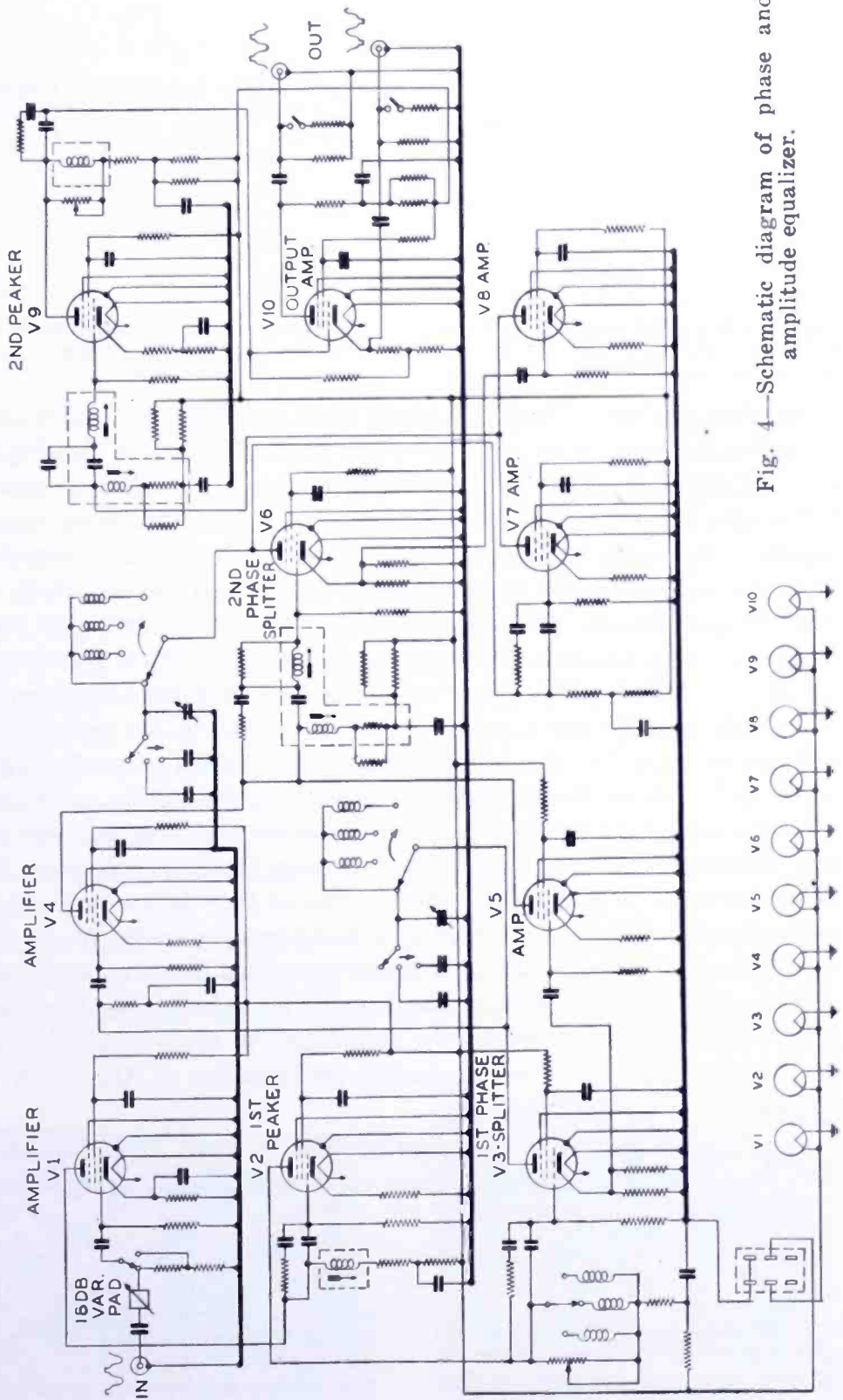


Fig. 4—Schematic diagram of phase and amplitude equalizer.

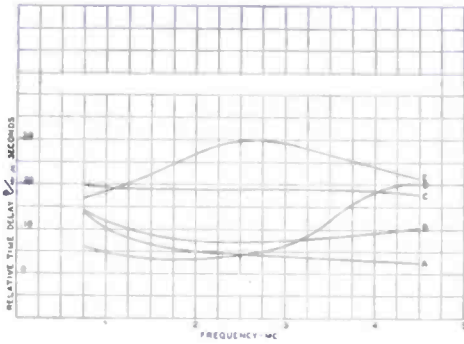


Fig. 5—Measured relative time delay characteristic obtained with various settings of phase controls.

increasing frequency. This has the effect of producing an anticipatory or leading transient as shown. By judicious juggling of the capacitance and resistance it is often possible to neutralize reasonably well a following transient or overshoot on the wave front. Practically speaking the use of such a phase section enables one to partially neutralize the following transient characteristic of an "overpeaked" chain of television equipment. In making the final overall adjustments on a chain of television gear it has generally been accepted practice to adjust the "high peaker" stage until either the following transient is objectionable or the noise level has been increased to the point where it becomes too noticeable. The peaking control is then reduced slightly to the point where the following transient and noise are acceptable. If, in the adjustment of such a chain, the noise level has not been the determining factor but rather the following transient has been the main limitation it is possible with the use of this device to partially neutralize the following transient, in some cases actually see it disappear from the right side of a transition from black to white and appear on the left side of the transition as an anticipatory transient. It is then possible to "repeak" the circuit and in many cases snap up the pictures and improve the overall performance of the chain of equipment.

In Figure 9 is shown the effect produced on the square wave of the various inductances in the phase section when they are added in

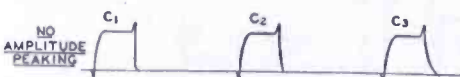


Fig. 8—Effects produced on a square wave by the introduction of various values of capacity in the phase shifting sections.

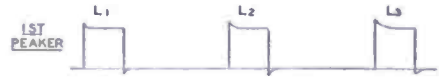


Fig. 6—Effect produced on a square wave with the peaker potentiometer open for various values of inductance (first peaker).



Fig. 7—Effect on a Square Wave with the peaker potentiometer open (second peaker).



Fig. 9—Effects produced on a square wave by the introduction of various values of inductance in series with a small fixed capacity in the phase shifting sections.



Fig. 10—Effects produced on a square wave by the introduction of various values of inductance in series with additional capacity in the phase shifting sections.

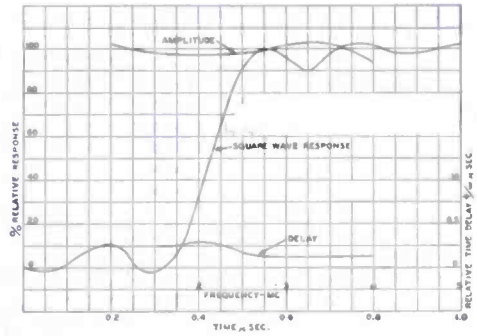


Fig. 11—Measured characteristics of equalized picture transmitter vestigial side band filter and WM-12A Monitor.

series with a small amount of capacitance. Figure 10 shows the effects produced on a square wave of the same coils in series with a larger capacitance. When the  $L$  and  $C$  are properly chosen it is possible to produce an overall phase versus frequency curve which is convex away from the frequency axis throughout a limited range of frequencies. For this range of frequencies the slope of the phase curve increases with frequency. This has the effect of producing an overshoot on the wave front or following transient similar in some respects to that produced as a result of overpeaking. Practically, such an adjustment of the phase equalizer has been used to advantage to partially compensate for or minimize the leading or anticipatory transient introduced by the side band filter at the transmitter.

In Figure 11 the overall amplitude, relative time delay and transient characteristics of a typical television transmitter after equalizations are shown.

When using the equalizer with the  $LC$  combination in the circuit as mentioned before the slope of the phase curve increases with increasing frequency only throughout a given range of frequencies.

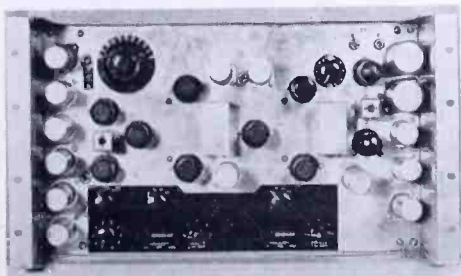


Fig. 12—Phase and amplitude equalizer (front view).

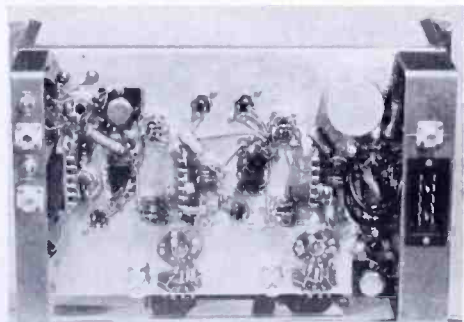


Fig. 13—Phase and amplitude equalizer (rear view).

Thereafter the slope reverses and starts to decrease with increasing frequency. The effect on a square wave then may be to produce, as in Figure 10, both leading and following overshoots. Generally speaking it has been found desirable to avoid this condition.

### CONCLUSION

This type of equalizer has been successfully used at Station WNBT for over a year. Other similar units have been fabricated and used in conjunction with a new system of high speed communication called Ultrafax,<sup>9</sup> the kinescope recording of television images on film,<sup>10</sup> and outside plant shows originating in the field or out of town where noticeable deterioration of picture quality had taken place during transmission. In many cases a noticeable improvement in overall picture quality resulted from the use of the equalizer.

### ACKNOWLEDGMENTS

Credit should be given the Television Operating Group of Station WNBT, and especially to T. J. Buzalski, for the excellent cooperation rendered during testing of the device, and to RCA Laboratories Division, in particular to G. L. Fredendall, for assistance in making the overall phase delay measurements.

<sup>9</sup> D. S. Bond and V. J. Duke, "Ultrafax," pp. 99-115 of this issue.

<sup>10</sup> R. M. Fraser, "Motion Picture Photography of Television Images," *RCA Review*, Vol. IX, No. 2, pp. 202-217, June, 1948.

# DEVELOPMENT OF A LARGE METAL KINESCOPE FOR TELEVISION\*

BY

H. P. STEIER, J. KELAR, C. T. LATTIMER AND R. D. FAULKNER

Tube Department, RCA Victor Division,  
Lancaster, Pa.

*Summary*—In recognition of the desirability of providing larger directly viewed television pictures at reasonable cost, a 16-inch metal kinescope has been developed. This tube provides a picture size intermediate between that obtained from the popular 10-inch kinescope and the large screen of projection television systems.

The envelope of this tube consists of a truncated metal cone. To the large end of the cone is fused a relatively flat glass face plate; to the smaller end, a tubular glass neck section containing the electron gun. The metal cone is made of a high-chromium iron alloy chosen for its excellent characteristics for sealing to high-quality inexpensive sheet glass. The shape of the cone was chosen after consideration of methods of tube fabrication adaptable to mass production and determination of strength requirements of the finished tube. Unique features of the tube are the large-area vacuum-tight seal between face plate and metal cone, and the stress system which permits the use of a relatively thin face plate of uniform curvature.

In order to fit into a wide range of applications, the tube was designed to operate either with a lower-cost power supply such as used in present 10-inch receivers, or at much higher voltages. Elimination of ion-spot blemishes is assured through the use of an ion trap in the electron gun. The ion-trap system employed separates a stream of mixed ions and electrons by means of a combined electrostatic tilted-lens and external magnetic fields.

## INTRODUCTION

IN January, 1948, the development of a 16-inch directly-viewed metal kinescope was announced to television receiver manufacturers. This tube, the 16AP4, is the first metal kinescope ever developed and is the outgrowth of 13 years of research, development, and production in metal receiving tubes.

The 16-inch metal kinescope adds a very significant milestone in the quest for larger and brighter television pictures at reasonable cost in the home. Development of the metal-cone kinescope marks a distinct cleavage with past practice in the manufacture of large television picture tubes. In fact, the metal construction of the 16AP4 is the factor which makes volume production of large directly-viewed kinescopes practical. The  $10 \times 13\frac{1}{3}$ -inch picture obtained with this tube

\* Decimal Classification: R138.31×R331.

bridges the gap, both in entertainment value and cost, between the now popular 6 × 8-inch picture of the 10-inch kinescope and the 15 × 20-inch picture provided by home projection receivers. The picture size afforded by the 16AP4 answers the popular demand for larger pictures at a lower cost than is possible with all-glass construction for a directly-viewed tube with the same screen size.

A cathode-ray tube for television consists of three fundamental parts: an electron gun, a fluorescent viewing screen, an an elongated envelope which contains the electron gun and fluorescent screen and through which the electrons are directed. As the picture size requirement increases so does the size of the tube envelope, and with that increase the advantages of the metal construction become increasingly evident.

This paper describes the design and construction problems encountered in the development of the new 16-inch low-cost kinescope for mass production. The discussion covers highlights of the metal kinescope design and structural requirements, the method used for sealing glass to metal, application of the screen materials and tube coatings, details of the ion-trap electron gun, and general electrical and physical characteristics of the tube.

#### REQUIREMENTS OF LARGE-SIZE KINESCOPE

In the development of the 16AP4, it was recognized first that to make a large-size picture available to a sizable portion of the television public, the kinescope to do the job must be designed for mass production and low cost. A design suitable for high-speed production by automatic machinery is inherently low in cost. A design with electrical requirements within the range of inexpensive high-voltage and deflection power supplies makes for lower-cost television receivers. A design having minimum volume and weight for a given picture size lowers cabinet cost which is important because of the critical relationship of cost to cabinet size. In addition, a kinescope must have a face of good optical quality and little curvature to provide high-quality pictures on an essentially flat viewing screen.

The 16AP4 metal kinescope meets these important criteria of low-cost design and quality quite effectively.

#### SELECTION OF ENVELOPE MATERIAL

The reasons for the selection of metal as a material for a cathode-ray tube envelope are lower cost, plentiful supply of raw materials,

ease of control of the dimensions of the fabricated part, durability, and adaptability of the tube assembly to mass production.

The cost of an all-glass envelope to obtain a picture size equivalent to that of the 16AP4 is, from all present indications, considerably greater than the cost of the metal and glass assembly used for this new tube. The formation of large masses of glass into the shape now common to kinescopes involves techniques which are inherently expensive. The art of heating and forming, and annealing and cooling heavy masses of glass is highly specialized. The extent of the art and science of metal working, on the other hand, is so vast that the supply and control of metal components gives the user the ability to make rapid changes at low cost. Glass as a raw material is not expensive compared to the high-quality chrome-iron alloy used for the metal cone of the 16AP4, but here the advantage ends. Large all-glass tube designs suffer in flexibility, because each minor change in shape or dimension often necessitates extensive developmental work and major tooling expense.

The manufacture of large glass products with accurate dimensions is very difficult. Tolerances of  $\pm 0.030$  inch or less are considered expensive in glass kinescope bulbs, while in metal forms of the shape used in this tube, tolerances of  $\pm 0.010$  inch are easy to maintain. Mass production of tube assemblies by high-speed automatic equipment requires close dimensional control if a high-quality product is to be assured.

The foregoing comparisons between glass and metal kinescopes are, of course, based on present conditions. They are not meant to imply that progress in glass has stopped. Indeed, when one considers the vast progress that has been made in the fabrication of large glass envelopes since the end of the war, the very considerable force of skilled technicians who are currently attacking the problems, and the competitive threat of the metal envelope, it is to be expected that additional improvements will be made. However, the art of using metal in kinescope envelopes is relatively new and, like all new techniques, is subject to rapid improvement. In certain respects, notably in weight, accuracy of dimensions, strength, and relative ease of manufacture it appears to have inherent advantages.

#### ESSENTIALS OF METAL-CONE KINESCOPE

The basic construction of a kinescope consists of a circular, nearly flat, glass plate on which is formed the picture image, and a conical body to the large end of which is attached the viewing screen and to

the small end a cylindrical neck containing the electron gun. The gun, cone, and screen have coaxial symmetry.

Associated with the tubes of this type are external magnetic, electron-beam-deflecting and focusing coils and ion-trap magnets. Because a minimum of magnetic shielding is desired between these external magnetic fields and the electron beam, glass serves best as the neck material. Also, there must be sufficient electrical insulation between the external magnetic coils and the high-voltage anode area of the metal cone.

As can be seen in the cross section of the tube given in Figure 1, the metal tube consists of a truncated metal cone to the large end of which is fused a relatively thin, nearly flat face plate, and to the smaller end of which is fused a glass flared neck section containing the

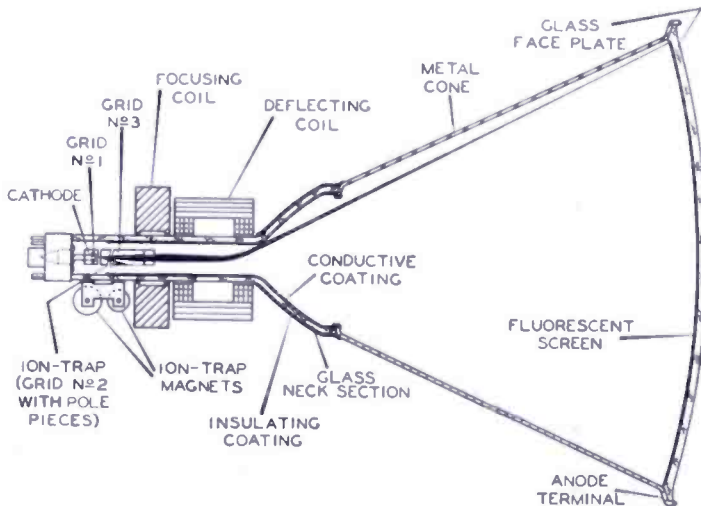


Fig. 1—Cross section of metal kinescope 16AP4.

electron gun at its lower end. The flared section provides electrical insulation between the deflecting coils which operate at ground potential and the exposed metal cone surface which operates at high potential.

### SELECTION OF METAL FOR CONE

In the selection of a metal for use in the cone portion of the tube the primary concern is with its glass-sealing properties. The major properties required of a good glass-sealing alloy are:

1. The coefficient of expansion of the metal must match that of the glass.
2. The metal oxide formed in heating the metal must be soluble in glass.
3. The metal oxide must have excellent adherence to the base metal.

4. The metal shall not be readily over-oxidized to form a thick porous oxide.

Of all the glass-sealing alloys available, those including chromium in their composition have the above properties to the largest degree. The investigation of metal suitable for the cones was, therefore, limited to the chromium-bearing alloys.

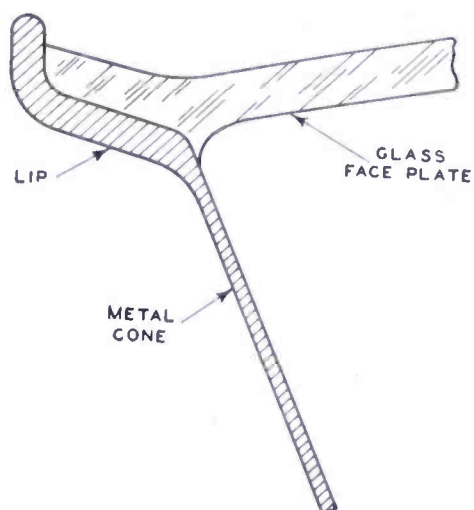
Additional requirements imposed on the metal by the use for which it is intended are that it have a high tensile strength, both at room temperature and at tube baking temperatures, that it have good corrosion resistance, and that it be vacuum tight.

The metal chosen after considerable experimentation was a modification of a commercially available high-chromium alloy — S.A.E. Type 446. Fortunately, it has most of the desired properties although it is difficult to form.

#### METAL-CONE DESIGN CONSIDERATIONS

In addition to the selection of a suitable metal, design of the metal cone involved a mathematical analysis of the mechanical stresses. As was anticipated, the critical point in the structure was found to be the junction between the glass face plate and the metal cone.

Atmospheric pressure on a face plate 16 inches in diameter exerts a total force of about  $1\frac{1}{2}$  tons. For safety purposes, however, the 16-inch kinescope was designed to withstand a minimum of three atmospheres or 4.5 tons. In an all-glass bulb the loading created by the atmospheric pressure is supported by a relatively heavy wall near the maximum diameter of the bulb. In the case of the metal cone this support is achieved by building up the face-plate-sealing surface of the cone in the shape of a truncated rim-cone supported at one end by a cylindrical rim and at the other end by the main cone. Figure 2 gives a cross section of the face sealing area. The rim of the cone is shaped to afford maximum resistance to tangential tension forces applied to it by the face plate. This rim shape was designed during the early stages of development of the metal kinescope by Tube Department engineers in 1937 and has proved to be the most practical solution to the problem of providing sufficient strength at the tube face periphery where the forces of atmospheric pressure on the slightly curved face plate are concentrated. Figure 3 is a picture of the device used to measure mechanical deformation of the sealing rim during the experimental work on the tube. In making these measurements the tube was gradually evacuated and deformations of the rim and face were measured by the gauges shown in the picture.



The conical shape was chosen for the metal cone to keep the volume as small as possible. The cone is fabricated by a spinning process, and, as is shown in Figure 2, the main cone wall thickness is thinner than the sealing surface. The extra strength is not needed in the side wall and so it is made proportionately thinner.

Fig. 2—Cross section of cone rim.

#### SELECTION OF FACE-PLATE MATERIAL

Most kinescopes, at the present time, have faces made by pressing molten glass in an iron mold. Face plates made by this method are characterized by roughness, light scattering, and visible foreign particles which cause noticeable reduction in picture quality. Improving the face plate quality without incurring additional cost was accomplished in the 16AP4 by selecting high-quality window glass for the face plate.

In a kinescope, some face curvature is made necessary by the fact that to support atmospheric pressures, an evacuated envelope must be curved or have an excessively thick wall. The glass face of even a 10-inch kinescope is subject to a total force of about 1200 pounds. As the glass kinescope becomes larger, the force on it becomes greater and the face, therefore, must be relatively thicker. With increasing

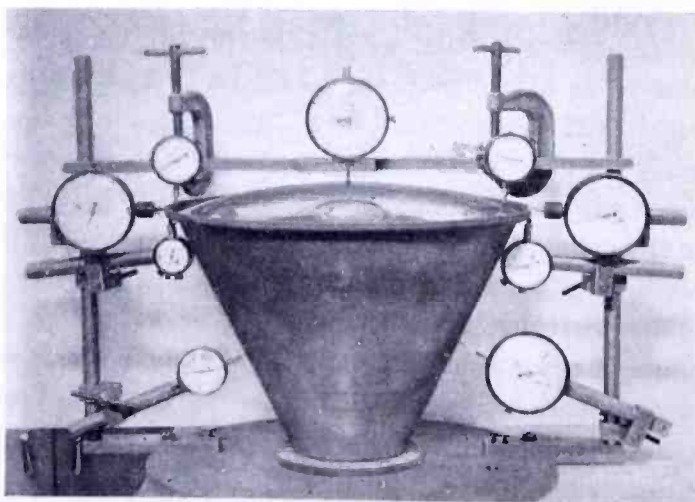


Fig. 3—Pressure deformation test equipment.

thickness, of course, the problem of achieving good optical quality becomes greater. The 16-inch metal kinescope was designed to have high strength in the metal rim so that the face plate can be relatively thin and nearly flat. The face plate is only  $3/16$  inch thick and has a radius of curvature of about 27 inches. With glass of this thickness good optical quality is easily obtained.

An examination of the expansion curves of all the available brands of window and plate glass manufactured in the United States showed that they all had practically identical expansion curves. To check the expansion, however, samples of every brand of window glass that could be located were purchased and seals made. One of these glasses showed a substantial reduction in seal strain, being about one-half that of the other samples tested. This glass had a lower *setting* point which made the over-all expansion difference between the metal and glass lower. Because the glass was lower in expansion than the metal, the metal would contract more than the glass when cooling from the annealing point, and thereby would put the glass into compression. Since glass is very strong in compression it was decided to develop face plates of this glass. The initial seals proved disappointing because little was known of the sealing and annealing techniques necessary for the new glass-to-metal seal. As more experience was gained, however, a practical method was evolved which permitted control of the stress distribution in the face plate, so that finally both tangential and radial compression was obtained. The resulting assembly is considerably stronger than an all-glass envelope of comparable size.

The face plate used in this tube is made by either pressing or sagging window glass. It takes the form of a section of a sphere 27 inches in radius. This curvature was adopted as a compromise between cost, strength, and flatness after face plates of various radii of curvature were tested. The face-plate radius of curvature is uniform from center to edge. In an all-glass construction the face radius of curvature usually becomes smaller near the rim of the tube in the region where the television picture corners are located.

#### GLASS-NECK CONSIDERATIONS

The glass neck section for this tube requires a glass which matches the expansion characteristic of the chrome-iron cone, has softening and annealing temperature properties which permit its use and processing with the glass chosen for the face plate, and has expansion properties suitable for sealing to the stem glass containing the electrode connector leads. In addition, high electrical resistance between the

outside and inside of the neck is required. Lead glass, #0120 meets these qualifications fairly well and was adopted for use. As stated previously, insulation between the deflecting yoke coils and the metal cone is necessary. This requirement was met by the flared design of the lower portion of the glass cone as shown in Figure 1. The feasibility of manufacturing the lower cone by a pressing operation on high-production equipment reduced the cost of the part.

A butt seal between the lower glass cone and the metal lip at the small end of the metal cone was needed so that the operation of sealing the two parts could be performed on automatic machinery. The butt seals have been quite successful and a very clean sealing operation results between the two parts, although the expansion properties of #0120 glass are not matched to the chrome-iron of the cone as advantageously as are those of the face-plate glass. By a selective system of strain distribution through parts design and a proper annealing and cooling cycle, the correct structural strength is obtained.

#### GLASS-TO-METAL SEALING

Until now the discussion has been limited to the design and economy of components. The processing costs, however, as reflected in processing speeds are just as important to low-cost design.

The processing of bulbs in the manufacture of kinescopes involves heating, annealing, and cooling of the tube envelope. The time required for these three processes is approximately dependent upon the square of the glass thickness. Any reduction of glass thickness, therefore, permits reduction of processing time. Because the glass required for the 16AP4 is  $\frac{1}{4}$  to  $\frac{1}{3}$  the thickness used in an all-glass construction, a large reduction in processing time is possible.

As previously mentioned, the "sealing" of glass and metal parts depends, in general, upon the ability of glass in the molten state to partially dissolve strongly adherent metallic oxides, thus forming a mechanically strong bond between the glass and metal. The sealing process, therefore, consists of oxidizing the metal and then melting the glass in contact with the metal and holding it in the molten state until the bond is formed. The process used for sealing the glass face plate and the metal cone consists of placing the face plate and cone on the sealing machine, rotating the assembly, and heating it uniformly until it is close to the annealing point (temperature at which glass is fluid enough to allow stress relief without deforming) of the glass. At this time, the sealing heat is applied to the sealing area so that the glass in contact with metal is melted and the seal formed. Air

pressure is used inside the cone during this operation to hold the face plate in position and to work and form the seal. The shape of the seal is important, because a smooth contour eliminates points of high stress concentration in the seal area. Such stresses weaken the glass and may cause glass breakage. At the completion of the sealing operation, the bulb is transferred to an oven maintained near the annealing temperature of the glass and allowed to temperature-equalize. It is at this point that the most radical change in processing has been made. Normally, when glass is cooled from its annealing point, it is necessary to lower the temperature of the glass very slowly to avoid excessive strains. In the case of the metal kinescope, it was found that this slow cooling is not necessary and that the bulb can be removed from the oven at a temperature near the annealing temperature and then allowed to cool in air at room temperature. This operation is possible because cooling and shrinking of the metal places the glass in both tangential and radial compression to limit the formation of tensile stress.

Prior to the face-plate sealing operation, the neck assembly is sealed on by conventional glass-to-metal sealing methods and then flame annealed.

#### BULB STRENGTH TESTS

The mechanical strength of the bulb is extremely important. After the sealing operation, the cone-face plate-neck assembly should be able to withstand air pressure of 60 pounds per square inch, or pressure one atmosphere greater than specified for the finished tube. This extra strength is necessary to allow for any additional strain that might be caused during processing.

Figure 4 is a picture of a pressure-test failure which occurred at a higher-than-normal test pressure. Radial cracks indicate that the sealing lip was expanded under pressure, placing the glass in tangential tension.

In addition to the standard pressure test, other tests have been made to test the strength of the metal bulb. One of these was a thermal shock test in which the face end of the bulb was taken from boiling water and plunged into liquid air, allowed to temperature-equalize, and then transferred back to the boiling water. No breakage of the glass



Fig. 4—Pressure test failure.

occurred. Other tests have been made on the effects of deformation or impact *while the bulb is under vacuum*. It is interesting to note that the failure of a glass bulb under similar conditions is usually accompanied by an implosion which shatters the entire bulb. To date, all test failures of metal kinescopes have shown the typical radial crack pattern shown in Figure 4. The face plate is held together by compression until the vacuum is relieved. At worst, a portion of the face plate may then fall in and bounce out, but with insufficient force to cause appreciable damage. Failure of an all-glass bulb face is accompanied by a failure of the glass rim inward toward the bulb center where the glass meets and is again broken into smaller particles by the impact.

### SCREEN APPLICATION

The phosphor employed in the screen of the 16AP4 is a mixture of blue-emitting zinc sulphide and yellow-emitting zinc cadmium sulphide. This combination, when properly manufactured, blended, and applied to the kinescope face plate, is a very efficient emitter of white light.

A most important preliminary step in the application of screens to the 16AP4 consists of a thorough cleaning of the interior of the bulb assembly. The slightest trace of dirt or grease would prevent the phosphor particles from adhering properly to the face plate. Handling marks such as fingerprints and etched areas on the face plate, would harm the appearance of the screen and the resulting picture. The presence of traces of certain metallic impurities, for example iron, cobalt, or nickel, can "poison" or decrease the efficiency of the phosphor. It is interesting to note that the limits of most chemical purification processes coincide with the order of magnitude of activator usually necessary to produce efficient phosphors, and with the magnitude of a poisoning element detrimental to phosphors. The magnitude of the activator is in the range of one thousand to one hundred million parts of phosphor to one part of activator or impurity.

The cleaning of the metal kinescope bulb is more difficult than that of a glass bulb because of the matte surface of the metal. In addition, the large areas of metallic oxide formed by the heat of the glass-sealing fires and the attendant possibility of scaling add to the problem. The cleaning process consists of flushing with solutions of sodium hydroxide and hydrofluoric acid, and rinsing thoroughly with tap and distilled water. Vigorous agitation is required to remove small flakes of metallic oxide hanging loosely from the metal. The washing is done by automatic machinery.

The screen is applied to the 16AP4 bulb by settling the phosphor from a suspension of double-distilled water and phosphor containing a suitable binder to promote adherence of the phosphor particles to the glass face plate. A "cushion" layer containing a dilute potassium silicate solution is poured into the bulb assembly and the suspension of screen material evenly distributed over the surface of the cushion layer.

In manufacture, the screens are applied to the bulb assemblies on a continuously moving belt, similar to that developed for the 10-inch television tubes. The bulbs are loaded into pockets on one end of the belt, face plate downward, and settling solutions introduced. All operations are conducted while the belt is advancing at the rate of a few inches per minute. By the time the bulb assembly has reached the opposite end of the belt, the screen has settled to the face plate, and the settling suspension is decanted as the belt moves around a large pulley at the end of the belt. When the neck end of the assembly is inverted and all the settling suspension drained off, the glass neck is cleaned with a dilute solution of hydrofluoric acid to remove the remaining silicate. As the bulb assembly moves along the underside of the belt, the screen is dried and the assembly is then removed by the same operator who loaded it.

Each screen is inspected by transmitted and reflected light, and with ultraviolet radiation before the tube is completed so that no defects such as spots, holes, or colored areas are present which can be detected by the eye at normal viewing distance.

#### COATING APPLICATION AND TUBE ASSEMBLY

A graphite conductive coating is applied to the inside of the glass neck section from the flared end down to just beyond the middle of the tubular section. This coating, shown in Figure 1, connects with the metal cone and is the conductor which maintains the inside of the glass neck section at the same potential as the metal cone. The screen and the conductive coating are baked to insure their adherence to the glass surfaces.

The electron gun is sealed into the bulb assembly and the tube is then exhausted by a straight-line exhaust machine initially developed for the 10-inch kinescope. The base is cemented to the tube neck. The cathode is aged to stabilize emission and the tube is then tested. Finally, the large sealing rim is wire-brushed to remove oxides in order to insure a good electrical connection for the anode high voltage.

Externally, the tube receives three different coats of paint. One is a conducting paint applied to the metal rim used as the anode con-

necter, the second is applied to the main cone as a decorative finish, and the third is an insulating paint applied to the flared part of the glass neck section. This coating prevents electrical leakage between the anode and the deflecting coils under conditions of high humidity.

### ION-SPOT PROBLEM

The electron gun of the 16AP4, although it uses conventional assembly methods and parts, has some novel features worthy of discussion in detail. One of these features is the tilted-lens ion trap.<sup>1</sup> This particular type of ion trap is a post-war development and was first used in the television kinescope type 10BP4. The ion-spot problem, which was so common in earlier television tubes, will be reviewed briefly and the operation of the ion trap explained.

An ion spot is a dark discoloration which may appear on the screen of a cathode-ray tube using magnetic deflection after operating for, in some cases, only a few hours and in others, a few hundred hours. The discoloration often increases in intensity and becomes darker as the tube is operated. The spot is the result of deterioration or fatigue of the screen phosphor in the area bombarded by the relatively heavy negative ions in the beam. In 1935, Freisenwinkel<sup>2</sup> and Von Ardenne<sup>3</sup> reported the presence of negative ions in the cathode-ray tube and discussed the effect of these ions on the screen. A number of methods have been proposed since then to prevent screen bombardment by negative ions. The problem can be approached in several ways. The most obvious method would be to prevent the formation of negative ions in the tube. If it were possible to evacuate the tube so that all residual gas were removed, positive ions, which are generally formed by direct electron collisions with gas molecules in the space, would not be formed along the path of the beam. The residual gas in the space, however, is not always the major source of ions. During the normal operation, the cathode as well as other parts in the tube are heated and some gases and ions are continuously emitted. H. Schaefer and W. Walcher<sup>4</sup> indicate that the negative ions originate at the thermionic cathode largely as a result of positive ion bombardment and possibly as a result of direct emission. Exhaust methods alone, therefore, cannot be considered as a means of eliminating ion spot formation but serve merely

<sup>1</sup> J. Kelar—U. S. and Foreign Patents Applied For.

<sup>2</sup> Freisenwinkel—*Archiv für Elektrotechnik*, Vol. 29, 1935, p. 272.

<sup>3</sup> Von Ardenne—*Archiv für Elektrotechnik*, Vol. 29, 1935, p. 731.

(Translation in *Television and Short Wave World*, Nov., 1936, p. 626.)

<sup>4</sup> H. Schaefer and W. Walcher—*Zeitschrift für Physik*, Vol. 121, pp. 679-701, 1943.

to delay this formation. Another approach is to use a screen phosphor which can withstand ion bombardment without damage. However, such phosphors capable of fluorescing in the proper colors and with reasonable efficiency are, at present, not available.

Ever since the effect of ions on the screen was recognized, attempts have been made to prevent them from reaching the screen. Such attempts have usually been concerned with removal of negative ions from the beam. The fundamental principle of separating streams of particles of different mass by passing the mixed beam through a magnetic field is well known and has been used for a long time in the mass spectrophotograph to obtain an ion spectrum. It was used by Strigel<sup>5</sup> to separate positive ions from mixed beams of electrons and ions.

Because, in an electrostatic field, deflection of a beam of particles is independent of the mass of the particle and, in a magnetic field, is not, a method is available by which the electrons can be extracted from a mixed beam of electrons and relatively heavy ions. A number of designs have been proposed which use electrostatic and magnetic fields separately or in combination to separate electrons and ions.<sup>6</sup> In television tube applications, it is desired to use the electron beam but to discard the ions. The device used to separate and discard the ions is called an ion trap.

#### TILTED-LENS ION TRAP

Most ion traps proposed in the past have used combinations of non-symmetrical gun structures, bent necks, and extra electrostatic deflecting electrodes which required additional connections for the application of voltages. Such designs were complicated and, therefore, added to the cost of the tube. Because of the need for a simple but dependable ion trap, a development program was undertaken which resulted in the tilted-lens ion trap used with the 16AP4. This design has been tested on many thousands of 10-inch tubes and has proved highly satisfactory. The principal feature of this method is the electron gun which has a tilted electron lens formed by cutting the adjacent ends of grid No. 2 and grid No. 3 at a slight angle to the plane normal to the gun axis. The arrangement is shown in Figure 5. The tilted lens deflects the mixed beam of electrons and ions away from the axis of the electron gun. In order to return the electron stream toward the axis of the gun a magnetic field of proper direction and strength is positioned in the

<sup>5</sup> Strigel—U. S. Patent 1,911,976.

<sup>6</sup> Branson—U. S. Patent 2,274,386. Bowie—U. S. Patent 2,211,613/4 and others.

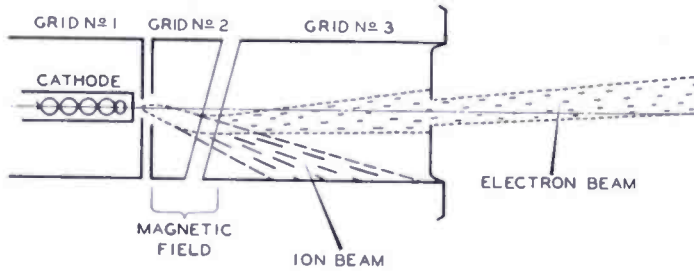


Fig. 5—Single-magnet ion-trap system.

vicinity of the bend. Because it is difficult to obtain a magnetic field which will, at all points along the axis, exactly neutralize the effect of the electrostatic field, the electron beam does not quite succeed in returning to the axis of the gun but can only approach or cross it. Operation of the tube with the beam off the neck axis is undesirable because it usually leads to spot distortion and requires additional centering current. A better solution was needed before the development could be considered complete.

The eventual solution was to use a second magnetic field on the ion-trap magnet. The first magnetic field was located as in Figure 5 but its strength was adjusted to cause the beam to cross the axis within the gun. The second field was of opposite polarity and of lower strength. It was located at the point where the beam crossed the axis and served to align the beam to coincide with the gun axis. Figure 6 shows the approximate path of the beam when the double magnetic field is used. It is obvious that, theoretically at least, both fields should be independently adjustable for each operating voltage on grid No. 2 and grid No. 3. In practice, however, the ratio of the two field strengths is fixed at the time of installation of the magnet assembly on the receiver, and by slight adjustment of position with respect to the gun a satisfactory adjustment is obtained. Various designs of ion trap magnets have been announced commercially ranging from double electromagnets to various permanent-magnet designs. The ion trap is a positive method of eliminating ion spots and is independent of gas pressures over a very wide range.

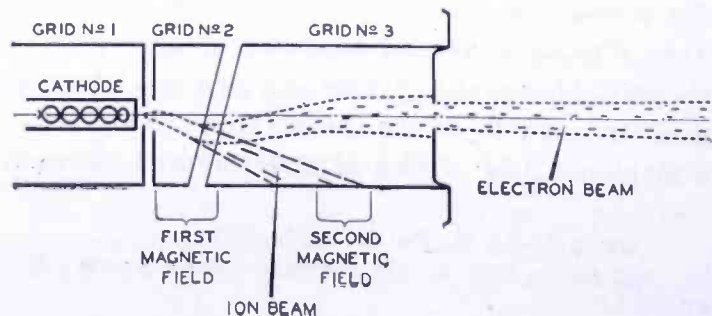


Fig. 6—Double-magnet ion-trap system.

The gun for the 16AP4 was designed for magnetic focus and deflection, and incorporates the tilted-lens ion-trap system. The gun is a tetrode type having a heater, thermionic cathode, and three grids. Magnetic pole pieces attached to grid No. 2 form part of the tilted-lens system of the ion trap.

Figure 6 shows the gun system and how the external ion-trap magnets and tilted-lens system affect the electron beam and ion stream. The limiting aperture in grid No. 3 serves to mask off the edges of the electron beam including most secondary electrons which may arise from collision with parts of the gun near the cathode. This action of the limiting aperture serves to produce a well-formed spot with clean edges and improves detail resolution. Although not shown in Figure 6, the edge of grid No. 2 in practice is rounded in the manner of a corona shield. This construction has been found necessary to reduce cold-emission of electrons from grid No. 2 to grid No. 3. Such emission is caused by the high potential difference, amounting to nearly the full anode voltage, between these two electrodes. Grid No. 3 is connected to the metal cone by the internal conductive coating on the flared glass section. As noted previously, this coating is carried up to the metal envelope. Contact to the coating is made by means of spring contacts on grid No. 3. Figure 1 shows that the limiting aperture in grid No. 3 is placed not at the end but inside the grid cylinder. This arrangement prevents extension of the magnetic focus field into the aperture. Such extension would result in interference with the normal path of the electron beam through the aperture depending upon the alignment of the focusing coil on the tube neck.

#### PHYSICAL AND ELECTRICAL CHARACTERISTICS

Many considerations determined the final physical dimensions and electrical characteristics of this tube, but the major aim was to develop a low-cost tube to provide a large picture of high quality and brightness which could be operated from low-cost power supplies. The 16AP4 kinescope as finally developed, and as shown in Figure 7, has a maximum outside diameter of 16 inches, and a length of  $22\frac{1}{4}$  inches. Its shape permits efficient utilization of cabinet volume for component placement. The great strength of the metal lip to which the face plate is sealed provides a most efficient relationship between the outside tube diameter and picture size. In addition, it permits the use of a uniform face curvature right up to the corners of the picture area. Tests of the mechanical strength of this tube, have shown it to be unusually resistant to impact and air pressure.

Because a major portion of the external area of this tube is metal, a large anode contact is available. Provision for positive contact has been provided in the form of a low-resistance area on the outside of the cone lip at the face end of the tube. Over 30 square inches of contact area are available for the anode contact. Either a spring or the weight of the tube may be used to insure good contact between the contact area and a metal connector. For protection against corona, the upper rim lip of the tube is rounded. The 16AP4 weighs about 11 pounds and, thus, compares very favorably in weight with the 10BP4 kinescope which also weighs about 11 pounds.

Fig. 7—Metal Kinescope 16AP4.



The 16AP4 may be operated with an anode voltage ranging from 9 kilovolts to 14 kilovolts which is a wide range for a tube of this size. These voltages may be obtained from low-cost pulse-operated or radio-frequency-operated power supplies. With the chosen deflection angle of 53 degrees, full scanning of the useful screen area is possible without increasing deflection-power requirements over that needed for 10-inch picture tubes operating at the same voltages.

The 16AP4 provides a picture of approximately 130 square inches which is  $2\frac{1}{2}$  times that of a 10-inch tube. Highlight brightness of 60 foot lamberts at an anode voltage of 12 kilovolts provides enough light so that the picture may be viewed under average conditions of ambient light in the home. Picture definition surpasses that required by present-day television practice.

# THE GRAPHECHON — A PICTURE STORAGE TUBE\*

BY

L. PENSAK

Research Department, RCA Laboratories Division,  
Princeton, N. J.

*Summary*—Long time storage of television quality pictures is possible with a new type of storage tube consisting of two independent cathode ray guns and a target plate coated with a thin film of insulating material. A new type of bombardment-induced conduction effect provides high sensitivity and stability. The two guns can operate simultaneously, the one to "write" down any arbitrary pattern to be stored and the other to scan repeatedly over it to both generate signals and erase the pattern at a controlled rate. The tube makes possible television pictures of oscillograms or radar patterns that can be viewed for several minutes.

## INTRODUCTION

THE problem which gave rise to this tube was that of providing a means for electrically storing complete radar plan position indicator (PPI) type patterns and generating from them signals which could provide television pictures of the radar patterns. This problem arose in the Teleran System<sup>1</sup> for airborne navigation. Here it was highly desirable to be able to broadcast a composite television picture of a radar pattern, its associated ground map and other information. The tube that was developed to meet this need proved to have several other interesting applications. However, it seemed preferable to describe it below in terms of its major initial application.

The problem is one of obtaining a means of converting radar signals to television signals without loss of the pattern geometry. This implies storage of the radar signals for at least several seconds because it can take this long to complete one PPI pattern. Also, because television pictures are generated at the rate of thirty per second, it may be necessary to generate several hundred television copies of a radar pattern before it fades out. Such conversion of signals has been obtained by using an image orthicon camera tube with a reflection type optical system to pick up the relatively weak afterglow of a radar cathode ray tube with a P7 or similar fluorescent screen. Much better

\* Decimal Classification: R583.15.

<sup>1</sup> D. H. Ewing and R. W. K. Smith, "Teleran," *RCA Review*, Vol. VII, No. 4, pp. 601-622, December, 1946.

results have been obtained with a special, high capacity orthicon<sup>2</sup> picking up the initial flash of a cathode ray tube without any afterglow, the picture being retained in the capacity of the orthicon photocathode. Both these schemes require a high-brightness cathode-ray tube and an optical system, which are unnecessary in principle because the light is used only as a link between two electrical signals. In order to obtain an all-electronic converting scheme, a new type of tube, called a graphechon, was built. This name is derived from the Greek words "Graphe" (to write) and "echo" (to keep or to hold). The tube can be regarded as a kinescope and iconoscope in one bulb, with the mosaic and kinescope screen replaced by a charge-sensitive, high-capacity, storage target. The kinescope gun will be referred to as the "writing" gun which takes the radar signal and "writes" it on the target. The other gun will be called a "reading" gun. Its function is to generate the television signal and gradually remove the stored signals.

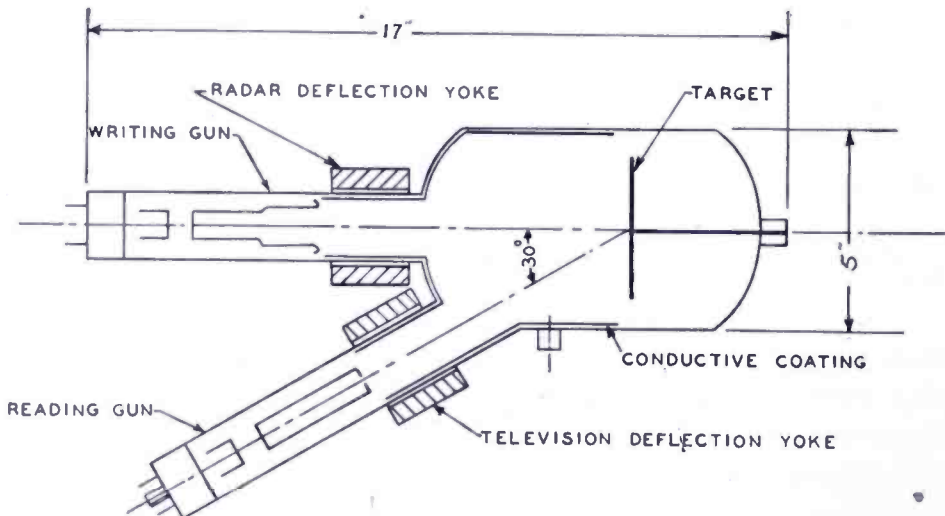


Fig. 1—Single sided target, magnetic deflection Graphechon.

#### CONSTRUCTION OF THE TUBE

The design of the bulb is not critical and is largely determined by the requirements of the cathode ray guns. Figure 1 shows a sketch of one type of tube using magnetic deflection. In order to simplify the circuit requirements, the writing gun is mounted perpendicular to the target, which avoids the necessity for keystone correction for a radial deflection pattern. This correction has been solved very simply for the iconoscope, and so the reading gun is mounted off the axis at the same angle as is used for the standard iconoscope. The dimensions of

<sup>2</sup> Stanley Forgue, "The Storage Orthicon," *RCA Review*, Vol. 8, No. 4, p. 633, December, 1947.

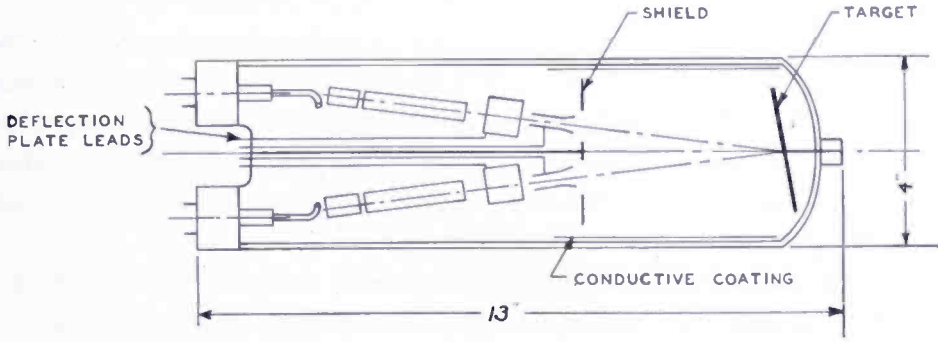


Fig. 2—Single sided target, electrostatic deflection Graphechon.

the bulb are determined by the space requirements of the deflection yokes, by the deflection angles required for obtaining adequate resolution, and by the desired target dimensions.

When preferable, a tube can be built with all-electrostatic focus and deflection. It is more suitable for oscillograph operation or, where weight and size are critical, it permits eliminating the deflection yokes. Figure 2 is a sketch of such a tube which can be made smaller and more compact than the magnetic deflection type, but is necessarily subject to the lower resolution limits imposed by the electrostatic deflection system.

Figure 3 is a sketch of the most recent form of the tube. This modification was built to make possible mounting the guns on a common axis and thereby avoid the need for keystone correction. The target construction was modified to permit the "writing" beam to penetrate through the target as will be described below.

For the magnetic deflection writing gun it is possible to use a standard kinescope gun with either magnetic focus (type 12DP7) or electrostatic focus (type 12AP4). Both types have been used for radar purposes and have adequate resolution at the rated voltages of 6,000 to 10,000 volts, which is also the range of voltage which is used in the Graphechon. The reading gun can be a standard iconoscope gun and runs at standard iconoscope voltages, which is 800 to 1,000 volts.

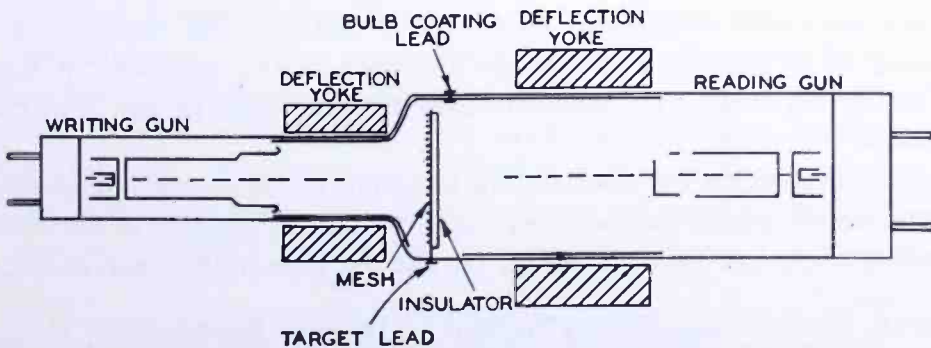


Fig. 3—Double sided target, magnetic deflection Graphechon.

The target consists of a plate of metal upon which is deposited a film of insulating material of the order of 6,000 Angstrom units thick (approximately half a micron). Where the two guns are on the same side, any of a number of metals, thick enough to be self supporting, can be used for the target. The insulator film can be any good insulator like silica or magnesium fluoride, applied by any suitable means, such as evaporation.

In tubes where the guns are on opposite sides of the target, it is necessary to make the metal backing transparent to electrons and yet strong enough to support the insulating layer. This can be done by using very fine mesh with a high transmission factor to provide the mechanical support. Then an organic film is spread over the mesh to act as a base upon which to evaporate a thin layer of aluminum. The insulating layer is then evaporated onto the aluminum and the target is complete. The high voltage "writing" gun is located on the mesh side of the target. The mesh is made fine enough so that it does not limit the resolving power of the tube. Sample targets have employed approximately 500-per-inch mesh.

#### PRINCIPLES OF OPERATION

The reading beam, operating at 1,000 volts, has a secondary emission ratio greater than unity. It scans uniformly over the insulator surface and therefore brings it approximately to the potential of the collector, which is the conductive wall coating. This is true regardless of the potential of the underlying metal. It is therefore possible to adjust the potential drop across the thickness of the insulating film to approximately the difference in potential between the target metal and the wall coating.

It is possible to regard the insulator as the dielectric in a condenser, one of whose plates is the target metal and the other is the surface scanned by the electron beam. As a starting equilibrium condition, the condenser is charged up uniformly over its area. Because the one plate is the insulating surface of the dielectric and does not conduct transversely, it is possible to discharge any part of the condenser without affecting the rest of it. Such discharging can occur in any arbitrary pattern.

The mechanism for discharging the dielectric is a newly discovered phenomenon<sup>3</sup> which can be observed in films thin enough to be wholly penetrated by an electron beam. It can be shown that currents can

---

<sup>3</sup> L. Pensak, "Conductivity Induced by Electron Bombardment in Thin Insulating Film," *Phys. Rev.*, February 1, 1949.

flow through the film which are many times larger than the bombarding beam, that the currents flow in the direction of the gradient, and that the insulation recovers on removal of the beam. Since the penetration of an electron beam increases with the square of the voltage, a film may be chosen of such thickness that, though fully penetrated by a 10,000 volt beam, it is scarcely penetrated at all by a 1,000 volt beam. If the latter, low-velocity, beam is employed to charge up the dielectric, the 10,000 volt beam may be used to discharge it. The second, high-velocity, beam is the "writing" beam which can be deflected and modulated in any arbitrary manner such as for a PPI pattern or an oscillograph trace.

The mechanism for signal generation is a simple form of that in the iconoscope.<sup>4</sup> The target surface is brought to equilibrium potential with the target metal at approximately 50 volts negative. Where the writing beam has struck and driven the surface negative, the second-

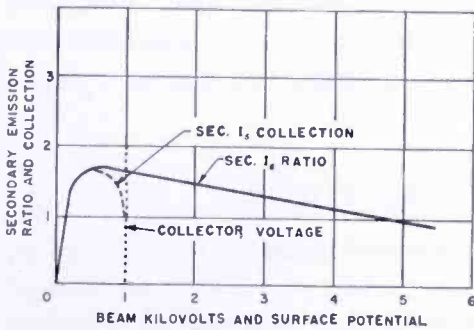


Fig. 4—Typical curve for secondary emission from silica.

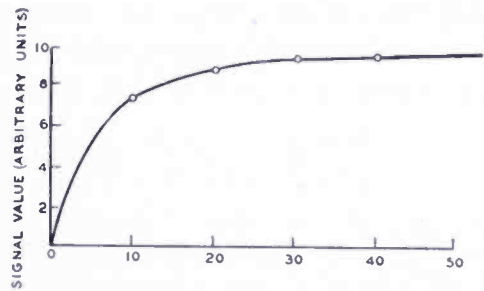


Fig. 5—Surface potential in volts below collector potential.

ary emission collection is greater than unity and some charge is removed every time the reading beam scans those areas. This removal of charge produces the signal which is amplified to operate the viewing kinescope. As is true for all condensers, removal of charge from one electrode causes an equal charge to flow onto the other, which, in this case is the signal plate. This current produces an  $IR$  drop across the load resistor  $R$  (see Figure 7) and thereby produces the signal.

The magnitude of the signal depends on the deviation from the equilibrium described above. When the surface is at collector potential, the secondary emission collection is equal to the beam current and no signal results. The dotted line in Figure 4 shows how the secondary emission collection approaches the true secondary emission curve when the surface potential falls below the collector potential. Figure 5

<sup>4</sup> Zworykin, Morton and Flory, "Theory and Performance of the Iconoscope," *Proc. I.R.E.*, Vol. 25, pp. 1071-1092, August, 1937.

shows this in terms of signal value for a typical electrode configuration. The curve levels off at the higher voltages because the secondary emission collection tends to saturate at relatively weak fields, and the signal current therefore remains almost constant at the higher fields.

The saturation of secondary emission provides a means of obtaining many television pictures of the writing pattern. The saturated secondary emission is proportional to the beam current so that it is only necessary to reduce the beam current to reduce the amount of charge removed on each scan. However, this also reduces the signal output and the lower limit in this direction is the noise inherent in the video amplifier.

A quantitative approach to the duration of a writing signal can be based on regarding the target as a group of elemental condensers, each the size of the focussed spot of the reading beam (one picture element by television standards). The signal plate is common to all of them and the electron beam provides the other electrode. Assuming that the writing beam has completely discharged the elemental condenser, the reading beam will charge it up again to collector voltage. The charge per element will then be

$$Q = Vc \quad \text{where } V = \text{collector voltage}$$

$$c = \text{element capacity.}$$

Assuming that the average charging current is a constant, which is reasonably correct for the condition of constant beam current and saturated collection of secondaries

$$Vc = I_c T \quad \text{Where } I_c = \text{average charging current}$$

$$T = \text{charging time.}$$

The charging current is the difference between the secondary emission current and the average current  $\bar{I}$  reaching the element or

$$I_c = r\bar{I} - \bar{I} = (r - 1)\bar{I} \quad r = \text{secondary emission ratio}$$

$$\bar{I} = \text{average beam current per element.}$$

Therefore

$$Vc = (r - 1)\bar{I}T$$

However, since the beam scans over the target, the average current to each element is  $1/n$  of the total beam current  $I$ , where  $n$  is the number of elements in the target.

$$\text{Therefore } Vc = (r-1) \frac{I}{n} T \quad \text{or} \quad T = \frac{Vcn}{(r-1) I}$$

But  $nc$  is the total capacity of "C" of the whole scanned area so that

$$T = \frac{VC}{(r-1) I}$$

The formula for the capacity of a parallel plate condenser is

$$C = .0885 \times 10^{-12} \frac{kA}{d} \text{ farads}$$

$k$  = dielectric constant  
 $A$  = area of condenser  
 $d$  = thickness of dielectric.

Substituting this in the equation above

$$T = .0885 \times 10^{-12} \frac{kAV}{d(r-1) I} \text{ seconds.}$$

An experimental value for  $T$  of 5 minutes was obtained with  $V = 100$  Volts,  $d = 5 \times 10^{-5}$  centimeters and  $r = 1.3$ . One to two minutes of continuous viewing is more usual. Several thousand scans at television standards are therefore quite feasible.  $T$  can be called the viewing or charging time, or the period during which the element will produce a detectable signal in the reading amplifier. The storage time is much greater and is determined only by the leakage resistance of the insulator. A value of ten days was obtained in one test.

It should be noted that the expression for  $T$  does not involve the number of elements in the picture, nor does it require scanning, but is exactly that which would be obtained by calculating the charging time, if it is assumed that the current  $I$  is spread out uniformly over the whole area of the target of capacity  $C$ .

A second thing to be noted is the fact that the charging time is proportional to the total area of the target. A reduction in tube size will hence result in a proportional reduction in the maximum viewing time. However, in applications where it is not necessary to keep the reading beam scanning constantly, the combination of storage time and viewing time can make the picture available for periods of time greater than  $T$  as given by the equations.

The factor of insulator thickness, however, does not necessarily vary the maximum charging time even though it varies target capacity.

If it is assumed that the dielectric strength of the insulator is constant, then varying the thickness also permits varying the voltage across it in proportion. As the capacity per element goes down, the voltage can go up, and the charge per element remains constant. Therefore, the charging time remains constant and the maximum viewing time is independent of the insulator thickness. Normally, voltage and thickness are determined by other considerations. In actual practice, the tube is built to have a maximum viewing time in excess of that required and the reading beam current is adjusted to provide the desired value.

The film thickness is subject to a basic limitation arising from the requirements of the conduction effect which depends on the penetration of the film by the writing beam. The efficiency of the effect, i.e., the number of conduction electrons per primary, depends on the absorption of the energy of the beam. There is, therefore, an optimum writing beam voltage for each film thickness such that the maximum amount of beam energy is absorbed in the insulator. This voltage is somewhat greater than that required for complete penetration alone. Fortunately, this value is not very critical. Another factor affecting the efficiency is the gradient through the film which should be as high as possible if it is desired to obtain the greatest sensitivity to the writing beam.

Varying the film thickness also varies the degree of half-tone reproduction. Half-tones are obtained in the voltage range where the output signal varies with the surface potential (the sloping part of the curve in Figure 5). Beyond this slope, the signal is independent of surface potential and so produces a "black and white" picture, i.e., the signal is either at its maximum value or is not present. If the film is thin or the total film voltage is less than ten volts for any other reason, the reproduction will be all half-tone and the viewed picture will decay continuously. On the other hand, a thick layer can take a large voltage and the signal will be black and white for most of the charging time. The picture will stay at constant level for a while and then decay. The choice of film thickness will, therefore, be determined by the desired ratio of half-tone to black and white viewing times and by the penetration limitations. A typical curve of signal output versus time is shown in Figure 6. The actual duration of the signal can be made to vary by varying the reading beam, but the ratio of the times in the two modes of operation stays constant for any given voltage change on the film. Reducing this voltage from the maximum possible reduces the viewing time as well as the ratio of black and white to half-tone time.

PRACTICE OF OPERATION

One of the applications of the tube is as a direct current or single trace oscillograph which can provide a bright picture of the complete trace for adjustable periods of time. The circuits for such a function are relatively complex, compared to an oscillograph with an afterglow type phosphor, but there

are several advantages that may justify the extra equipment. The problem of large screen oscillography, for viewing by large numbers of people, can be met by using a commercial television projection set and operating the Graphechon as an oscillograph-iconoscope combination. The problem of photography of very short duration transients can be met by recording the trace in the Graphechon and photographing the picture on a standard kinescope. If the interval between transients is long, the reading beam and kinescope need only be turned on when desired for photographing. In either case, the tube can be made very sensitive to the writing beam and thereby reduce the need for a very high voltage type oscilloscope which ordinarily might be required for high writing speeds.

For such applications, where the writing beam is not modulated in intensity, the circuit requirements are shown in block form in Figure 7. The components are all of a type that can be found described in television and oscillography literature.

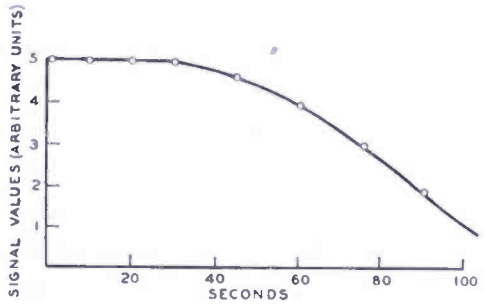


Fig. 6—Typical signal output against viewing time.

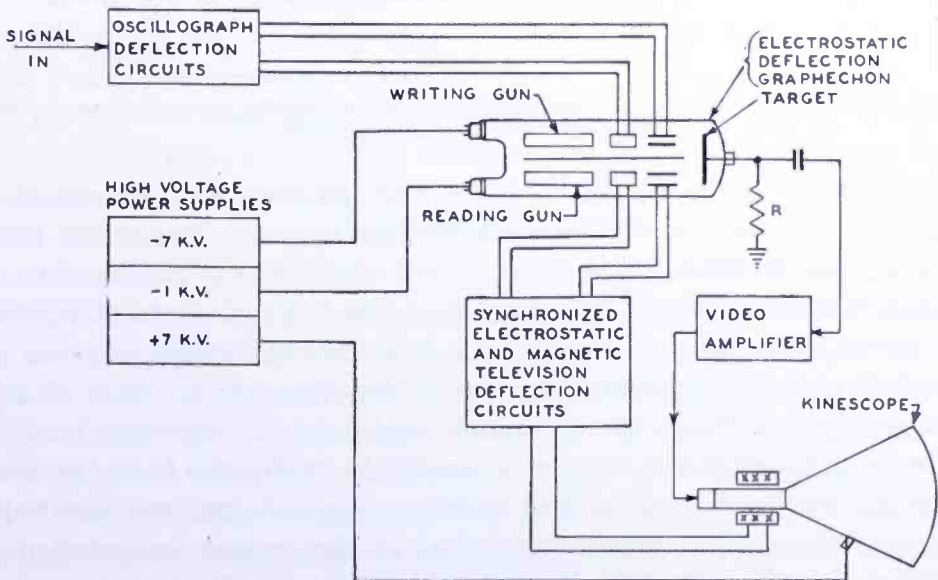


Fig. 7—Block diagram of circuits for using Graphechon as oscillograph.

The requirement that the writing beam not be modulated in intensity arises from the fact that it will produce a video signal in the target of the same form as the modulation and of an intensity that could be many times that of the signal produced by the reading beam. This occurs because, as was shown above, any removal or addition of charge to the target produces a signal and the writing beam, being above the second crossover point, tends to put down charge which will vary in amount with the intensity of the beam. As long as the writing beam intensity is constant, it produces only a direct current type of signal which is blocked by the input condenser of the video amplifier.

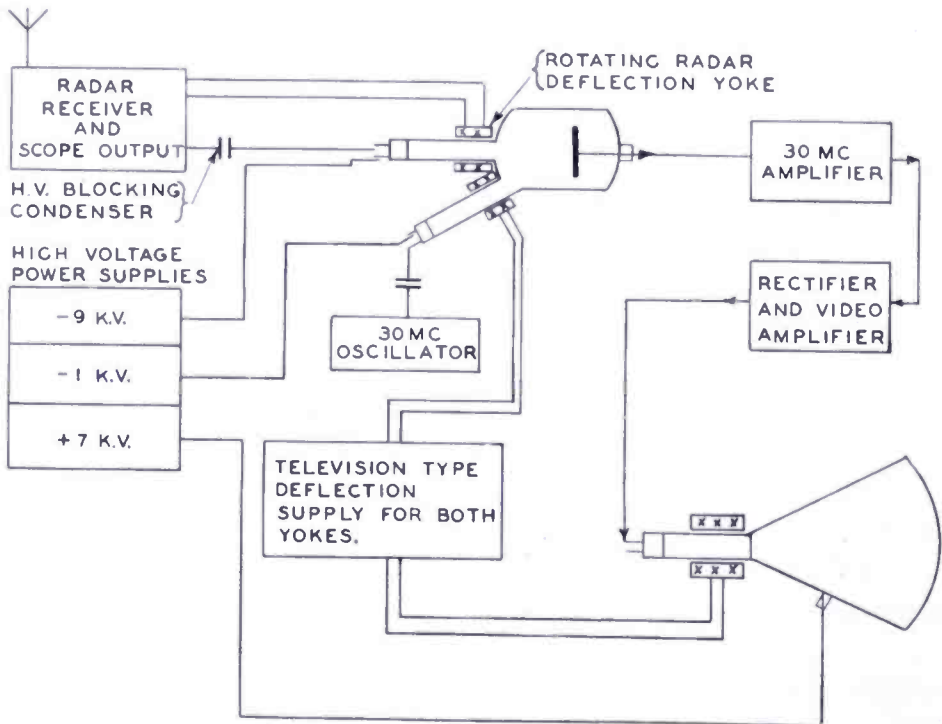


Fig. 8—Block diagram of circuits required for using Graphechon to view PPI type radar presentation.

However, for many applications, such as for radar conversion, it becomes necessary to modulate the writing beam at frequencies in the same range as that of the video output signal and it is therefore not possible to separate the two signals on the basis of signal frequency. However, it is possible to create a frequency difference between the reading and writing signals by modulating the reading beam at some frequency well above the maximum contained in the writing signal. The output signal will now be an amplitude modulated high frequency carrier, which can be amplified by conventional means and rectified to provide the desired video signal free of the writing modulation. A typical circuit is shown in block diagram form in Figure 8, giving the

components required to operate the tube as a radar converter. The operation of the tube in this manner is quite satisfactory provided suitable precautions are maintained.

The original objective and main application of this tube is to provide means of viewing radar PPI patterns. A number of advantages can be attained over conventional practice with systems using tubes made with the P7 type phosphor. A few of these will be mentioned without description:

The decay curve of the brightness of a signal is very much improved over the exponential decay of phosphors (see Figure 6).

The brightness level is limited only by what the best cathode ray tubes can do, so that ambient light level is not important.

The size of the picture can be made as large as desired by television projection techniques.

The viewing time is continuously adjustable over the range of a few seconds to several minutes.

A means is provided for obtaining television type signals and this means can be used to reduce the bandwidth requirements for relaying purposes.

Improvements in signal-to-noise ratio are possible by the integration effects of superposing successive radar patterns.

A block diagram of a system is shown in Figure 8. In the tests performed, the radar system was adjusted to a rotation period of approximately 6 seconds and the sweep times were operated at both 800 microseconds (80 mile range) and 100 microseconds (10 mile range) with adequate performance at both ranges. This showed that the writing speed was adequate to record the short range radar which required much higher sweep speeds and peak currents in the writing beam than the long range radar.

The high writing speed makes possible operation of the writing gun with television type scan in which the modulating signal is applied for a thirtieth of a second (one frame time) during which time the whole target can be covered. The writing beam can then be turned off for one or more seconds before another picture is flashed on, but the reading beam, operating continuously, produces a signal for a steady picture on the kinescope. This type of operation provides a means of viewing continuously a television type picture that is generated at a rate too slow for normal viewing due to excessive flicker. Such a problem is encountered in the Teleran system, in the receiver unit on board the airplane. Because the different pictures for each altitude level are sent out as successive frames, each receiver obtains the pictures for its altitude level at a rate of between one and four pictures

per second. The flicker thus produced is very objectionable, but can be reduced if viewed on a kinescope with special phosphor having a suitable afterglow. However, the picture brightness is down by the ratio of time "off" to time "on" of the signal, which can be compensated for by the use of a storage tube in the manner described above. Such operation has been tested and found satisfactory both in terms of storage time and resolution.

The resolution of the stored picture is best discussed in terms of television practice. Because the picture is formed by the action of a moving cathode ray beam, the smallest discrete picture element possible is the size of the focused spot. Therefore, the maximum picture content possible is the number of elements or adjacent spot areas that can cover the total area of the target. This is true regardless of the type of scanning used. A television type scan is the most efficient because it arranges the elements as close together as possible without producing any overlapping. The PPI type scan has considerable overlapping near the center of the picture, but this does not appreciably affect the resolution. Its only effect is to increase the bandwidth of the signal required to send its pictures over that required for the same picture rate with television type scan.

It can be shown too, that the number of picture elements possible does not vary with the target size. A larger target must be moved farther away from the electron lens of the gun if it is to be covered by the same deflecting angle of the beam. The increased gun-to-target distance causes the spot area to increase in direct proportion to the increase in target area, and so the number of elements stays constant. This property, inherent in the electron optics of cathode ray tubes, applies when all other factors stay constant.

In view of the above, it is customary to refer to the number of elements contained in a picture by the number of parallel lines in which they can be arranged, which is the number of scanning lines used to build up the picture. A standard television picture has approximately 500 lines and, if it were of square aspect, (as high as it is wide) it would have 250,000 elements. For aesthetic reasons, it has an aspect ratio of 4:3 or its height is three-fourths of its width, and it therefore contains over 300,000 elements. This is the order of magnitude of the picture content available in the graphechon with present standard guns and techniques.

Writing speed is customarily measured, in oscillographic practice, in feet or meters per second. So measured, the writing speed of the graphechon is considerably better than 4,000 feet per second. Expressed in more meaningful terms, this is equivalent to better than

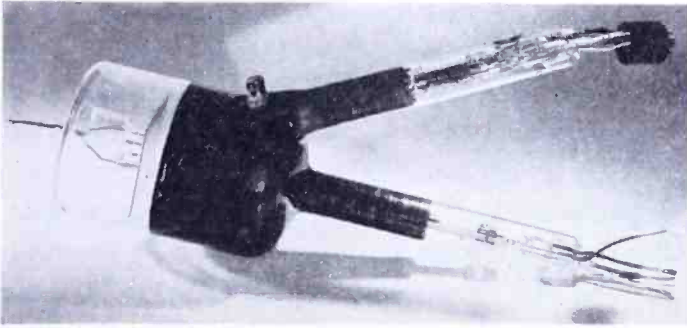
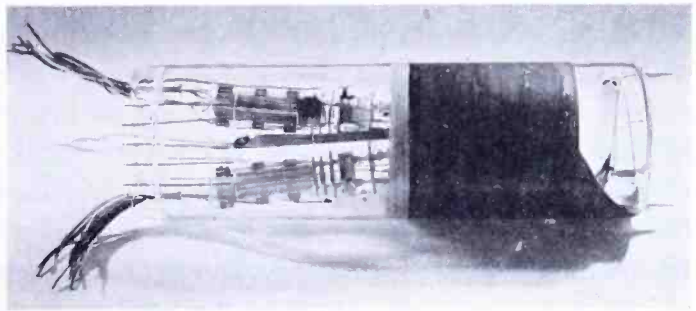


Fig. 9—Single sided target, magnetic deflection Graphechon.

nine million elements per second. This speed has been demonstrated by the test of television operation in which a picture containing 300,000 elements was written onto the target in one thirtieth of a second. Still higher writing speeds can be obtained, though only at the expense of resolution, because they require higher beam currents and this causes the spot size to increase, everything else held constant.

Figures 9, 10, and 11 are photographs of actual tubes built and operated.

Fig. 10—Single sided target, electrostatic deflection Graphechon.



#### GENERAL COMMENTS

When the voltage across the film becomes excessive, breakdown occurs, and in an interesting manner. When the signal plate is given an increment in its negative voltage the picture on the kinescope goes white all over, indicating increasing secondary emission as a transient condition until the surface comes to collector potential. But before this equilibrium can occur, there is a sudden appearance of a large, round patch of white over part of the target. The center of this area is the point at which the film broke down with the emergence



Fig. 11—Double sided target, magnetic deflection Graphechon.

into space of a stream of electrons which sprayed over the adjacent portions of the target and charged them negative. The discharge removes the gradient from the film and gives it a chance to heal. The reading beam then proceeds to remove this surface charge and tries again to bring the surface to collector potential, but breakdown may again prevent this. No permanent damage seems to result to mar operation at normal voltages if breakdown is not permitted to occur repeatedly.

Another effect that will be noticed under some conditions, is called the co-planar grid effect. A strong writing signal produces an area of negative potential on the target which suppresses the secondary emission around it for some distance, depending on the value of the potential and the size of the area. In the viewed picture this can be shown by adjusting the appearance of the blank target to an intermediate shade of gray. A strong signal will show up as a white patch, outlined by a black border which shades off to the normal gray. The extent of this border will decrease linearly with viewing time, even though the signal from the area holds constant, because it is a function of the surface potential which decreases steadily even during the time when the secondary emission is saturated. While this effect serves to distort the picture, it may be regarded as a useful type of distortion in that it tends to emphasize the information.

Another factor that varies with viewing time is the resolution in the picture as affected by the redistribution of secondary electrons. Immediately after the writing beam produces its record, the picture has its full resolution, which is the best that the beam can do, but as the reading beam scans over the target in repeated frames, the resolution of the pattern will change in a manner depending on its configuration. An isolated spot will tend to decrease in size whereas two spots close together will tend to merge into one large spot. These effects are only apparent in the fine detail which requires better than 200 line definition to be resolved. It occurs because the strong gradients at the edges of the negative area causes complete removal of all secondary electrons emitted and so that area tends to reduce in size. These secondaries are collected by the adjacent positive areas, from which they are removed faster than they can accumulate, unless the negative areas are close together. In this case, the region between them slowly goes negative and the spots appear to merge,

Some qualitative observations were made on the two kinds of noise that relate to the operation of this tube. The first is the noise generated by the tube and its associated circuits. This occurs when the reading beam current is reduced to a very low value in an attempt to

obtain the maximum viewing time. The output signal approaches the noise level of the amplifier, which causes a grainy appearance in the viewed picture that is characteristic of this type of noise. However, for most radar applications there is enough reserve viewing time so that this type of noise is not serious.

The most important type of noise is that generated by the radar receiver when its signal-to-noise ratio is low. By proper adjustment of several factors, it is possible to obtain an improvement in signal-to-noise ratio due to the superposition of successive radar scans. The true signals will occur in the same part of the target repeatedly and their effects will be added, whereas the noise is a random pattern and will not add to the same extent over any given period of time. Signals that can only be detected by such integrating arrangements can therefore be observed in the final picture.

Another important gain in this type of operation arises from the fact that the target is not completely discharged by small writing beam currents, such as occur with the noise pulses. The viewing time for these pulses will be shorter than for the stronger signal pulses which can be made to discharge the target completely. Therefore, after a short interval, the signal is still visible but the noise is largely gone except for the few noise pulses that happen to be as large as the signal.

The tubes and results described in this paper have all been produced in a research laboratory. However, because some of the processing techniques are critical, much additional development work remains to be done before consistently reproducible tubes can be produced on a commercial basis.

#### ACKNOWLEDGMENT

The author wishes to acknowledge the invaluable advice and assistance of L. E. Flory, A. Rose, and H. B. Law, and many others at these Laboratories.

# CERTAIN ASPECTS OF TRIODE REACTANCE-TUBE PERFORMANCE FOR FREQUENCY MODULATION AT ULTRA-HIGH FREQUENCIES\*

BY

C. L. CUCCIA

Research Department, RCA Laboratories Division,  
Princeton, N. J.

*Summary*—This paper extends the already published low-frequency investigation of reactance-tube properties to include ultra-high-frequency considerations of transit-time, distributed parameter circuits and inter-electrode capacitances. Expressions for the frequency deviation and  $Q$  of a transmission line—reactance-tube system are derived. It is shown that an important limitation of any basic reactance-tube system is the fact that the grid swing limits the magnitude of the radio frequency voltages in the system thereby making such systems inherently low-level. An illustrative transmission line—reactance-tube system is discussed with respect to mechanical detail, design, and performance—5 megacycles frequency deviation being obtained.

## INTRODUCTION

DURING the course of a general investigation of the problem of producing frequency modulation at the ultra-high frequencies which resulted in the use of spiral electron beams as frequency modulators<sup>1</sup> in a one-kilowatt, 900 megacycle cavity magnetron<sup>2</sup>, an auxiliary study was made of the performance, problems, and limitations which are encountered in the use of triode reactance-tubes at these frequencies. This paper discusses the results of this study and is intended to serve as an introduction to the general engineering problems involved. It also essentially extends the general low-frequency investigations of triode reactance-tube properties which have been published by Vilbig<sup>3</sup>, Reich<sup>4</sup>, and others<sup>5</sup>, to include considerations of

\* Decimal Classification: R135×R148.2×R310.

<sup>1</sup> Lloyd P. Smith and Carl I. Shulman, "Frequency Modulation and Control by Electron Beams," *Proc. I.R.E.*, Vol. 35, No. 7, pp. 644-657, July, 1947.

<sup>2</sup> J. S. Donal, Jr., R. R. Bush, C. L. Cuccia, and H. R. Hegbar, "A 1-Kilowatt Frequency-Modulated Magnetron for 900 Megacycles," *Proc. I.R.E.*, Vol. 35, No. 7, pp. 664-669, July, 1947.

<sup>3</sup> Von F. Vilbig, "Blindwiderstande mit negativen induktivem oder kapazitivem Widerstandsverlauf," *Hochfrequenztechnik und Elektroakustik*, Band 55, pp. 120-132, April, 1940.

<sup>4</sup> H. J. Reich, "The Use of Vacuum Tubes as Variable Impedance Elements," *Proc. I.R.E.*, Vol. 30, No. 6, pp. 277-288, June, 1942.

<sup>5</sup> August Hund, FREQUENCY MODULATION, pp. 155-182, McGraw-Hill Book Company, Inc., New York, N. Y., 1942.

distributed parameter circuits, transit-time, and interelectrode capacitances which become important factors at the ultra-high frequencies<sup>6</sup>.

The discussion will be limited to the more practical aspects of ultra-high-frequency systems inasmuch as only a limited number of triodes have been developed for use at the ultra-high frequencies, and the radio-frequency voltages, which are encountered in triode reactance-tube systems, are limited in magnitude due to restrictions in grid swing.

### BASIC REACTANCE-TUBE THEORY

In Figure 1(a), a schematic diagram of a basic triode reactance-tube circuit<sup>3-5</sup> at low frequencies is pictured. Here a triode with a certain  $\mu$ ,  $r_p$ , and  $g_m$  is shown connected to a resistance-condenser network across which is placed the output of an alternating-current generator whose voltage output is  $e_{ab}$ . The voltage across the condenser will be  $e_g$  and, if  $R$  is much greater than  $1/\omega C$ ,  $e_g$  will lag  $e_{ab}$  by 90 degrees and the triode will pass a lagging current,  $i_p$ , thereby causing the reactance-tube system to exhibit reactive properties.

In general, the admittance,  $Y_{ab}$ , seen by the generator will be

$$Y_{ab} = \frac{i}{e_{ab}} \quad (1)$$

For the circuit in Figure 1,

$$i = i_p + i_1 \quad (2) \quad e_g = e_{ab} \frac{-jX_c}{R - jX_c} \quad (3)$$

where

$$i_p = g_m e_g + \frac{e_{ab}}{r_p} \quad (4) \quad i_1 = \frac{e_{ab}}{R - jX_c} \quad (5)$$

Substituting (2), (3), (4), and (5) into (1), yields

$$Y_{ab} = \frac{g_m X_c^2 + R}{R^2 + X_c^2} + \frac{1}{r_p} - j \frac{X_c [g_m R - 1]}{R^2 + X_c^2} \quad (6)$$

$$= G_{ab} - jB_{ab} \quad (7)$$

<sup>6</sup> Simon Ramo, "Electrical Concepts at Extremely High Frequencies," *Electronics*, Vol. 15, No. 9, pp. 34-82, September, 1942.

If  $R$  is much greater than  $X_c$ , then in general, letting  $X_c = \frac{1}{\omega C}$ ,

$$G_{ab} = \frac{1}{R} + \frac{1}{r_p} \quad (8) \quad B_{ab} = \frac{1}{\omega} \left[ \frac{g_m R - 1}{c R^2} \right]. \quad (9)$$

It is evident from (9) that for  $g_m R > 1$ , the inductive susceptance presented by the reactance-tube system may be written as follows:\*

$$B_{ab} = \frac{1}{\omega L_{ab}} \quad (10)$$

where

$$L_{ab} = \frac{C R}{g_m}. \quad (11)$$

As the system frequency-of-operation increases, then considerations of interelectrode capacitance become important. Figure 1(b) shows the nature of the circuit at fairly high frequencies. The interelectrode capacitances,  $C_{gp}$ ,  $C_{kp}$ , and  $C_{kp}$  are seen to form a delta network whose members must be included in the system network. (It is convenient to use the grid-to-cathode interelectrode capacitance,  $C_{kp}$ , as the capacitance member of the  $RC$  network at ultra-high frequencies.) The grid-to-plate interelectrode capacitance,  $C_{gp}$ , may be tuned out, together with any other capacitances appearing from grid to plate, by using a tuning stub\*\* such as will be described in the latter part of this paper. The effect of the cathode-to-plate interelectrode capacitance on overall reactance-tube-system frequency will be discussed in the next section. In this equivalent circuit, a voltage generator,  $\mu e_p$ , in series with the plate resistance,  $r_p$ , is connected between  $k$  and  $p$ .

\* When the tube is biased beyond cut-off such that  $g_m = 0$ , the reactance tube system presents a shunt susceptance,  $1/\omega CR^2$ , due to the  $RC$  network. As  $g_m$  is increased from zero, this positive susceptance is decreased by the negative susceptance due to the reactance tube current until  $g_m R = 1$  at which point the two cancel. For  $g_m R > 1$ , the shunt susceptance of the reactance tube is negative and is described for all practical purposes by Equation (11).

\*\* If an inductance is connected across  $gp$  in Figure 1(b) such that the admittance between these terminals is written as

$$Y_{gp} = 1/R + j\omega C_{gp} [1 - (f_1/f)^2]$$

where  $f_1$  is the resonant frequency of the resonant circuit made up of the inductance and  $C_{gp}$ , then it is easily shown that for small deviations of frequency from  $f_1$ ,

$$B_{ab} \cong [g_m/\omega RC + \omega C_{gp} (\Delta f/f_1)]$$

where  $\Delta f$  is the frequency deviation. For values of  $C_{gp}$  and  $\Delta f$ , to be considered in this paper, the second term in the bracket is very small compared to the first term and will be neglected.

As the frequency increases into the ultra-high-frequency region, transit time effects<sup>7-9</sup> must be included in the reactance-tube performance. The delta network, as pictured in Figure 1(b), becomes exceedingly complicated when an attempt is made to include these effects and a star network based on a network<sup>9</sup> due to F. B. Llewellyn and L. C. Peterson, as shown in Figure 1(c), becomes very useful. In this star network, which is transformed from the delta network, a fictitious grid plane, *G*, is included which can be shown to be located

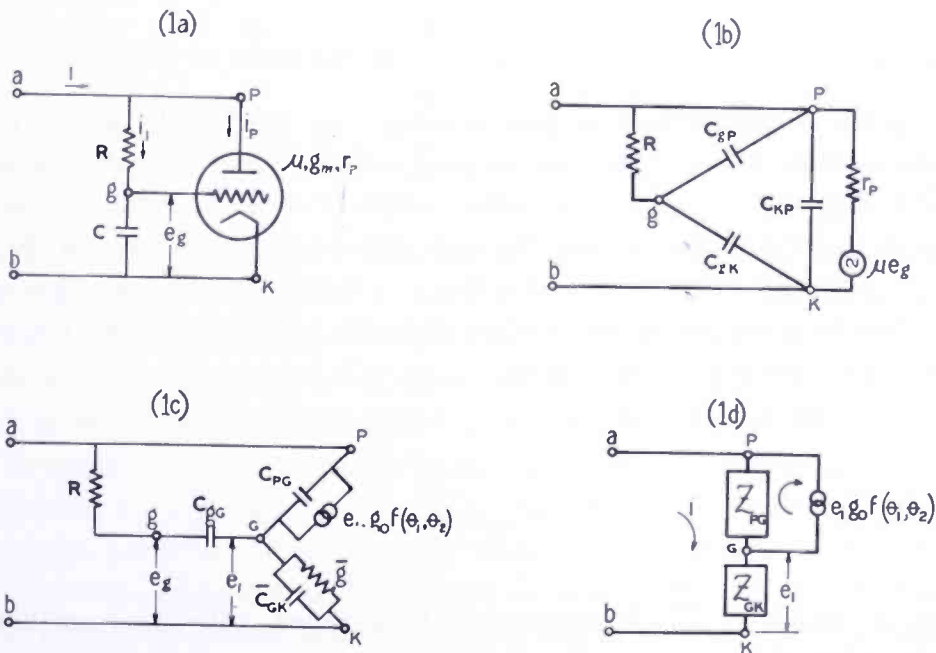


Fig. 1(a)—Basic reactance-tube circuit, suitable for ultra-high-frequency use, which will exhibit the properties of an inductive reactance. (b)—Equivalent circuit of the reactance-tube circuit at high frequencies, using a delta-network. (c)—Equivalent circuit of the reactance-tube circuit, using a star-network, for use at the ultra-high frequencies. (d)—General equivalent network of a reactance-tube circuit.

extremely near to the grid wires but does not quite include them. The capacitance,  $C_{Gp}$ , is very nearly equal to  $C_{gp}$  being the capacitance as measured between the plate and a solid conducting plane, substituted for the grid.  $C_{Gg}$  can be shown to be related to  $C_{Gp}$  by the relationship

$$C_{Gg} = \mu C_{Gp} \tag{12}$$

<sup>7</sup> F. B. Llewellyn, "Equivalent Networks of Negative Grid Vacuum Tubes at the Ultra-High Frequencies," *Bell Sys. Tech. Jour.*, Vol. 15, pp. 575-586, 1936.

<sup>8</sup> F. B. Llewellyn, "Vacuum Tube Electronics at Ultra-High Frequencies," *Proc. I.R.E.*, Vol. 21, pp. 1532-1574, November, 1933.

<sup>9</sup> F. B. Llewellyn and L. C. Peterson, "Vacuum Tube Networks," *Proc. I.R.E.*, Vol. 32, No. 3, pp. 144-166, March, 1944.

In many problems involving high- $\mu$  tubes at the ultra-high frequencies, this capacitance may be neglected.

Between the cathode and the grid,  $G$ , is located a conductance,  $\bar{g}$ , in shunt with a capacitance,  $\bar{C}_{Gk}$ , the bar denoting transit-time dependency. While their analytic forms are very complicated, the behavior of  $\bar{g}$  and  $\bar{C}_{Gk}$  as functions of transit time is well known\*. At low frequencies,  $\bar{g}$  is the transconductance,  $g_o$ , of the tube, as referred to the effective potential of the grid. It is related at these low frequencies to  $g_m$  by a slight factor whose magnitude is approximately equal to  $\mu/(1 + \mu + \frac{4}{3} \frac{x_2}{x_1})$  where  $\frac{x_2}{x_1}$  is the ratio of the grid-to-plate spacing to the cathode-to-grid spacing. As the transit angle,  $\theta_1$ , in the cathode-to-grid space increases,  $\bar{g}$  behaves somewhat cosinusoidally and goes to zero at  $\theta_1 = 2\pi$ , after which it oscillates with decreasing peak amplitude and passes through zero at transit angles of  $4\pi$ ,  $6\pi$ , . . . and approximately  $3\pi$ ,  $5\pi$ ,  $7\pi$ , . . . being negative in sign when  $\theta_1$  lies between any whole number of cycles and that number increased by approximately a half cycle.

At low frequencies

$$\bar{C}_{Gk} = \frac{3}{5} C_{Gk} \quad (13)$$

As  $\theta_1$  increases,  $\bar{C}_{Gk}$  increases and approaches, with some oscillation, the value,  $C_{Gk}$ .

In order to complete the transformed network, a constant-current generator, of magnitude,  $e_1 g_o f(\theta_1, \theta_2)$ ,\*\* where  $e_1$  is the effective potential of the grid and  $\theta_2$  is the transit-time in the grid-to-plate region, is connected between the fictitious grid and the plate.  $g_o f(\theta_1, \theta_2)$  is a transadmittance whose magnitude as a function of both  $\theta_1$ , and  $\theta_2$  is somewhat involved.† However, when  $\theta_2$  is very small as is the case in many ultra-high-frequency triodes, then  $f(\theta_1, \theta_2)$  reduces to the form

$$f(\theta_1, 0) \cong e^{-j \frac{11}{30} \theta_1} \quad (14)$$

\* See Figure 4 of Reference 9.

\*\* Omitted here is a factor of around 0.75 which is related to the capture of electrons by the grid.

† See Equation (26), Reference 9.

The network in Figure 1(c) may be generalized\* into the form shown in Figure 1(d) in which the impedances may include other resistances, capacitances, and inductances which may be present. For this circuit, assuming the loop currents,  $i$ , and  $e_1 g_0 f(\theta_1, \theta_2)$  as shown,

$$e_{ab} = [i - e_1 g_0 f(\theta_1, \theta_2)] Z_{Gp} + e_1 \quad (15)$$

$$e_1 = i Z_{Gk}. \quad (16)$$

Substituting (16) into (15), it follows that

$$Y_{ab} = \frac{i}{e_{ab}} = \frac{1}{[1 - g_0 f(\theta_1, \theta_2) Z_{Gk}] Z_{Gp} + Z_{Gk}}. \quad (17)$$

This is a perfectly general expression and since the behavior of  $\bar{g}$ ,  $\bar{C}_{Gk}$ , and  $f(\theta_1, \theta_2)$  as a function of transit-time is known, the shunt conductance and susceptance of any triode reactance tube circuit, whose basic low-frequency circuit is based on that shown in Figure 1(a), may be determined for any values of  $\theta_1$  and  $\theta_2$ .

It would be relatively simple to derive the complete set of equations describing the circuit in Figure 1(c); however, the resulting general equations would not be particularly rewarding due to their great complexity. The important aspects of the general system may be deduced as a function of transit-time by utilizing the following approximations in equation (17):

$$\begin{aligned} \bar{g} &\approx g_m \cos \frac{\theta_1}{4} & Z_{Gp} &\approx R \\ g_0 &\approx g_m & Z_{Gk} &= \frac{1}{g_m \cos \frac{\theta_1}{4} + j\omega C_{Gk}} \\ \bar{C}_{Gk} &\approx C_{Gk} & & \\ \theta_2 &= 0 & & \end{aligned} \quad (18)$$

Substituting equation (14) and the approximations listed in (18) into equation (17), gives

\* The generalization is tempered by various vacuum-tube equivalent-network conditions which arise from the analysis; i.e., that the electron flow is perpendicular to the plane electrodes, that the emitted electrons have a single velocity rather than the Maxwellian distribution which actually exists and that no electrons move toward the cathode.

$$Y_{ab} = \frac{1}{R} \frac{g_m \cos \frac{\theta_1}{4} + j\omega C_{\rho k}}{g_m \left[ \cos \frac{\theta_1}{4} - \cos \frac{11}{30} \theta_1 \right] + \frac{1}{R} + j\omega C_{\rho k} \left[ 1 + \frac{g_m}{\omega C_{\rho k}} \sin \frac{11}{30} \theta_1 \right]} \quad (19)$$

which is valid for transit angles up to  $\theta_1 = 2\pi$ .

When  $\theta_1 = 0$  and when  $R \gg \frac{1}{\omega C_{\rho k}}$ , equation (19) reduces to

$$Y_{ab} = \frac{1}{R} - j \frac{g_m}{\omega C_{\rho k} R} \quad (20)$$

which is the low frequency case and consists of the same quantities as those yielded by equations (8) and (10) with the exception of the term,  $1/r_p$ , which is absent in Equation (20) due to nature of the approximations involved.

For values of  $\theta_1$ , from zero to  $\theta_1 \approx \pi$ , Equation (19) may be closely represented by the expression,

$$Y_{ab} = \frac{1}{R \left[ 1 + \frac{g_m}{\omega C_{\rho k}} \sin \frac{11}{30} \theta_1 \right]} - j \frac{g_m}{\omega C_{\rho k} R} \frac{\cos \frac{\theta_1}{4}}{\left[ 1 + \frac{g_m}{\omega C_{\rho k}} \sin \frac{11}{30} \theta_1 \right]} \quad (21)$$

which shows that in this range of transit angles, the shunt conductance and susceptance will decrease in magnitude slightly depending on the

ratio,  $\frac{g_m}{\omega C_{\rho k}}$ . Consider now the limiting case of  $\theta_1 = 2\pi$  (beyond this value, the expressions for  $\bar{g}$  and  $f(\theta_1, 0)$  as given by (18) and equation (14) will no longer be valid): it follows that

$$Y_{ab} = \frac{1}{R} \cdot \frac{\left[ 1 + 0.742 \frac{g_m}{\omega C_{gk}} \right]}{0.448 \left[ \frac{g_m}{\omega C_{gk}} \right]^2 + \left[ 1 + 0.742 \frac{g_m}{\omega C_{gk}} \right]^2} + j\omega C_{gk} \frac{g_m}{R} \cdot \frac{0.670}{0.448 \left[ \frac{g_m}{\omega C_{gk}} \right]^2 + \left[ 1 + 0.742 \frac{g_m}{\omega C_{gk}} \right]^2}. \quad (22)$$

Note that the susceptance has now changed sign such that the reactance-tube circuit presents a shunt capacitive susceptance. It can easily be shown\* that the transit-angle,  $\theta_{1c}$ , at which the crossover from inductive to capacitive susceptance takes place, is described by the equation

$$\cos \frac{\theta_{1c}}{4} \sin \frac{11}{30} \theta_{1c} = \frac{\omega C_{gk}}{g_m} \left[ \frac{1}{R g_m} - \cos \frac{11}{30} \theta_{1c} \right]. \quad (23)$$

If  $\frac{1}{R g_m} < 0.1$ , then the crossover will take place in the range,  $4.3 < \theta_1 < 5.5$ , for  $0 < \frac{g_m}{\omega C_{gk}} < 2$ . As the reciprocal,  $\frac{1}{R g_m}$ , increases in magnitude, the crossover point shifts to slightly smaller values of  $\theta_1$ . This change in sign of the susceptance is due to the shift in phase of the output of the constant-current generator. As  $\theta_1$  increases in magnitude beyond  $\theta_1 = 2\pi$ , the phase of this current will change even more rapidly and other crossovers will take place; under certain conditions, the reactance-tube may be made to display the properties of a negative conductance. Throughout the equivalent network formulation and analysis, such conditions as transit-time loading<sup>10,11</sup> are implicitly included.

---

\* The imaginary portion of any expression of the form,  $\frac{a + jb}{c + jd}$ , is zero when  $cb = ad$ .

<sup>10</sup> D. O. North, "Analysis of the Effects of Space Charge on Grid Impedance," *Proc. I.R.E.*, Vol. 24, No. 1, pp. 108-136, January, 1936.

<sup>11</sup> John M. Miller, and Bernard Salzberg, "Measurements of Admittances at Ultra-High Frequencies," *RCA Review*, Vol. 3, No. 4, pp. 486-504, April, 1939.

The term,  $\frac{g_m}{\omega C_{gk}}$ , which occurs in Equations (19-23) may be shown to be related to the transit-angle,  $\theta_1$ , as follows: Since

$$\theta_1 = \frac{3 x_1 \omega}{\sqrt{\frac{e}{2m} V}} \quad (24)$$

$$g_0 = \frac{3}{2} \cdot \frac{A}{9\pi} \cdot \sqrt{\frac{e}{m} \frac{V^{\frac{1}{2}}}{x_1^2}} \quad (25)$$

where  $V$  is the effective potential of the equivalent diode and  $A$  is the area, then, combining these equations

$$g_0 \theta_1 = \frac{A \omega}{2\pi x_1} \quad (26)$$

$$= 2\omega C_{gk} \quad (27)$$

whereupon, as a close approximation,

$$\frac{g_m}{\omega C_{gk}} \cong \frac{2}{\theta_1} \quad (28)$$

where  $\theta_1$  is measured in radians,  $C_{gk}$  is measured in farads and  $g_m$  in mho's (see Equation (63) for a numerical example). While Equation (28) permits the calculation of transit-angles in terms of  $g_m$ ,  $\omega$ , and  $C_{gk}$ , this equation cannot be directly combined into any of Equations (19-22) in view of the practical relationship between  $g_m$  and  $\theta_1$ . As will be seen,  $g_m$  is the only convenient variable in a triode reactance-tube system and since it will be varied from a maximum value, which is a function of the tube, to a minimum value, the transit-angle will increase from its minimum value (which should be much less than  $\theta_{1c}$ ) to infinity, should the minimum value of  $g_m$  be zero. Since Equations (19-22) are only valid for  $0 < \theta_1 < 2\pi$ , their representation would fail for a great portion of the useful range of  $g_m$ . It is evident that in the practical design of a reactance-tube system, the value of  $g_m$  corresponding to  $\theta_{1c}$  should occur as close to cutoff as possible.

## ULTRA-HIGH-FREQUENCY TRIODES

A relatively small number of types of triodes have been engineered or are available for use in the ultra-high-frequency region. Of those which are available commercially, the types which utilize coaxial construction have achieved widespread use since they may be used in coaxial enclosed systems. Coaxial ultra-high-frequency triode types in general fall into two categories—the coplanar-electrode type which is best exemplified by the “lighthouse” or disk-seal variety<sup>12</sup> in which planar electrodes with circular symmetry are used, and the coaxial-electrode type<sup>13-15</sup> in which the plate, grid, and cathode are mutually coaxial being concentric cylinders. An RCA developmental triode, A-2231<sup>13</sup>, is typical of the latter type. These tubes of either type may vary with respect to current capacity, interelectrode capacitances, and specific construction but they are all capable of high  $g_m$  and have very small spacing between the tube elements in order to reduce the electron transit-time<sup>16</sup> to a minimum.

DEVELOPMENT OF AN EXPRESSION FOR THE FREQUENCY DEVIATION  
THEORETICALLY POSSIBLE WITH A TRIODE REACTANCE TUBE  
TERMINATING A SHORTED TRANSMISSION LINE

Let a suitable low-transit-time ultra-high-frequency triode reactance-tube be connected across the open end of a shorted transmission line as shown in Figure 2. The self impedance of the transmission line alone<sup>17</sup>, as measured across the terminals,  $a$ ,  $b$ , is

$$Z_s = j Z_o \tan \frac{\omega l}{c} \quad (29)$$

<sup>12</sup> E. D. McArthur, “Disk-Seal Tubes,” *Electronics*, Vol. 18, No. 2, pp. 98-102, February, 1945.

<sup>13</sup> R. R. Law, D. G. Burnside, R. P. Stone, W. B. Whalley, “Development of Pulse Triodes and Circuit to Give One Megawatt at 600 Megacycles,” *RCA Review*, Vol. 7, No. 2, pp. 253-264, June, 1946.

<sup>14</sup> L. S. Nergaard, D. G. Burnside, R. P. Stone, “A Developmental Pulse Triode for 200 KW Output at 600 Mc,” *Proc. I.R.E.*, Vol. 36, No. 3, pp. 412-416, March, 1948.

<sup>15</sup> S. Frankel, J. J. Glauber, and J. P. Wallenstein, “A Medium Power Triode for 600 Megacycles,” *Proc. I.R.E.*, Vol. 34, No. 12, pp. 986-992, December, 1946.

<sup>16</sup> J. R. Whinnery and H. W. Jamieson, “Tracing of Electron Trajectories Using the Differential Analyzer,”—Part III—“Study of Transit-Time Effects in Disk-Seal Power-Amplifier Triodes,” *Proc. I.R.E.*, Vol. 36, No. 1, pp. 76-83, January, 1948.

<sup>17</sup> Ware and Reed, COMMUNICATION NETWORKS, Chapter VI, John Wiley and Sons, Inc., New York, N. Y., 1944.

where  $Z_o$  is the characteristic impedance of the line,  $l$  is the length of the line, and  $c$  and  $\omega$  are the velocity of light and the angular frequency respectively.

If the reactance-tube produces the inductive reactance,  $\omega L_{ab}$ , in order to achieve resonance it must be shunted across the line such that the reactances of the tube network and the line are equal in magnitude but opposite in sign. Then, as a condition of resonance,

$$Z_o \tan \frac{\omega l}{c} = \omega L_{ab}. \quad (30)$$

This is a cumbersome expression since in order to determine the values of frequency which will satisfy the equation, each side must be computed simultaneously. Of more value and interest is the following approximate solution:

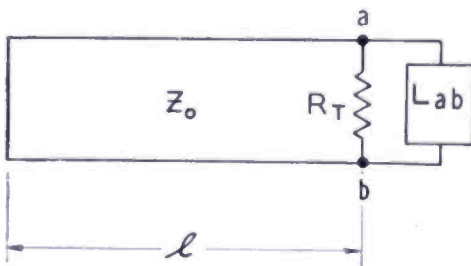


Fig. 2—Schematic diagram of a reactance tube and a shunt load terminating a shorted transmission line.

The transmission line must be slightly longer than a quarter wavelength in order to resonate with the inductance which is presented by the triode. Let

$$\frac{\omega l}{c} = \frac{\pi}{2} + \alpha \quad (31)$$

where  $\alpha$  is a small fraction of  $\pi/2$  radians. Then equation (30) may be rewritten as follows:

$$-Z_o \cot \alpha = \omega L_{ab}. \quad (32)$$

The expression for  $\cot \alpha$  may be replaced by the first term in its series expansion; i.e.,

$$\cot \alpha = 1/\alpha. \quad (33)$$

Substituting (32) and (33) into (31), the transmission line angle,  $\frac{\omega l}{c}$ , may be expressed as follows:

$$\frac{\omega l}{c} = \frac{\pi}{2} + \frac{Z_o}{\omega L_{ab}}. \quad (34)$$

From this, it follows that

$$\omega^2 - \frac{\pi c}{2l} \omega + \frac{Z_o c}{l L_{ab}} = 0. \quad (35)$$

In order to approximate the solution, let

$$\omega = \frac{\pi c}{2l} + \delta \quad (36)$$

where  $\delta$  is a small quantity. Then

$$\omega^2 = \left[ \frac{\pi c}{2l} \right]^2 + \frac{\pi c}{l} \delta + \delta^2. \quad (37)$$

Ignoring the term,  $\delta^2$ , substitute (36) and (37) into (35) to obtain the following expression for  $\delta$ :

$$\delta = -\frac{2 Z_o}{L_{ab}}. \quad (38)$$

Substituting (38) into (36), in terms of frequency,

$$f = \frac{c}{4l} - \frac{Z_o}{\pi^2 L_{ab}} \quad (39)$$

$$= f_o - \Delta f \quad (40)$$

where

- $c$  = velocity of light in centimeters per second
- $l$  = length of transmission line in centimeters
- $Z_o$  = characteristic impedance of the transmission line in ohms
- $L_{ab}$  = inductance presented by the reactance tube in henries.

The solution, (39), which identifies the frequency that satisfies (29) for small deviations is in two parts. The first term,  $f_o$ , is the frequency of resonance of the transmission line without the reactance-tube and the second term,  $\Delta f$ , is the change in frequency due to the addition of the reactance-tube — its magnitude being inversely proportional to the magnitude of the inductance presented by the reactance tube.

It would seem at first inspection that  $\Delta f$  could become large by making the effective inductance of the reactance-tube very small. This is not physically realizable since according to Equation (11),  $L_{ab}$  is directly proportional to  $R$  and  $C$  and inversely proportional to  $g_m$ .  $g_m$  can be increased only to a given limit which is a function of the tube used and as the product of  $R$  and  $C$  is reduced to zero, the reactance-tube will lose its quadrature characteristics and the transmission line will become shunted by the capacitive and resistive characteristics of the tube and its  $RC$  network.

In terms of Equation (11), (39) can be rewritten as follows:

$$f = \frac{c}{4l} + \frac{Z_o g_m}{\pi^2 RC} \quad (41)$$

Note that for all practical purposes,  $\Delta f$  is not a function of frequency. It is therefore evident that before the various other mechanical and electrical aspects of deviation limitation are considered, an increase in the resonant frequency of the transmission line will result in a reduction in the ratio,  $\Delta f/f_0$ , for a specific reactance-tube system.

If the reactance tube-transmission line system is shunted by a capacitance,  $C_{s1}$ , where  $C_{s1}$  may be the plate-to-cathode interelectrode capacity of the tube\* or a combination of stray capacitances, the frequency of the system can be described by the expression,

$$f = \frac{c}{4l} \left[ \frac{1}{1 + \frac{c C_{s1} Z_o}{l}} \right] - \frac{Z_o}{\pi^2 L_{ab}} \quad (42)$$

which differs from Equation (39) by the correction term,  $\frac{1}{1 + \frac{c C_{s1} Z_o}{l}}$ ,

which does not affect the frequency deviation.

\* Note that for a 2C43 triode, the plate-to-cathode interelectrode capacity is 0.02 micromicrofarad. Choosing the values,  $Z_o = 55$  ohms,  $l = 8$  centimeters, and  $c = 3 \times 10^{10}$  centimeters, it can be shown that

$$\frac{1}{1 + \frac{c C_{s1} Z_o}{l}} = \frac{1}{1 + 0.0041}$$

which shows that the presence of a 2C43 triode whose grid is biased beyond cut-off causes negligible frequency change.

## THE Q OF A TRANSMISSION-LINE—REACTANCE-TUBE SYSTEM

The  $Q$  of a transmission-line—reactance-tube system is an important consideration in the use of such a system since its magnitude will influence both the choice of tube and circuit parameters and the general circuit behavior. If a triode reactance tube is to be added to the tank resonator of an oscillator which is coupled to the load, for example, the increase in loading due to an improperly designed reactance-tube network may inhibit or prevent oscillation.

The  $Q$  of the transmission-line—reactance-tube system shown in Figure 2 may be found by considering the stored energy<sup>18,19</sup> and the losses in the system; i.e.,

$$Q = 2\pi \frac{U}{W/f} \quad (43)$$

where  $U$  is the stored energy of the system and  $W/f$  is the power lost in the system per cycle. Since the voltage varies sinusoidally along the line, Equation (43) becomes

$$Q = 2\pi \frac{\frac{C_0 c}{4\pi f} \int_0^{\phi_0} e_{ab}^2 \frac{\sin^2 \phi}{\sin^2 \phi_0} d\phi}{\frac{e_{ab}^2}{2f R_T}} \quad (44)$$

where

$$C_0 = \frac{1}{Z_0 c} \quad (45)$$

$$\phi_0 = \frac{\pi}{2} + \frac{Z_0}{\omega L_{ab}} \quad (46)$$

$$R_T = \frac{R R_s r_p}{R r_p + R R_s + R_s r_p} \quad (47)$$

<sup>18</sup> J. R. Ragazzini, "Ultrashort Electromagnetic Waves"—Part II, "Transmission Lines at Ultrahigh Frequencies," *Elec. Eng.*, Vol. 62, pp. 159-167, April, 1943.

<sup>19</sup> E. W. Herold and L. Malter, "Some Aspects of Radio Reception at Ultra-High Frequency"—Part I, "The Antenna and the Receiver Input Circuits," *Proc. I.R.E.*, Vol. 31, No. 8, pp. 423-438, August, 1943.

$C_0$  is the capacitance per unit length of line,  $\phi_0$  is the true angle of the transmission line in the length of which is included the apparent change in length due to the reactance-tube, and  $R_T$  is the combined shunt resistance due to the plate resistance,  $r_p$ , the  $RC$  network resistance,  $R$ , and the shunt resistance,  $R_s$ , which is due to all other shunt loads seen by the system.

Performing the integration in (44) and substituting (45) into the result, gives

$$Q = \frac{R_T}{2Z_0} \left[ \frac{2\phi_0 - \sin 2\phi_0}{1 - \cos 2\phi_0} \right] \quad (48)$$

Substituting (46) into (48), it follows that

$$Q = \frac{R_T}{2Z_0} \left[ \frac{\pi + \frac{2Z_0}{\omega L_{ab}} + \sin \frac{2Z_0}{\omega L_{ab}}}{1 + \cos \frac{2Z_0}{\omega L_{ab}}} \right] \quad (49)$$

For small values of  $\frac{Z_0}{\omega L_{ab}}$ , this expression reduces to

$$Q \approx \frac{\pi R_T}{4Z_0} \quad (50)$$

and when the tube is biased beyond cutoff,

$$Q \approx \frac{\pi R_s R}{4 [R_s + R] Z_0} \quad (51)$$

It is evident that as the grid voltage, starting at cut off, becomes less negative, for comparable values of  $R_s$ ,  $R$  and  $r_p$ , the system will undergo a small but rapid change in  $Q$  until it reaches the value predicted by Equation (50) from which point on, the changes in  $Q$  for practical values of  $\Delta f$  will be negligible unless transit-time loading becomes an important factor.

Equations (49-51) are based on the reactance-tube exhibiting mainly reactive properties. It is evident however, that if the magnitude of  $R$  is not sufficiently larger than the magnitude of the capacitive reactance,  $1/\omega C$ , the current through the reactance-tube will not be

in quadrature with  $e_{ab}$  and additional loading will take place which will reduce the  $Q$  of the system.

#### CONSIDERATIONS OF PLATE CURRENT IN DISTRIBUTED-PARAMETER REACTANCE-TUBE SYSTEMS

The current through a reactance-tube system which is shunted across a distributed parameter circuit across which is impressed the voltage,  $e_{ab}$ , is

$$i = \frac{e_{ab}}{2\pi f L_{ab}} \quad (52)$$

If, for example,  $f = 5 \times 10^8$  cycles per second and  $L_{ab} = 2 \times 10^{-6}$  henries, then  $i$  will be 159 microamperes per volt (effective value) which may be designed for without undue difficulty.

If the reactance-tube is connected across a shorted transmission line as shown in Figure 2, it is interesting to compare this tube current with the largest current which flows in the system; i.e.,  $i_{sc}$  — the current in the shorted end of the line whose magnitude may be determined from the expression

$$I_{sc} = \frac{e_{ab}}{Z_0} \quad (53)$$

If  $Z_0 = 50$  ohms,  $i_{sc}$  is 20 milliamperes per volt (effective value). This value is 126 times greater than the reactance-tube system current. This example illustrates what is in general the case in reactance tube-distributed parameter systems; i.e., the reactance-tube is utilized in the low current portion of the resonant system in such a manner that unduly high current capacity demands, which might inhibit the performance of the overall system, are not made on the tube.

#### LIMITATIONS DUE TO GRID SWING IN REACTANCE-TUBE SYSTEMS

The alternating-current voltage,  $e_g$ , which is impressed on the grid due to the system voltage,  $e_{ab}$ , is

$$e_g = \frac{e_{ab}}{j\omega RC - 1} \quad (54)$$

This describes the portion of  $e_{ab}$  which will appear across the grid-to-cathode circuit as a function of the ratio of the resistance,  $R$ , to the capacitive reactance,  $1/\omega C$ . Excluding for the moment considerations of grid bias, it is evident that if the grid is swung too far negatively,

the reactance-tube will be beyond cut-off for a portion of a cycle of  $e_{ab}$  whereas if the grid is swung too far in the positive direction, the grid circuit will draw current thereby producing a resistive loading across the capacitance,  $C$ , which will affect the qualities of the  $RC$  network. In order to maintain the validity of the mathematical expressions which are derived for Class A operation and in order to avoid plate current clipping, the grid swing must be confined to the region,  $-E_c < E_g < 0$ , where  $E_g$  is the instantaneous grid voltage and  $-E_c$  is the cut-off voltage. In order to insure a sinusoidally varying plate current, the actual alternating-current grid swing must be confined to a region much smaller than this region since the dynamic characteristic curve of a triode is approximated by a power law greater than unity and a large second-harmonic component of plate current will be produced if the grid is swung over too large a portion of  $-E_c < E_g < 0$ . This second-harmonic component will not be useful since only the fundamental component contributes to the frequency deviation.

A second limitation on grid swing in this region is that due to the fact that if the resonant system frequency is to be varied, the only system parameter which can be controlled is the  $g_m$  of the triode which can be varied only by changing the grid bias. It is evident that the maximum variations in grid bias, corresponding to the maximum values of the modulating signal, will depend on the

ratio of  $\left| \frac{E_c}{2} \right|$  to  $e_{g_{max}}$  since, if the magnitude of  $e_{g_{max}}$  is a large fraction of  $\left| \frac{E_c}{2} \right|$ , the range of  $g_m$  over which the effective variation of frequency can be achieved will be greatly reduced.

Therefore, the maximum permissible radio frequency system voltage will be determined by the cut off characteristics of the tube and by the ratio of  $R$  to  $1/\omega C$ . Note that the situation cannot be redeemed by simply increasing the magnitude of  $R$  since the capacitance will in general be determined by the system and such an increase in  $R$  will result in a decrease in the maximum frequency deviation which can be obtained. In like manner, any attempt to increase the cut-off voltage negatively by designing a tube with larger grid-to-cathode spacing may reduce both  $C$  and  $g_m$  which will also affect the maximum frequency deviation.\*

\* Note that it is possible to engineer an equivalent  $RC$  network in which the capacitance network is replaced by an amplifier which permits high voltage across the network but which delivers a quadrature voltage of the correct magnitude to the grid of the tube.

As the grid potential is varied from its least negative value to cut-off, the electron transit-time through the tube will increase and bring about a reduction in frequency deviation in the more negative regions of the grid swing. However, since the largest values of  $\Delta f$  and  $g_m$  occur at the least negative values of grid potential, these electron transit-time effects will merely serve to reduce the grid swing necessary to vary the frequency deviation from its maximum value to its zero value.

#### SYSTEM FREQUENCY LIMITATIONS IN COAXIAL-LINE — REACTANCE-TUBE SYSTEMS

As the resonant frequency of the unmodulated system is increased, then the geometry and size of the various system components and, in particular, the reactance tube, must be accounted for in the design since, in a coaxial line, it is desirable that the mean circumference of this line be less than a wavelength in order to insure operation in the proper mode. This size limitation will place restrictions on the type of tube used.

#### THE DESIGN AND PERFORMANCE OF AN EXPERIMENTAL FREQUENCY MODULATED COAXIAL-CAVITY SYSTEM USING A 2C43 TRIODE

##### A. *Description of the Experimental System*

The following discussion describes in detail the application of the theoretical aspects of frequency modulated reactance-tube systems to an ultra-high-frequency coaxial system utilizing a 2C43 triode. The system to be described must in no way be construed as being a definitive system; it was chosen because of its relative simplicity and because its assembly serves to illustrate many of the mechanical and electrical problems which are encountered.

A schematic diagram and a mechanical diagram of 2C43 tube mounted in a coaxial line are shown in Figures 3 and 4, respectively. In order to avoid mechanical complexity, the grid is placed at the same potential as the coaxial line and the plate and cathode are connected using blocking condensers — the cathode blocking condenser, which is an integral part of the 2C43 structure, and the plate blocking condenser, whose construction is illustrated in Figure 4.

The first system component to be considered is the  $RC$  network. It is evident that the capacitance,  $C'_{gk}$  between the grid and the radio frequency cathode (see Figure 3) of the 2C43 is suitable for use as the capacitance member of the network. Its capacity is 2.8 micro-

microfarads and its ohmic reactance in the frequency range from 500 to 1000 megacycles is seen in Figure 5 to vary from 115 to 57 ohms.

The resistive member of the  $RC$  network should be designed such that it fulfills the four following conditions:\*

1. Its magnitude in ohms should exceed the ohmic reactance of the condenser member of the network by an amount such that the voltage across the condenser lags, by as nearly 90 degrees as possible, the current through the network.

2. Its magnitude should be such as to yield the desired frequency deviation (see Equation (39)).

3. Since this resistance may be an important load of the resonant system, its magnitude, combined with the shunt load,  $R_s$ , and the plate resistance,  $r_p$ , should be such as to yield the desired  $Q$  of the system (see Equation (50)).

4. Since, as will be discussed next, this resistance may also be a member of an essential component resonant system in the grid-to-plate circuit of the triode, its magnitude should be such as to yield a bandwidth for this system which will be commensurate with the frequency deviation which is required of the main resonant system.

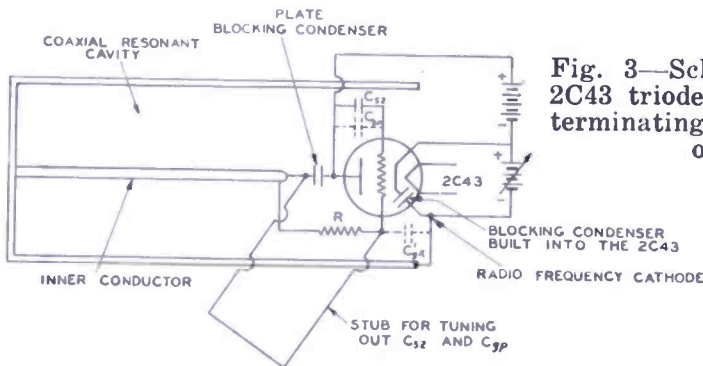


Fig. 3—Schematic diagram of a 2C43 triode reactance-tube system terminating a shorted coaxial resonant cavity.

In Figure 4 the resistance element is seen to be installed by connecting a low wattage resistor from the grid connector to the end of the inner conductor of the main resonator. Note that this resistance is shunted by two capacitances in series—the plate blocking condenser and a capacitance made up of the grid-to-plate interelectrode capacitance  $C_{gp}$  in shunt with any additional capacitance,  $C_{s2}$ , which appears across the grid-to-plate electrode. The blocking condenser will be neglected in the considerations to follow because of the large magnitude of its capacitance. The ohmic reactance of the grid-to-plate capacitance in the frequency range from 500 to 1000 cycles per second

\* As is seen in Equation (23),  $R$  is also a function of  $\theta_{1c}$ . The role of  $R$  here is of secondary importance due to the fact that the changes in value of  $\theta_{1c}$  are relatively small for a wide range of values of  $R$ .

is seen in Figure 5 to vary from 180 to 95 ohms. If the resistor,  $R$ , is to satisfy condition 1 in this frequency range, its magnitude should exceed 1000 ohms. It is evident that a tuning stub\* installed across  $R$ , will be necessary in order to tune out  $C_{gp}$  and  $C_{s2}$  so that the quadrature characteristics of the  $RC$  network will be maintained.

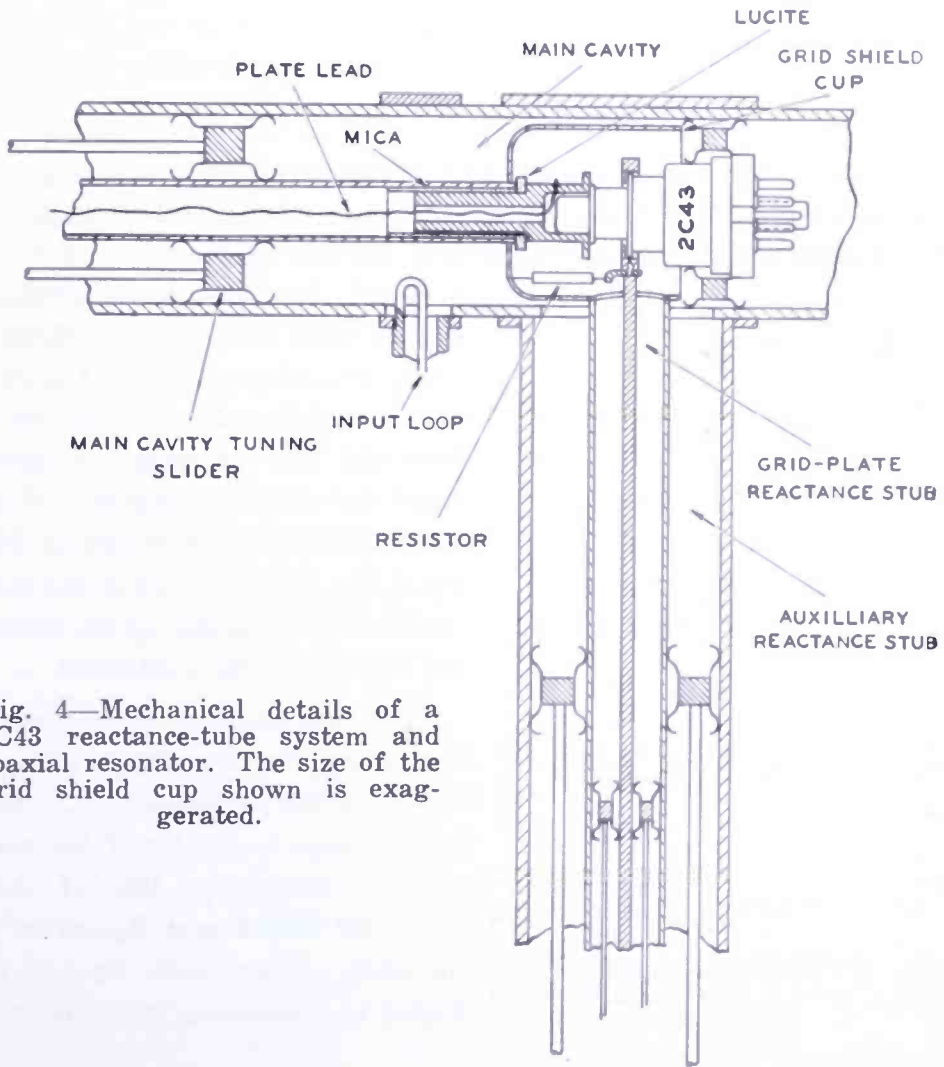


Fig. 4—Mechanical details of a 2C43 reactance-tube system and coaxial resonator. The size of the grid shield cup shown is exaggerated.

This tuning stub is shown in Figure 4 and it is easily verified that if the characteristic impedance of this stub is  $Z_{03}$ , the  $Q$  of this grid-to-plate resonant system (see condition 4) when considered alone as a component member of the total system will be<sup>19</sup>

\* As other illustrations of the use of tuning stubs to tune out inter-electrode capacitances, see, for example: W. M. Kellogg—U. S. Patent 2,416,322, Feb. 25, 1947; W. Van B. Roberts—U. S. Patent 2,344,734, March 21, 1944.

$$Q_3 = \frac{1}{2} \left[ \omega R |C_{gp} + C_{s2}| + \frac{2\pi l_3}{c} \frac{R}{Z_{o3}} |1 + (\omega Z_{o3} \{C_{gp} + C_{s2}\})^2| \right] \quad (55)$$

where  $l_3$  is the length of this stub. In a coplanar tube such as a 2C43, the grid-to-plate capacitance is small and this expression reduces to

$$Q_3 \cong \frac{\pi R}{4 Z_{o3}}. \quad (56)$$

In order to minimize the coupling between the grid-to-plate tuning stub and the main resonant cavity, a cup is placed over the grid-to-plate region of the tube, as pictured in Figure 4, in order to serve as a shield. In addition, an auxiliary tuning stub is installed which is concentric with respect to the grid-to-plate stub and which serves to tune out the impedance resulting from the stub sticking out of the main cavity. As is shown in Figure 4, the lengths of all of the three cavities which make up the system are independently controlled.

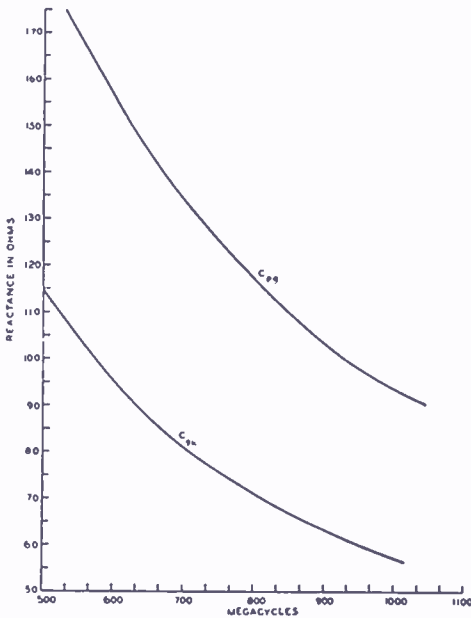


Fig. 5—Ohmic reactance of  $C_{gp}$  and  $C'_{pk}$  of a 2C43 triode versus frequency.

For calculations of frequency deviation, the auxiliary stub of characteristic impedance,  $Z_{o2}$ , which is connected to the tip of the main cavity transmission line of characteristic impedance,  $Z_{o1}$ , must be included. When each line is adjusted to resonance, it follows that

$$\Delta f = \frac{Z_{o1} Z_{o2}}{\pi^2 L_{ob} [Z_{o1} + Z_{o2}]}. \quad (57)$$

In considerations of the  $Q$  of the entire system, the stored energy in both the auxiliary stub and the grid-to-plate stub must be included with that of the main-cavity transmission line and if the principal loads of the system are  $R$ , and,  $r_p$ , it can be shown that the system  $Q$  is very nearly equal to

$$Q_{\text{system}} \cong \frac{\pi}{4} R_T \frac{Z_{o1} Z_{o2} + Z_{o1} Z_{o3} + Z_{o2} Z_{o3}}{Z_{o1} Z_{o2} Z_{o3}} \quad (58)$$

The electrical connections to the tube are made as follows: The cavity structure is at the same potential as the 2C43 grid. The plate lead is brought to the plate cap of the tube through the center conductor of the main cavity and appropriate potentials are applied between the cathode pin of the tube and the plate and grid.

### B. Determination of the System Characteristics

Let the system characteristics which can theoretically be obtained for such a 2C43 coaxial system be computed for the case where  $Z_{o1} = Z_{o2} = Z_{o3} = 55$  ohms and  $R = 1,500$  and  $3,000$  ohms—the smaller value of resistance being at least ten times greater than the ohmic reactance of the grid-to-cathode capacity in the frequency range from 500 to 1,000 megacycles.

Using the values,  $R = 1,500$  ohms,  $C = 2.8 \times 10^{-12}$  farad,  $r_p = 6,000$  ohms, and  $g_m = 8 \times 10^{-3}$  mho, for a set of sample calculations at the point of maximum frequency deviation, it follows from Equations (11), (57), (58), (56), and (28), that

$$L_{ab} = \frac{1,500 \times 2.8 \times 10^{-12}}{8 \times 10^{-3}} = 0.526 \text{ microhenry} \quad (59)$$

$$\Delta f = \frac{55 \times 55}{\pi^2 \times 0.526 \times 10^{-6} \times 110} = 5.28 \text{ megacycles} \quad (60)$$

$$Q_{\text{system}} = \frac{\pi \times 1,200}{4 \times 18.3} = 51.5 \quad (61)$$

$$Q_3 = \frac{\pi \times 1,500}{4 \times 55} = 21.3 \quad (62)$$

$$\theta_1 \cong \frac{4 \times \pi \times 5 \times 10^8 \times 2.8 \times 10^{-12}}{8 \times 10^{-3}} \cong 2.2 \text{ radians.} \quad (63)$$

Using the calculations of the type described in equations (59) and (60),  $\Delta f$  may be plotted as a function of  $E_g$  as shown in Figure 7\* using values of  $g_m$  from Figure 6 which is a derived curve from a set of 2C43

\* In deriving the curves in Figure 7, the contributions to  $\Delta f$  by the RC network (see Equation (9)) are neglected.

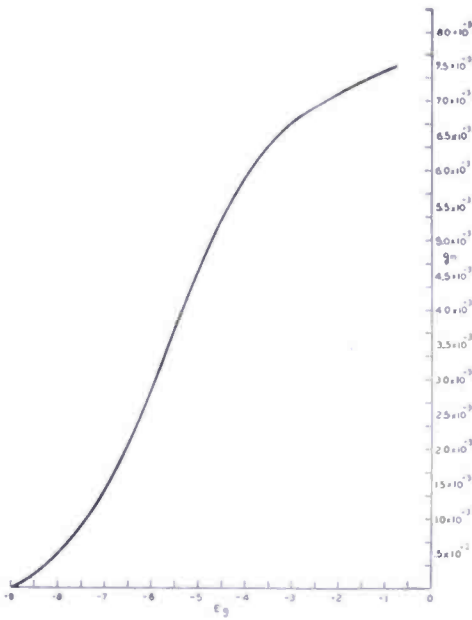


Fig. 6 — Transconductance of a 2C43 versus grid voltage for  $E_p = 250$  volts.

characteristic curves and pictures of a curve of  $g_m$  versus  $E_g$  for a constant plate voltage of 250 volts. Two  $\Delta f$  vs.  $E_g$  curves are shown in Figure 7—one corresponding to  $R = 1,500$  ohms and the other to  $R = 3,000$  ohms. Note that up to 5 megacycles of frequency deviation are possible for  $R = 1,500$  ohms—the frequency deviations being halved as the resistance is increased to  $R = 3,000$  ohms. Actually, as the grid is biased more negatively such that  $\theta_1$  increases, the  $\Delta f$  vs.  $E_g$  curve for the ultra-high-frequency curve will go to zero more rapidly than that predicted by the low frequency curve thereby narrowing the effective region in which the

grid swing can take place. According to Equation (23), which is based on an idealized tube using the approximations listed in (18), the shunt susceptance of the triode reactance tube will go to zero at  $g_m = 3.95$  and  $3.83$  for  $R = 1,500$  ohms and  $3,000$  ohms, respectively. As is seen in Figure 6, these values of  $g_m$  correspond to grid voltages in the vicinity of  $E_g = -5.5$  volts. Since  $g_m$  goes rapidly to zero as the grid bias is increased from  $E_g = -5.5$  volts to the cut-off voltage of  $-9$  volts, contributions of shunt susceptance in this range from the reactance tube will not be useful and the predicted effective range of grid voltage variation is seen to be  $-5.5 \leq E_g < 0$ .

Note that the predicted value of  $Q$  of the cavity system is high enough to permit measurements of sufficient accuracy (as will be pointed out, the measured  $Q$  is actually somewhat higher) and the bandwidth of the tuning stub will easily accommodate a frequency shift of 5 megacycles. The loading considered here is somewhat academic since no load is included in the system that would simulate a shunt load which would actually be

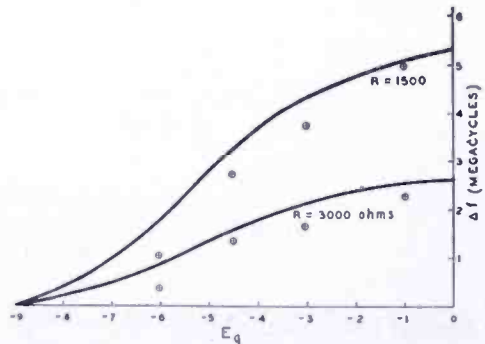


Fig. 7 — Theoretical and experimentally observed performance of the 2C43 reactance-tube system pictured in Figure 4 for  $R = 1500$  ohms and  $R = 3000$  ohms. The dots represent the experimental data.

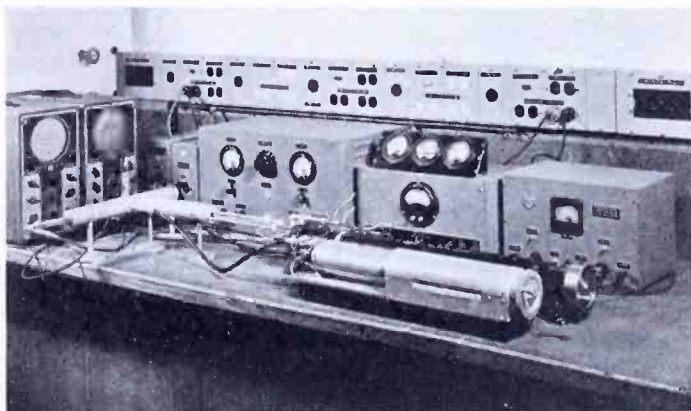
met in practice and which would lower the system  $Q$ .

Since the total grid swing variation is confined to a range of less than 6 volts, the maximum value of  $e_g$  is limited to around  $\frac{1}{2}$  volt. The ratio of  $R$  to  $1/\omega C'_{gk}$  varies from 13 to 30 in the frequency range from 500 to 1,000 megacycles for  $R = 1,500$  ohms and it is evident that the maximum value of radio frequency voltage,  $e_{ab}$ , cannot exceed 7 volts at 500 megacycles in order for the system to operate correctly and to permit variations of frequency.

### C. Operation of the Experimental System

Figure 8 pictures the laboratory set-up which was used for testing the reactance-tube system shown in Figure 4. Included in the photograph are the plate and grid power supplies, a modulated oscillator, a

Fig. 8—Photograph of the laboratory set up which was used for testing the reactance-tube system showing the driving oscillator, the power supplies and the wavemeters.



wavemeter assembly, and a crystal pickup, tuned-amplifier, and oscilloscope arrangement for detecting radio frequency fields in the coaxial cavity.

The system was operated\* at 500 megacycles for both values of  $R$  which have been discussed, with the driving loop from the oscillator adjusted to produce such field strengths in the resonator that the output of the crystal pickup was sufficiently above the noise level. As can be seen in Figure 6, the total variation of grid voltage which can be utilized for frequency modulation is in a range of less than 9 volts. 250 volts were applied between the plate and cathode and the cathode bias was varied from  $E_g = -9$  volts to  $E_g = -\frac{1}{2}$  volt in which vicinity, the grid began to draw current. The frequency deviations which were obtained for both values of  $R$  are included in Figure 7 as a set of points and it is seen that these deviations in the regions of smaller transit time compare favorably with those predicted, with up to 5 mega-

\* In these experiments, dynamic modulation characteristics and an extended transit-time investigation were beyond the scope of the investigation.

cycles of frequency deviation\* being obtained from  $R = 1,500$  ohms — the frequency deviation going to zero in the vicinity of  $E_g = -6.2$  volts. The measurements were made from point to point under steady-state conditions using the previously mentioned instruments with an accuracy of measurement, which was in the neighborhood of  $\pm \frac{1}{2}$  megacycle.

The measured  $Q$  of the resonator system with the reactance-tube in operation was found to be in the neighborhood of 65 which is somewhat higher than that predicted in Equation (61). This increase is readily attributable to the additional lumped capacity at the end of the transmission line which is provided by the grid-to-plate shield cup, the grid-to-plate interelectrode capacity and various stray capacitances all of which serve to increase the total stored energy of the system.

#### ACKNOWLEDGMENT

The author is indebted to several of his colleagues for valuable discussions; in particular, L. S. Nergaard, D. O. North, J. S. Donal, Jr., V. D. Landon, and E. W. Herold.

---

\* These deviations are commensurate with the deviations previously obtained in similar reactance tube systems by V. D. Landon and H. Kihn of this laboratory and with those obtained in the magnetrons using spiral beam frequency modulators which are reported on in Reference 2, although the powers involved are considerably different. In these magnetrons, using a spiral electron beam in each of nine cavities of a twelve cavity magnetron, a total frequency deviation of 3.5 megacycles at 1 kilowatt output and about 4 megacycles at 750 watts output was obtained in the 850 to 900 megacycle range.

# ULTRAFAX\*

BY

DONALD S. BOND† AND VERNON J. DUKE‡

*Summary*—An experimental high-speed system of record communication known as *Ultrafax* is described. It is a facsimile transmission method capable of operating at speeds of over a million words per minute. Electronic scanning and many of the other techniques of television are employed. At the sending terminal a flying-spot kinescope using a single-line sweep scans copy previously recorded on photographic film. A 7000-megacycle radio-relay system of band width of 4 to 6 megacycles has been employed for transmission tests. At the receiving terminal a second projection kinescope is modulated in intensity by the received video wave. Moving photographic film records the focussed kinescope image. This film is then rapidly developed in a film-processing apparatus with a total delay of less than 45 seconds.

System tests over microwave circuits up to 28 miles in length have given speeds of 500,000 words per minute of adequate commercial quality. This is 60 to 100 times as fast as is possible in mechanical facsimile systems currently used.

## INTRODUCTION

RECENT advances in the communication field have made it technically possible to transmit wider and wider bands of frequencies over long distances. Major economies in operation are foreseen from these developments, particularly from wide-band radio-relaying circuits in the ultra-high-frequency and super-high-frequency ranges.

A study has been undertaken of new methods and apparatus for the terminal points to keep pace with the greater intelligence-handling capabilities of the transmission circuits. The system to be described is adapted to the transmission of written or recorded messages. It is capable of handling a large volume of traffic over a wide-band communication system. The principle of operation and the terminal apparatus required are relatively simple and give promise of economical operation. This system of record communication<sup>1</sup> has been designated "Ultrafax."

There are various fundamental methods of utilizing a transmission

\* Decimal Classification: R580×R581.

† Research Department, RCA Laboratories Division, Princeton, N. J.

‡ Engineering Department, National Broadcasting Company, Inc., New York, N. Y.

<sup>1</sup> Examples of *record communication* include written or printed material, photographs, line drawings, or other illustrations.

system for the sending of a sequence of unrelated messages by telegraph, facsimile, or telephone. Some such multiplexing methods divide the frequency spectrum while others operate on a time-sharing basis. Probably the simplest of all — and it is of the time-division type — is one in which *complete messages* are transmitted in sequence.

In the case of the older open-wire or cable-pair circuits, the outside plant cost was relatively high in comparison with that of terminal equipment on a long circuit. Consequently it became desirable to economize on band width wherever possible. This necessitated rather elaborate terminal equipment. On the other hand, with radio-relay systems having intelligence bands ranging from hundreds of kilocycles up to a number of megacycles in width, it is found that annual costs *per kilocycle* of communication band width are only a small fraction of the corresponding wire-line costs. When these wide-band

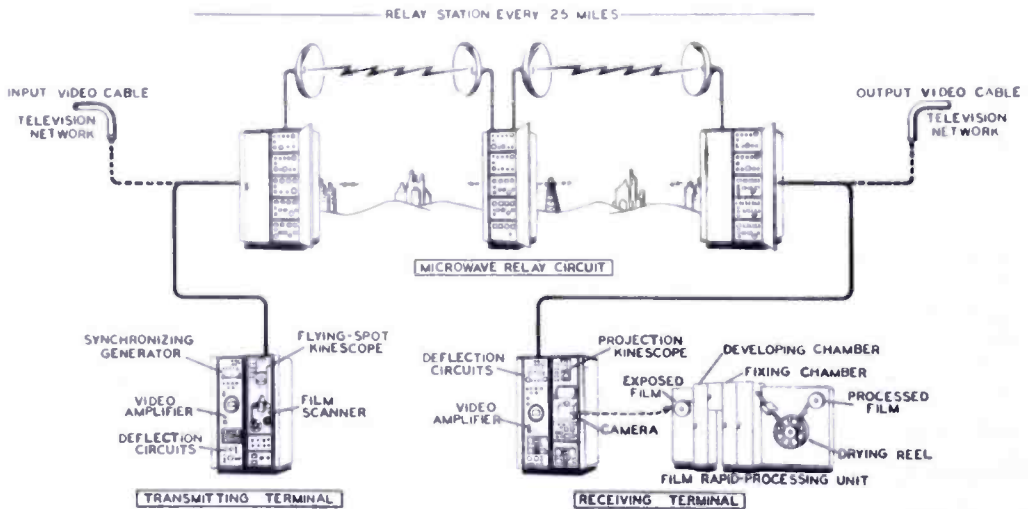


Fig. 1—Functional diagram of Ultrafax system.

relay systems are employed, entirely different types of equipment become practical for large traffic volume.

### SYSTEM DESCRIPTION

Ultrafax is a facsimile transmission method employing electronic scanning and many of the other features of television. Photographic means are employed for recording the messages. With intelligence band widths of the order of 3 to 5 megacycles, Ultrafax has proved capable of transmitting written copy at rates up to 480 or more pages per minute.

The elements of the basic Ultrafax system are shown diagrammatically in Figure 1. At the transmitting end a flying-spot kine-

scope unit scans copy previously recorded on photographic film. The resulting video signals are mixed with synchronizing pulses and transmitted by a microwave radio-relay system. At the receiving terminal a second kinescope is modulated in intensity by the received video wave and deflected in synchronism with the scanner. This kinescope is imaged on moving photographic film in the camera. The film is then rapidly developed. The finished film may then be used in several different ways: to make enlarged prints of each page, to be projected onto a screen for immediate reading, or to be re-scanned on a slower-speed outgoing branch circuit.

The following detailed description refers to an experimental Ultrafax system used to test and demonstrate some of the potentialities of the method.

### FLYING-SPOT SCANNER

The method of scanning that uses a projection kinescope tube as the source of light<sup>2</sup> is particularly well adapted to the Ultrafax application. Good definition, freedom from shading difficulties, and absence

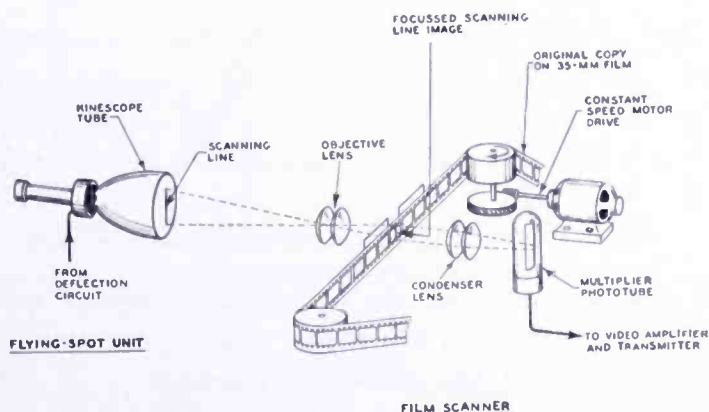


Fig. 2—Method of operation of Ultrafax sending terminal.

of image-storage requirements are factors in favor of its use. Single-line deflection is used. The circuits for this are similar to those of horizontal scanning in television. Scanning in the direction perpendicular to the line scan is accomplished by uniform movement of the copy to be transmitted.

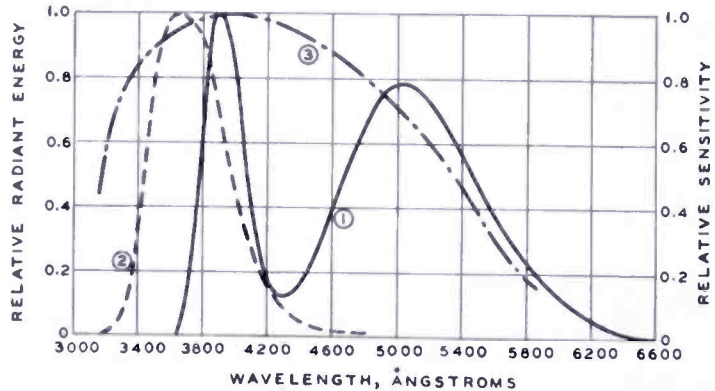
In Figure 2 the elements of the scanning system are shown. The line-deflection circuits produce a linear sweep and quick retrace during the blanking interval at a repetition rate that can be adjusted from 6 to 16 kilocycles. Blanking signal is applied to the kinescope control grid. Light from the illuminated spot on the tube screen passes

<sup>2</sup> G. C. Sziklai, R. C. Ballard, and A. C. Schroeder, "An Experimental Simultaneous Color-Television System, Part II," *Proc. I.R.E.*, Vol. 35, p. 862, September, 1947.

through the lens system, where it is focussed on the film. This light in passing through the film is modulated in intensity. The modulated light is then focussed on the multiplier phototube by the condensing-lens system. The output of the phototube constitutes the video signal.

The projection kinescope of the flying-spot scanner has a flat screen 5 inches in diameter. The tube operates at a second-anode potential of 24 to 27 kilovolts. Depending upon the type of phosphor used, the second-anode current may be adjusted to an average value of 1 to 30 microamperes. The commercially-available type 5WP15, which at the present time has a zinc-oxide screen, has been used for this purpose. Improved results have been obtained by the use of experimental tubes in which a smaller spot diameter was obtained by limiting the maximum beam current to about the limit given above. Improved phosphor materials having high ultraviolet output and shorter persistence have also been employed with resulting better performance.

Fig. 3—Spectral characteristics. (1) Radiant energy from 5WP15 kinescope phosphor. (2) Radiant energy from experimental phosphor. (3) Sensitivity of phototube cathode.



Spectral response characteristics of the zinc-oxide phosphor and of the experimental type are given in Figure 3. The decay time of the principal visible component of the zinc-oxide phosphor is of the order of a microsecond, while for the improved phosphor it is perhaps only 10 per cent as long. Phosphors having very short decay time are desirable in order to produce the necessary detail resolution.

The objective lens of the scanner is corrected for aberrations and is designed to give a flat field. Enlarging lenses<sup>3</sup> of 75- to 100-millimeter focal length and with speeds of  $f:4.5$  or faster have been found suitable for use with 35-millimeter film.

The disposition of the various parts of the scanner may be seen in Figure 4. The film on which the copy to be transmitted has been recorded is fed from supply reel  $S_1$  through the optical system and to the take-up reel  $S_2$ . Drive roller  $D$  is rubber-covered. It is driven through a gear reduction from a synchronous motor located directly

<sup>3</sup> The Eastman projection Ektar lens  $f:4.5$  of 75-millimeter focal length has been used extensively in the tests.

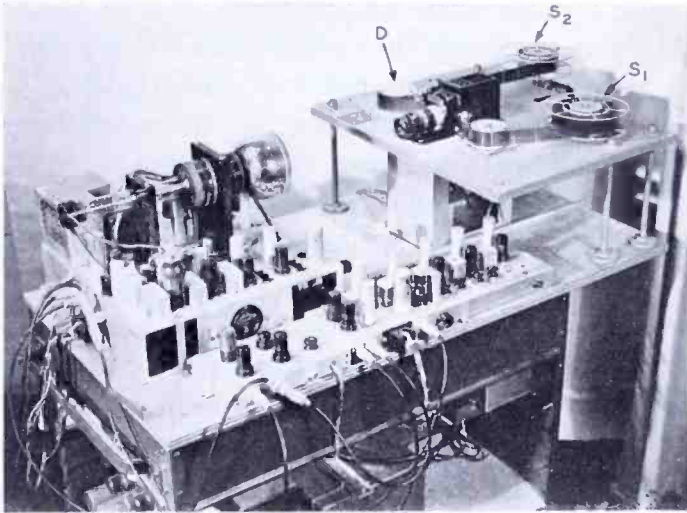
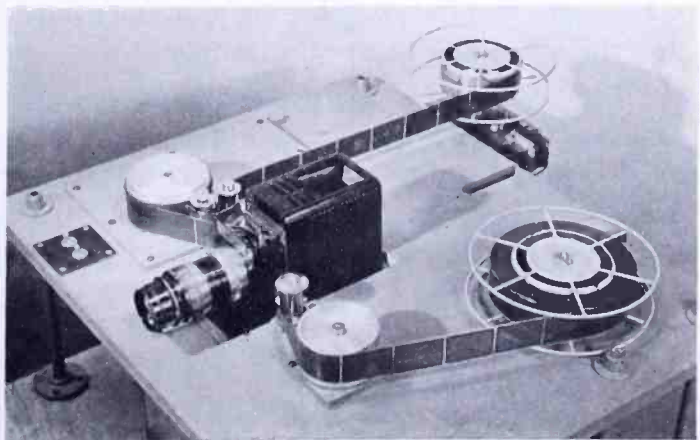


Fig. 4—Flying-spot scanner.

beneath *D*. A friction drive of this sort permits greater constancy of speed of the film as the latter is pulled through the optical gate than is possible with a sprocket drive. Furthermore, unperforated film may be used with resulting larger image size.

In the housing behind the optical gate are located the condensing-lens system and the phototube. As is seen in Figure 5, a commercially-available projector for 2 x 2-inch slides was converted for this use by replacing the incandescent projection lamp by the phototube. The latter is a type 931-A or a 1P21 9-stage multiplier type. The maximum sensitivity is at a wave length of 4000 angstrom units. The spectral characteristic is shown in Figure 3 for comparison with the kinescope phosphor light-emission curves. The maximum potential between cathode and anode of the phototube is 700 volts. This value is adjustable. One video amplifier stage is closely associated with the phototube and serves as a low-impedance source of video signal to feed into the equalizing amplifier.

Fig. 5—Optical system of flying-spot scanner.



A block diagram of the video chain is shown in Figure 6. The preamplifier previously described feeds into a four-stage video amplifier. A phase-inverter stage may be switched into the circuit if the opposite polarity of video signals is desired. Two of the video stages have adjustable resistance-capacitance networks in the cathode circuits to provide compensation for the persistence of the kinescope phosphor and to adjust the over-all high-frequency response. Blanking signal is introduced on the plate of the fourth video stage from a separate blanking amplifier. Video gain is controlled ahead of this point by grid-bias adjustment on several video stages and by variation of the phototube dynode voltage. The narrower line-synchronizing pulses are fed into the equalizing amplifier at the video output stage.

In transmission the variations in background brightness may be abrupt and occur with each new page of copy scanned. It is desirable for black-and-white (i.e. not continuous-tone) material like printing, line drawings, and handwriting that the background should be represented by a uniform video level. Low-frequency transmission must be maintained throughout the system, and correction must be made for poor low-frequency response before its cumulative effect becomes too great. The clamping amplifier that follows the equalizing amplifier acts to maintain the dc<sup>4</sup> and low-frequency response. If the blanking signal were limited after being added to the video wave, the clamp circuit should precede the blanking mixer stage.

A double diode tube is connected to form part of the grid-return circuit of the video output stage of the clamping amplifier of Figure 6. The two diode sections are keyed on during the latter portion of the blanking interval by pulses derived from the synchronizing signal. The bias conditions obtained during this interval are then maintained through the remainder of the line-scanning interval. The output composite video signal coming from the clamping amplifier is carried to a kinescope monitor, oscilloscope (for checking video and setup levels), and the video line to the transmitter.

High voltage for the projection kinescope used in the flying-spot scanner is obtained from a radio-frequency power supply.<sup>5</sup> The second-anode voltage is adjustable up to 27 kilovolts. The first-anode supply is from a bleeder across one-third of the output and is adjustable. For the experimental high-definition tubes, a potential of 5 to 6 kilovolts is required for focus.

<sup>4</sup> K. R. Wendt, "Television DC Component," *RCA Review*, Vol. 9, No. 1, p. 85, March, 1948.

<sup>5</sup> R. S. Mautner and O. H. Schade, "Television High Voltage R-F Supplies," *RCA Review*, Vol. 8, No. 1, p. 43, March, 1947.

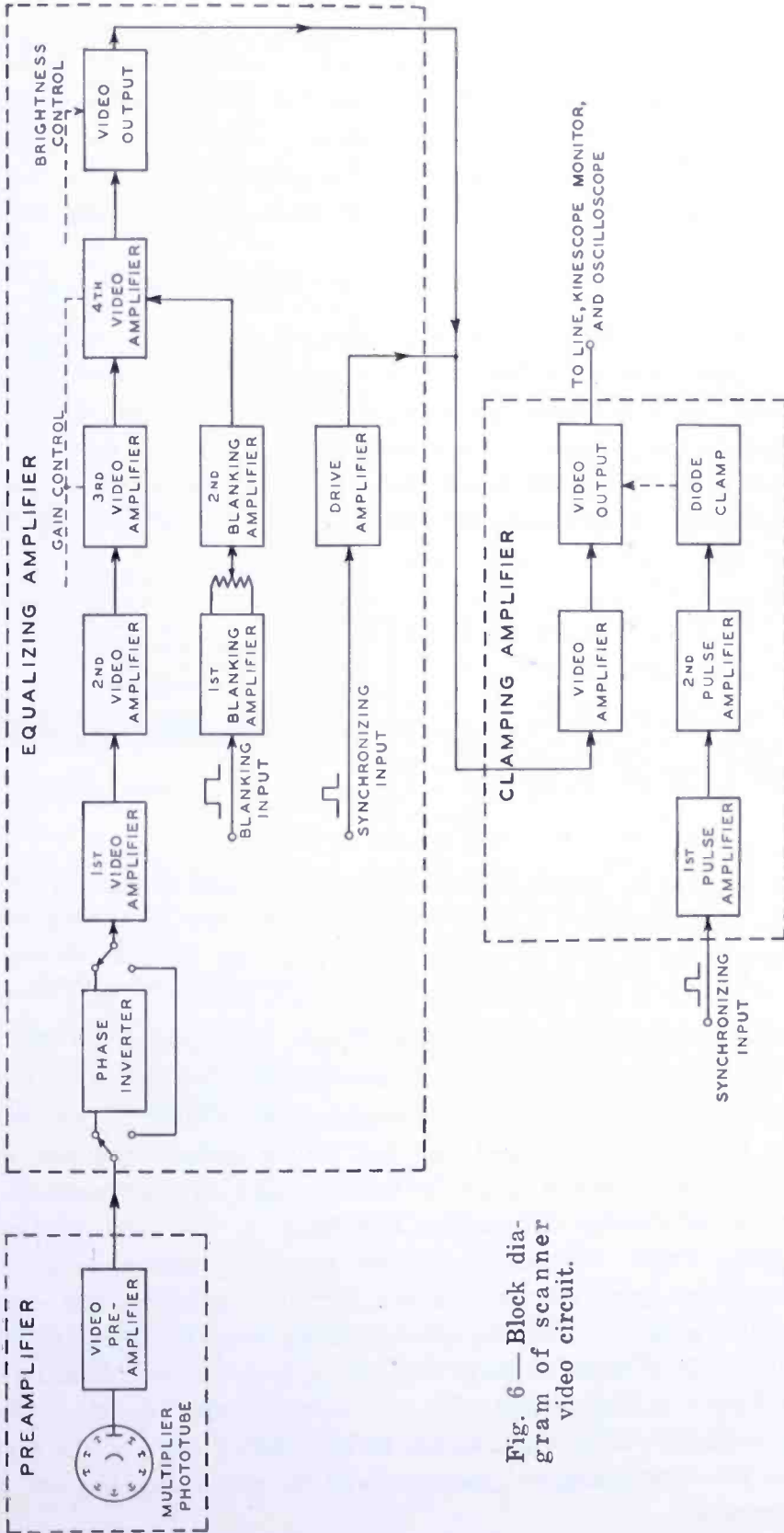


Fig. 6—Block diagram of scanner video circuit.

While deflection in the direction normal to line scanning is not required during actual transmission, it is convenient to make provision for scanning a complete raster for preliminary adjustment purposes. This deflection, which will be referred to as "vertical" deflection from its counterpart in television operation, is derived from a free-running blocking oscillator and is set to approximately 60 cycles.

### SYNCHRONIZING GENERATOR

The synchronizing generator is required to furnish output at only one frequency, viz., line-repetition frequency. As is shown in Figure 7, the source is a free-running sine-wave oscillator. This is ordinarily operated at a frequency of 6.3 kilocycles. Its output is converted into a square wave by a limiter and then into alternate positive and negative pulses by a differentiator circuit. Only the positive pulses are

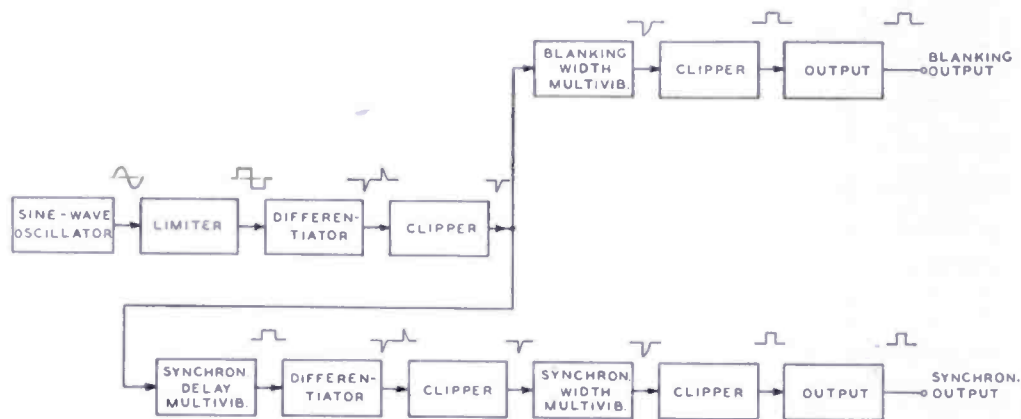


Fig. 7—Block diagram of synchronizing-generator circuit.

transmitted through the following clipper. The output of the latter then consists of pulses of about 1-microsecond length which key two multivibrators. One of these determines the width of the blanking pulse. Its output is clipped and fed into a cathode-follower output stage. The pulse width is set between 12 and 18 microseconds. The second multivibrator determines the delay in the start of the synchronizing pulse. A pulse is derived from the trailing edge of the synchronizing multivibrator output by differentiating and clipping. This pulse is used to key the synchronizing-pulse-width multivibrator. The latter then feeds circuits similar to those in the blanking chain to produce a second output of 5 to 8 microseconds' duration, delayed about 3 microseconds with respect to the leading edge of the blanking pulse. The synchronizing generator and its power supplies are shown in Figure 8.

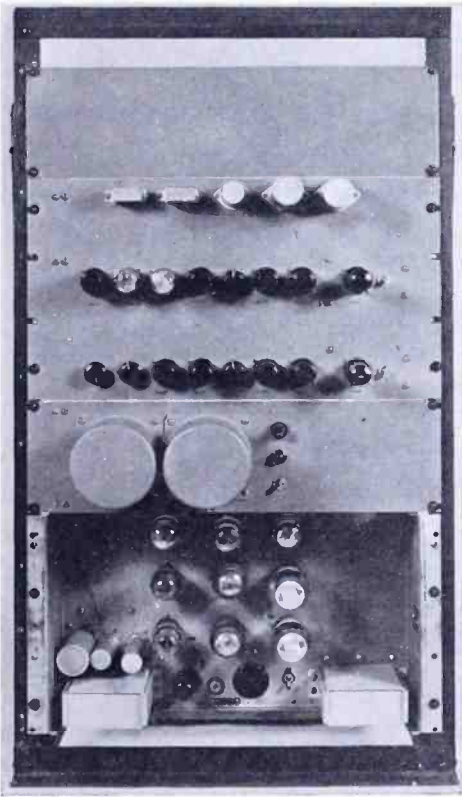


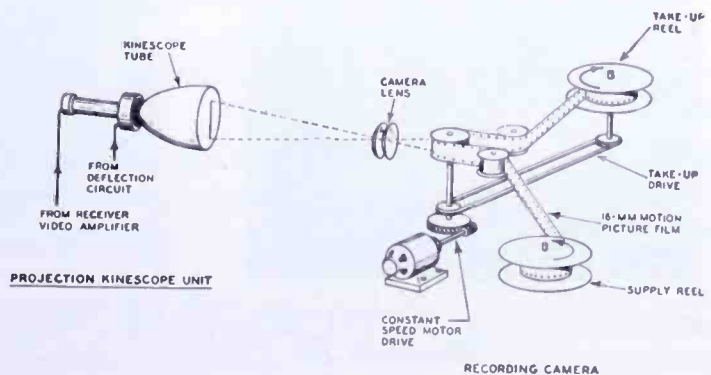
Fig. 8—Synchronizing generator.

### RECEIVING TERMINAL

The Ultrafax receiving-terminal equipment employs the same type of single-line sweep as in the scanner. The principle of operation will be seen in Figure 9. The beam of the projection kinescope is modulated in intensity by the video signal applied to its control grid. The light strikes the objective lens of the recording camera and is focussed as a transverse line on the 16-millimeter film. The latter moves continuously from a supply reel, past the lens system, and to the take-up reel. A synchronous motor with gear reduction drives a rubber-covered roller or capstan directly behind the lens, and this roller drives the film. Linear speed of the film is about 22 feet per minute.

The projection kinescope used in the receiving terminal is similar to the 5WP15 of the scanner except that a P-11 phosphor is used. The actinic value of the light from this screen is high when used with blue-sensitive recording film. The spectral response of the P-11 phosphor is shown in Figure 10. Its peak is at a wave length of about 4600 angstrom units, corresponding rather closely to the region of maximum film sensitivity.

Fig. 9 — Method of operation of Ultrafax receiving terminal.



The camera uses a Zeiss Biotar f:2 lens of 45-millimeter focal length. Apertures of f:2.4 to f:3.5 give adequate exposure with positive-type motion-picture film<sup>6</sup> at average kinescope beam currents of 3 to 10 microamperes. These values of current vary with different types of copy and correspond to peak currents in highlights 5 to 10 times as great.

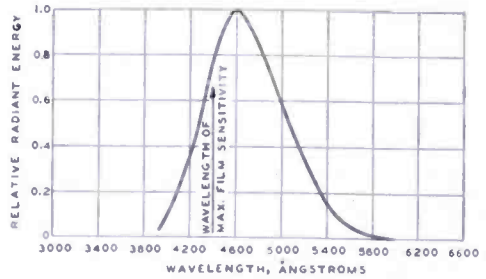


Fig. 10 — Spectral characteristic. Radiant energy from kinescope P-11 phosphor.

The complete receiving-terminal electrical equipment is shown in Figure 11, with a view of the camera with its cover removed in Figure 12. On the left rack of Figure 11 are located the deflection circuits, the video amplifier and synchronizing-signal separator, a monitor unit, and power supplies. At the top on the right side is the kinescope projector unit. The cathode-ray tube is located in the cylindrical housing with its face down. On the panel associated with this unit are the video-output and clamping-amplifier circuits.

Beneath the kinescope projector unit is located the high-voltage radio-frequency power supply, below which is the camera. Next is a

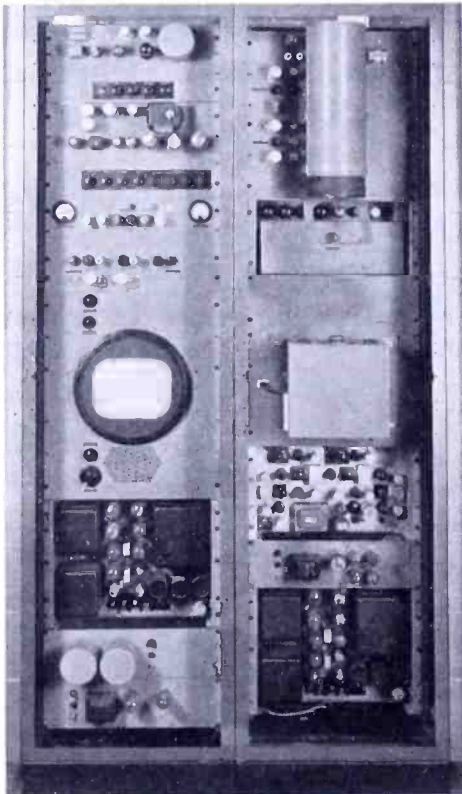


Fig. 11—Receiving terminal equipment.

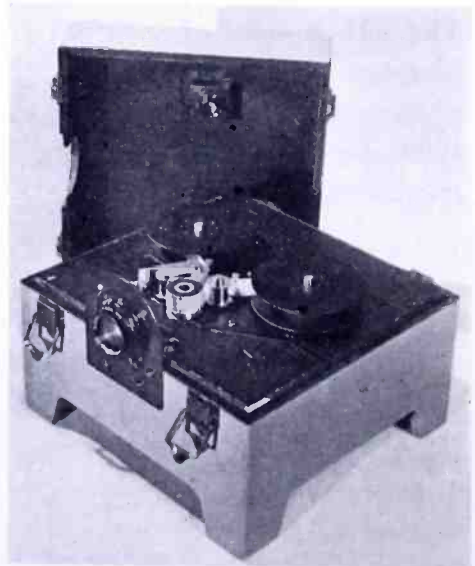


Fig. 12 — Recording camera with cover removed.

<sup>6</sup> Eastman Fine-Grain Release Positive Safety Film Type 7302.

compensating amplifier which may be switched into the video chain to correct for certain types of high-frequency phase distortion introduced during transmission. Additional power supplies are at the bottom of the rack.

From the block diagram of the receiving-terminal circuit in Figure 13 it will be seen that the arrangement is rather similar to that used in television receivers and monitors. After the synchronizing pulses have been separated from the video signal they control the deflection unit and also feed the clamping circuit. In the latter the pulses are delayed by approximately their own width by differentiation and re-forming. These delayed pulses then occur during the "back-porch" interval of the blanking signal. Both polarities are obtained from the final pulse amplifier and used to key the diode clamp stage.

#### FILM-PROCESSING EQUIPMENT

The high speed of transmission of information through the electrical part of the circuit would be of little value if there were to ensue a long delay in developing the film at the receiving point. The time lag of film processing is limited to a few seconds by the rapid-processing unit shown in Figure 14. This was built by the Eastman Kodak Company<sup>7</sup> as an experimental unit intended for the study of rapid processing of film in compact equipment. It was made available to RCA Laboratories for use in the Ultrafax tests and demonstrations. The machine develops, fixes, washes, and dries film continuously and with a total elapsed time of less than 45 seconds. The equipment shown in Figure 14 can process 16-millimeter film at a speed of 8 feet per minute. Larger machines have been built, operating at rates up to 90 feet per minute with shorter processing times and for use with either 16- or 35-millimeter film.

In Figure 14 the apparatus is shown set up for operation. Exposed film on a spool in light-tight compartment *A* feeds in sequence through three miniature tanks located in the processing chamber *P*. The film next passes through the spray wash at *W*<sub>2</sub>, an air squeegee at *B*, and then around heated drying rollers *R*<sub>1</sub> and *R*<sub>2</sub>. It is finally taken up on spool *S*.

Developing and fixing solutions flow from bottles *M* and *N* respectively to constant-level reservoirs, from which the liquids pass at a slow flow rate to the developing and fixing tanks. Each processing

<sup>7</sup> A similar development has been described by F. M. Brown, L. L. Blackmer, and C. J. Kunz, "A System for Rapid Production of Photographic Records," *Jour. Franklin Inst.*, Vol. 242, p. 203, September, 1946.

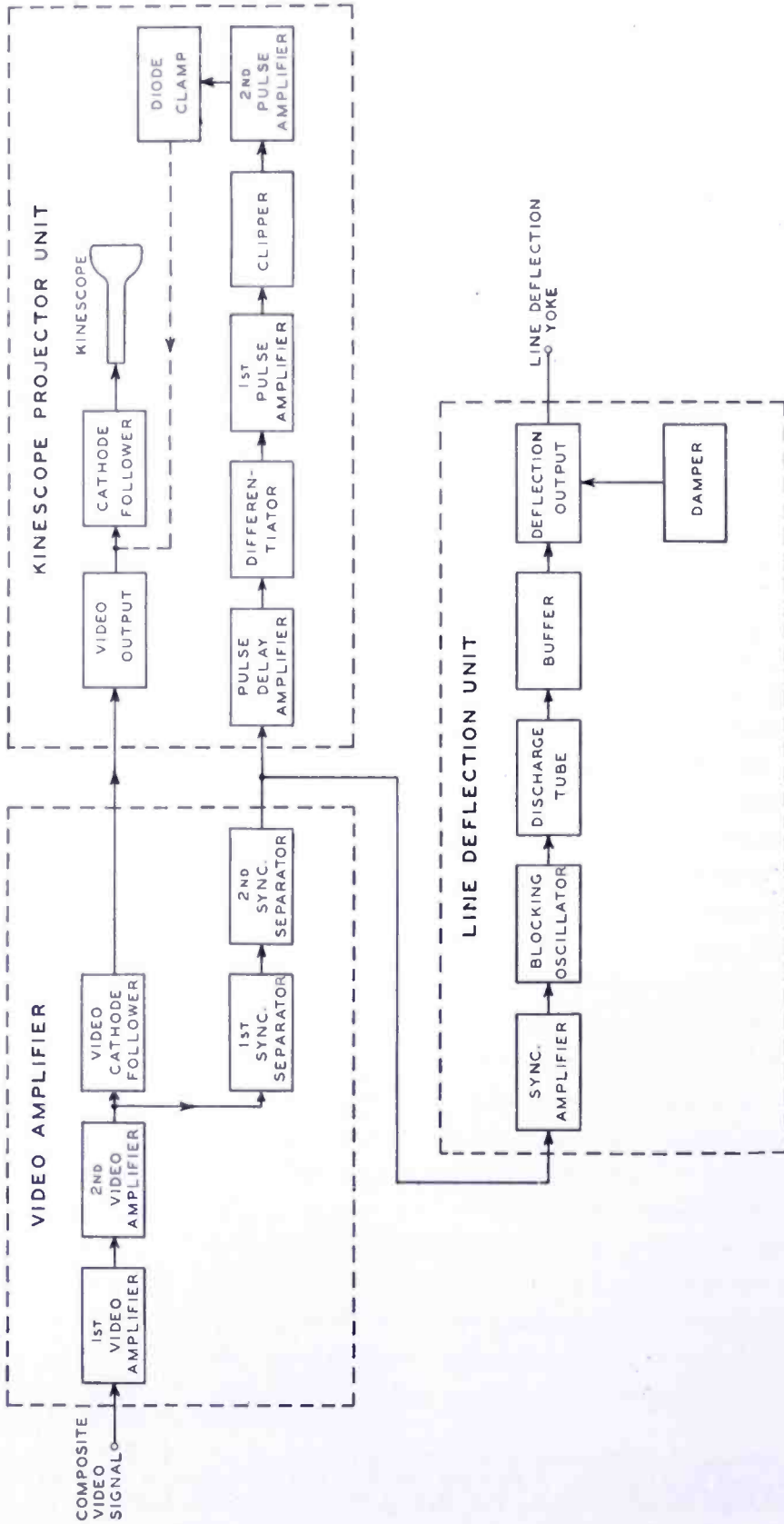


Fig. 13—Block diagram of receiving terminal circuit.

tank holds approximately one ounce of solution and is constantly being replenished.

A better view of the film path is obtained in Figure 15. The water-jacketed tank unit has been removed to show the developing, rinsing, and fixing tanks, *D*, *W*<sub>1</sub>, and *F*. The film loops *L*<sub>1</sub>, *L*<sub>2</sub>, and *L*<sub>3</sub> are formed in the tanks during threading as the film elevator which carries the racks is lowered to the position shown. Three loops are normally used, except when the film image is to be reversed.

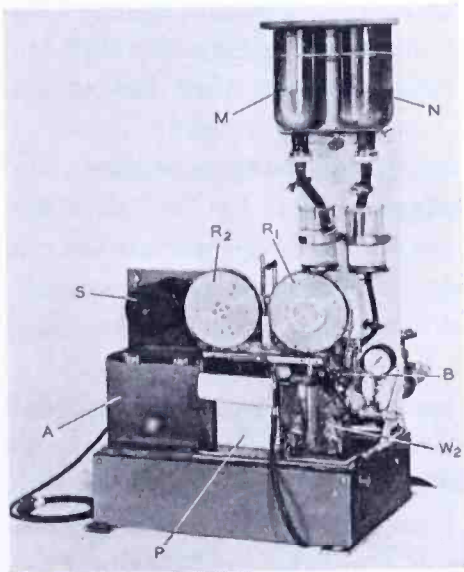


Fig. 14—Film-processing unit. Threaded and with processing chamber in place.

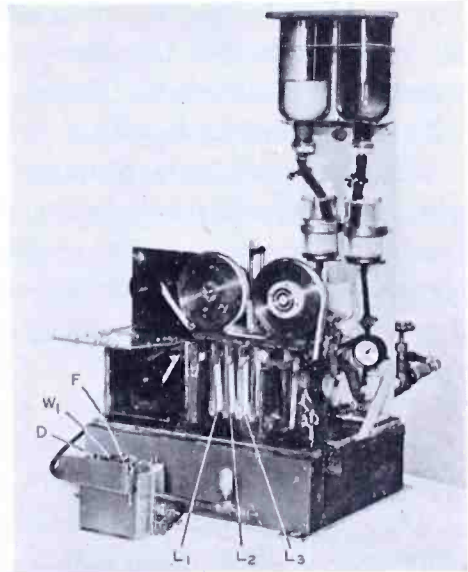


Fig. 15—Film-processing unit. Processing chamber removed to show film path.

The elapsed time in each processing tank is approximately 5 seconds. Final washing and drying require an additional 25 to 30 seconds. The unusually high developing and fixing rate results from the use of highly active chemical solutions at temperatures of 125 to 140 degrees Fahrenheit. The emulsion on the film is relatively hard, and the elapsed time in the hot solutions is very short. As a result there is no trouble due to softening of the emulsion. Fixing and washing are entirely adequate for long life of the finished film. The hypo content of film washed in this unit is such that it falls within the limit suggested for long-storage or *archival* use — for film of this type less than 0.010 milligrams of hypo per square inch.

#### SYSTEM TESTS

The Ultrafax equipment has been tested over both television-broadcast and point-to-point microwave radio circuits. In each case

intelligence band widths of the order of 4 to 6 megacycles were available. Early in 1947 tests were conducted with the predecessor of the equipment described over a 43-mile path. The transmitting terminal equipment was located at the laboratory of the National Broadcasting Company in the RCA Building, New York City. Video signals were sent through the regular television master-control facilities and then by coaxial cable to television station WNBT on the Empire State Building. The synchronizing pulses were re-formed by a "sync stretcher" before the composite signal passed into the transmitter. The Ultrafax signal was transmitted in the conventional manner for television in the 66-72-megacycle band. It was picked up at Princeton, New Jersey, and demodulated. The video signals were fed to the Ultrafax receiving terminal.

Demonstrations were made to various industry, military, and government groups during the period May to July, 1947. Fair detail resolution was obtainable at that stage, but because certain of the circuit features previously described were not incorporated, the resulting received images on the film suffered from hum patterns, "bounce," and geometric distortion.

The improved equipment was tested on a microwave television circuit in the spring of 1948. One link of the television-relay circuit operated by the National Broadcasting Company between Philadelphia and Washington was used. The transmitter was located at the Brandywine station of Western Union Telegraph Company near Wilmington, Delaware, while the receiving equipment was at the Elk Neck station of Western Union near Northeast, Maryland. The transmission distance was approximately 28 miles.

The relay transmitter<sup>8</sup> was an RCA type TTR-1A operating at approximately 7000 megacycles. This unit employs frequency modulation with a peak carrier deviation of 10 megacycles. An intelligence band of over 6 megacycles was available. This full amount was not utilized by the Ultrafax terminal amplifiers. The radio-frequency output of approximately 100 milliwatts was radiated from a six-foot parabolic antenna.

A similar antenna was used at the receiving point. This fed an RCA type TRR-1A receiver. The received signal was far above noise level throughout the tests. The Ultrafax terminal connected to the receiver output.

Operation could scarcely be distinguished from local video trans-

---

<sup>8</sup> W. J. Poch and J. P. Taylor, "Microwave Television Relay," *FM and Television*, Vol. 6, p. 30, August, 1946, also "Microwave Equipment for Television Relay Service," *Broadcast News*, No. 44, p. 20, October, 1946.

missions in the laboratory. Minor adjustments were required in the compensating amplifier to correct for altered high-frequency phase characteristics of the transmission circuit.

During these field tests transmissions were made of printed copy of typical book format as recorded on 35-millimeter microfilm. Pages set up in ten-point type were sent at the rate of 480 per minute, giving an equivalent of 300,000 words per minute. Definition and other characteristics of the received copy were much improved, approaching the quality of the same original material reproduced through only the photographic steps on 16-millimeter film.

Additional tests employing the same type of microwave radio-relay equipment were made in Washington, D. C., during September and October, 1948, preceding a series of public demonstrations. The propagation path was much shorter, the transmitter location being at the NBC station in the Wardman Park Hotel and the receiver point at the Library of Congress. Kinescope tubes for the flying-spot scanner were of the experimental type described above, with smaller spot size and ultraviolet-emitting phosphor.

Definition and uniformity of field brightness were better than on the previous tests. Measurements on the 16-millimeter-film image showed an over-all system resolution of 45 to 60 photographic lines per millimeter. This is the equivalent of about 85 to 115 lines per inch on the full-size original material.

Figure 16 illustrates a typical page of copy enlarged after transmission through the entire system. This was sent at the rate of 480 pages per minute. Printed material in much smaller type-size was also transmitted. Examination of the 16-millimeter recording film under a reading microscope showed that perfectly legible copy could be obtained at speeds of 1,000,000 to 1,200,000 words per minute while fair legibility was possible at 1,500,000 words per minute. Characters this small, however, would produce a rather poor enlarged print. Larger recording film, of perhaps 35-millimeter width, would help greatly in improving definition further. It is obvious that 45 to 60 lines per millimeter of over-all resolving power approaches the rated limit of 90 lines per millimeter for the recording film used.

#### CONCLUSION

As is evident from the foregoing discussion, the scope of this project has been limited to the demonstration of the possibilities of high-speed facsimile transmission. Methods of establishing a trunk circuit only have been investigated. The problems of concentrating

and distributing the traffic at the terminal points remain to be considered before a complete commercial service can be contemplated.

Electronic scanning means permit attaining speeds far greater than are possible with present-day mechanical facsimile methods. The Ultrafax system has been operated at speeds of 200 to 480 pages per minute with about 100-line-per-inch definition. This is 60 to 100 times as fast as the best mechanical facsimile system in current use. On printed or typewritten copy 300,000 to 500,000 words per minute with adequate commercial quality have been transmitted. Tests have been run up to speeds of 1,000,000 words per minute, and it appears reasonable to expect that further development will result in equally good commercial quality at such a speed. A comparison with printer-telegraph systems is shown in Table I. The equivalent number of voice bands, each of 3-kilocycle width, is shown for the carrier-telegraph cases.

### Gone with the Wind

171

even the plainest woman when she is utterly protected and utterly loved and is giving back that love a thousandfold.

They loved their men, they believed in them, they trusted them to the last breaths of their bodies. How could disaster ever come to women such as they when their stalwart gray line stood between them and the Yankees? Had there ever been such men as these since the first dawn of the world, so heroic, so reckless, so gallant, so tender? How could anything but overwhelming victory come to a Cause as just and right as theirs? A Cause they loved as much as they loved their men, a Cause they served with their hands and their hearts, a Cause they talked about, thought about, dreamed about—a Cause to which they would sacrifice these men if need be, and bear their loss as proudly as the men bore their battle flags.

It was high tide of devotion and pride in their hearts, high tide of the Confederacy, for final victory was at hand. Stonewall Jackson's triumphs in the Valley and the defeat of the Yankees in the Seven Days' Battle around Richmond showed that clearly. How could it be otherwise with such leaders as Lee and Jackson? One more victory and the Yankees would be on their knees yelling for peace and the men would be riding home and there would be kissing and laughter. One more victory and the war was over!

Of course, there were empty chairs and babies who would never see their fathers' faces and unmarked graves by lonely Virginia creeks and in the tall mountains of Tennessee, but was that too great a price to pay for such a Cause? Silks for the ladies and tea and sugar were hard to get, but that was something to juke about. Besides, the dashing blockade runners were bringing in these very things under the Yankees' disgruntled noars, and that made the possession of them many times more thrilling. Soon Raphael Semmes and the Confederate Navy would tend to those Yankee gunboats and the ports would be wide open. And England was coming in to help the Confederacy win the war, because the English mills were standing idle for want of Southern cotton. And naturally the British aristocracy sympathized with the Confederacy, as one aristocrat with another, against a race of dollar lovers like the Yankees.

So the women swished their silks and laughed and, looking on their men with hearts bursting with pride, they knew that love snatched in the face of danger and death was doubly sweet for the strange excitement that went with it.

When first she looked at the crowd, Scarlett's heart had thump-thumped

Fig. 16—Sample Ultrafax transmission. Sent over microwave circuit at rate of 480 pages per minute.

\* This page from GONE WITH THE WIND, by Margaret Mitchell, is reproduced by permission of the author and the publisher, The Macmillan Company, Copyright 1936 by The Macmillan Company.

Table I—Comparison of Telegraph and Ultrafax Traffic Capacities

Circuit	No. voice bands	Words per minute
Single teleprinter .....	....	60
One 4-channel multiplex .....	....	240
Ordinary wire line .....	1	1920
High-quality wire-carrier circuit .....	8	15,360
150-kilocycle radio-relay circuit .....	32	61,440
Ultrafax (present experimental system) ..	....	300,000-500,000

The circuit over which Ultrafax is to be transmitted must be of adequate band width and must have negligible delay distortion. Facilities that are satisfactory for the relaying of television signals may be used for Ultrafax. The present equipment actually utilizes a band only 50 to 75 per cent as wide as is needed for television. Flexibility in the operation of wide-band intercity circuits can result from the fact that television and Ultrafax services may be handled interchangeably.

The simplicity of the terminal apparatus in comparison with that required for the multi-channel frequency-division multiplex systems of Table I indicates that Ultrafax may have important economic advantages to communication organizations. This conclusion may be expected to hold even with the smaller volume of traffic now being handled on commercial circuits.

#### ACKNOWLEDGMENTS

The authors wish to acknowledge the assistance of and active encouragement by a number of individuals in the Radio Corporation of America, the National Broadcasting Company, and the Eastman Kodak Company in the carrying out of this joint development.

In particular C. J. Kunz of Eastman is responsible for the development of the film-processing unit and has cooperated in the tests and demonstrations. Advice and assistance of C. E. K. Mees and T. G. Veal of that organization are acknowledged. R. E. Shelby and R. M. Fraser of the National Broadcasting Company and C. J. Young and K. J. Magnusson of RCA Laboratories have contributed extensively in the development. Early proposals leading to the present system were made by C. W. Hansell.

Western Union Telegraph Company made available its facilities at the Brandywine and Elk Neck stations and assisted in some of the field tests. F. E. d'Humy of Western Union has given much encouragement to the engineering study.

# THYRATRONS IN RADAR MODULATOR SERVICE\*

BY

HUBERT H. WITTENBERG

Tube Department, RCA Victor Division,  
Lancaster, Pa.

*Summary*—This paper describes some of the wartime research which went into radar modulators. The relationship between the performance of thyratrons in radar modulator service and various thyatron characteristics and circuit parameters is shown. Analysis of the waveforms yields explanations of the various phenomena in terms of the deionization reignition potential.

## INTRODUCTION

THE characteristics of thyratrons were found to be ideal in radar modulator service where the requirements are high current (10-300 amperes), low tube drop, high voltage (500-15,000 volts), but low frequency (100-4000 cycles per second). For a more detailed discussion of the relative merits of thyratrons and other types of pulsers, as well as details of line modulators and some hydrogen thyratrons, reference can be made to "Pulse Generators" by G. N. Glasoe and J. V. Lebacqz, Vol. 5 of the Radiation Laboratory Series, chapters 1 and 6 to 10. Sufficient brief review is merely given in this article to enable the reader who is unfamiliar with the principles of operation of such devices to understand the effects on thyatron operation.

The first radars were modulated by vacuum-tube circuits in which the pulse was formed at low power and then amplified to drive the radio-frequency oscillator. The complexity, inefficiency, and power limitations of this type of modulator led to the development of the line modulator circuit.

A simplified line modulator circuit is given in Figure 1(a). Briefly, the operation of this circuit is as follows: the load is a radio-frequency oscillator, usually a magnetron, which sends out bursts of radio-frequency power when supplied with a square pulse of high voltage (Figure 1(b)). The pulse duration is of the order of 1 microsecond and the pulses may be 1000 microseconds apart. The pulses are produced by the closing of the switch. A negative wave front of voltage travels down the artificial line, is reflected at the open end without change of polarity, and returns, thus discharging the line. During this time, the current flowing through the switch and load is constant. When the

---

\* Decimal Classification: R337.12×R537.122.

negative wave front returns to the switch, however, the current ceases abruptly and a square pulse of current is produced. The interval between pulses is long enough so that the energy for charging the line may be supplied at a low rate or at a low power level. The discharge time is so short that the pulse power may reach megawatts.

The charging circuit consists of the power supply, charging impedance, line, and load in series. The power supply may be ac or dc, but the latter is more usual. Although the charging impedance may be supplied by either a resistor or a choke, the efficiency of the latter has made it standard. A typical charging waveform is shown in Figure 1 (c); this curve is for resonant charging which will be discussed later.

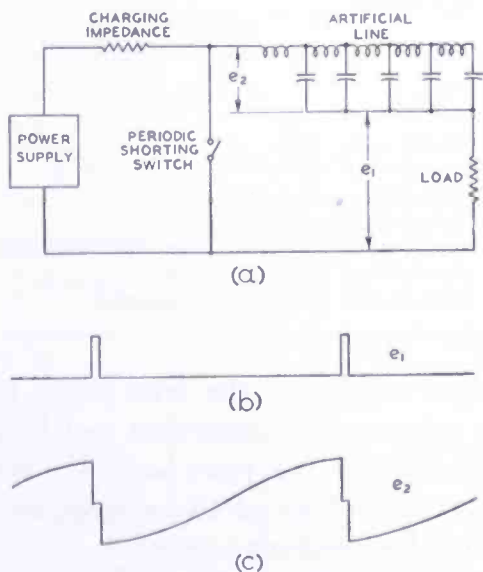


Fig. 1—(a) Simplified line modulator circuit.  
 (b) High-voltage pulse.  
 (c) Waveform of line charging voltage.

The periodic shorting switch is a gas discharge device of one of several forms. The early line modulator used a rotary spark gap, but the noise, maintenance problems, and time jitter of this device led to the use of fixed, triggered gas-discharge tubes. These tubes may be either of the cold-cathode or hot-cathode type. The cold-cathode types are: (1) two diodes in series triggered by a pulse of voltage applied to one diode, (2) trigatrons<sup>1</sup>, or (3) ignitrons. The hot-cathode type is the thyatron. It is the purpose of this paper to present some data on the frequency performance of thyratrons in radar modulator service.

DEVELOPMENT WORK ON THYRATRONS FOR RADAR MODULATOR SERVICE

Early in the war, the laboratories developing radar found that the type 884 thyatron operated very satisfactorily in a line-type pulse-former circuit. The low power output of this circuit, however, required amplification before use for modulation purposes.

In April, 1943, the RCA Laboratories at Princeton reported that two type 2050 thyratrons could be operated in parallel to give a peak power as high as 15 kilowatts. This amount of power was sufficient for direct modulation in low-power radars. Analysis of the circuit

<sup>1</sup> J. D. Craggs, M. E. Haine, and J. M. Meek, "The Development of Triggered Spark-Gaps for High-Power Modulators", *Jour. Inst. Elec. Eng.* (Brit.), Vol. 93 Part IIIA, No. 5, p. 963, March-May, 1946.

showed that each tube was passing 15 amperes. This amount of current was phenomenal for a tube rated at only 0.5 ampere in conventional service, but it was practical because the shortness of the pulse and the low duty cycle kept the average current low.

In the meantime, there was under development for airborne use a miniature 2050 now standardized as the type 2D21. This type was carefully tested for its pulse characteristics and was found, because of its small size, to be better in frequency performance than the 2050. Because of this fact, a concentrated effort to make the 2D21 suitable for pulse service ensued and the following pulse ratings were established.

Table I — Type 2D21

Heater Voltage (+5%, —10%)	7.0 volts
Peak Forward Anode Voltage	450 maximum volts
Control Grid Voltage	—100 maximum volts
Shield Grid Voltage	—100 maximum volts
Peak Cathode Current	25 maximum amperes
Average Cathode Current	20 maximum milliamperes
Rate of Rise of Cathode Current	75 maximum amperes per microsecond
Pulse Duration	6 maximum microseconds
Repetition Rate	90 maximum pulses per second

The type 3D22 thyratron is a larger version of the type 2050. It was developed for industrial use as a relay or grid-controlled rectifier, but was considered by the radar laboratories for pulse service. Its large cathode area permitted peak currents as high as 50 amperes, but the wide interelectrode spacings limited its frequency range.

The hydrogen thyratrons<sup>2</sup>, types 3C45, 4C35, and 5C22, developed especially for radar modulator service, were used for high-power radars. Some experiments were conducted in which hydrogen was substituted for the xenon normally used in types 2D21, 2050, and 3D22, but no new commercial tube types resulted. The results of these experiments are given in this paper.

The British had a concentrated program to apply the mercury thyratrons<sup>3</sup> to radar modulator service. In this they were quite successful in spite of the temperature-control equipment needed and the effects of cathode bombardment by heavy mercury ions.

The following chart gives the operating conditions at which various types were used in pulse service. Not all of the values, however, have been established as pulse ratings.

<sup>2</sup> Harold Heins, "Hydrogen Thyratrons", *Electronics*, Vol. 19, No. 7, p. 96, July, 1946.

<sup>3</sup> H. B. Knight and L. Herbert, "The Development of Mercury-Vapour Thyratrons for Radar Modulator Service", *Jour. Inst. Elec. Eng. (Brit.)*, Vol. 93, Part IIIA, No. 5, March-May, 1946.

Table II

Type	Peak Anode Volts	Peak Cathode Amperes	Peak Watts Output
884	350	0.5	88
2D21	450	25.0	5,620
2-2050's	1,000	30.0*	15,000
3D22	600	50.0	15,000
3C45	3,000	35.0	52,500
4C35	8,000	90.0	350,000
CV12**	15,000	200.0	1,500,000
5C22	16,000	325.0	2,600,000

\* 15 amperes per tube.

\*\* British type.

TEST PROCEDURE

Figure 2 shows the circuit used for comparing the performance of the various thyratrons in pulse service. In order to insure a basis for comparison, certain values of the circuit parameters were set up as standard.

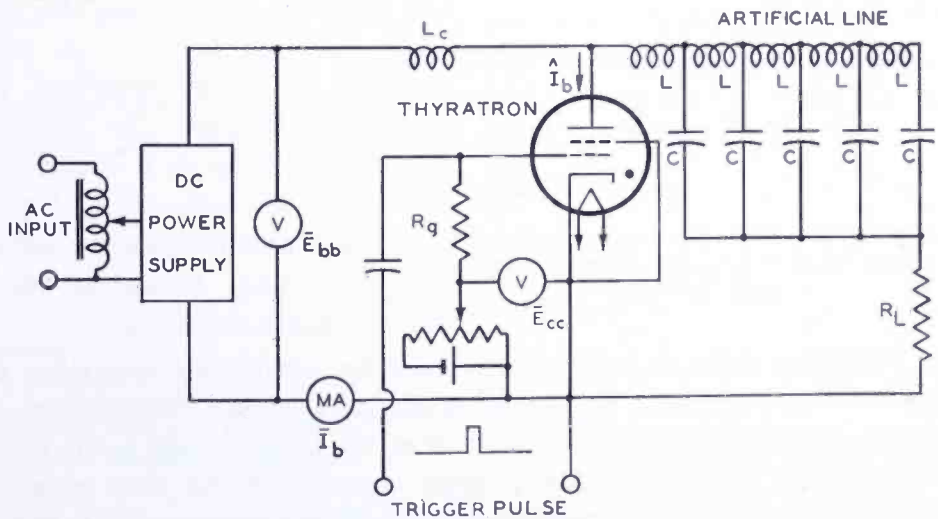


Fig. 2—Thyatron test circuit.

In the circuit of Figure 2, the thyatron is fired periodically by a trigger which is a voltage pulse of about 100 volts in magnitude and 15 microseconds in duration, produced by a multivibrator or blocking oscillator. Although most thyratrons can be maintained non-conducting by a small negative bias of about 5 volts, a much larger bias is needed to ensure rapid deionization. The standard value selected for these tests was -50 volts. The control-grid resistor ( $R_g$ ) is maintained at the standard value of 20,000 ohms. A smaller value would give a shorter deionization time, but would load the trigger circuit too much.

The artificial line is charged through the charging inductance,  $L_c$ . Because the charging inductance is approximately 1000 times as large as the inductance of the sections ( $L$ ) of the artificial line, the line can be considered as a lumped capacitor during the charging part of the cycle. It can be shown<sup>4</sup> that if the load ( $R_L$ ) is equal to or greater than the characteristic impedance ( $Z_n$ ) of the line, the voltage across the line just prior to the firing of the thyatron is double the supply voltage ( $E_{bb}$ ), irrespective of triggering frequency, magnitude of charging inductance ( $L_c$ ), or total capacitance of line ( $C_n$ ). However, in order to maintain a charging wave with an amplitude inde-

pendent of frequency,  $L_c$  is made much greater than  $\frac{1}{(\pi f)^2 n C}$  where  $n$  is number of sections in the line. Linear charging is obtained and, as a result, the voltage across the line rises at a constant rate. For

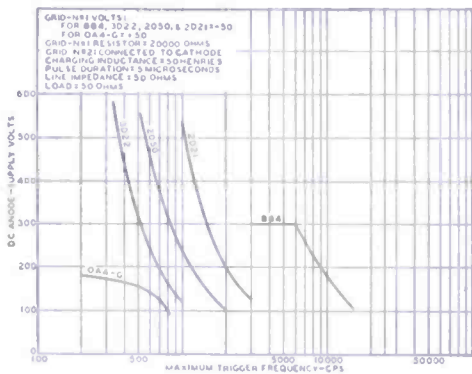


Fig. 3—Relationship between maximum trigger frequency and anode supply voltage.

the networks used, a value of 50 henries for  $L_c$  fulfills these conditions and was used in these tests.

As a standard condition the line was operated into a matched load<sup>5</sup> ( $R_L = Z_n$ ). In addition, a pulse duration of 5 microseconds was selected. Because the current through the tube is a function of ( $R_L + Z_n$ ), the value of  $Z_n$  depends upon the current capacity of the tube under test. Values of 10, 50, and 600 ohms were used.

Frequency runs on a tube were made by setting the frequency and then raising the supply voltage by means of a variac. With increasing voltage, the average current  $\bar{I}_b$ , as well as the peak current  $I_b$ , increases. At a certain voltage, normal pulsing ceases and the tube goes into continuous conduction or pulses at a frequency higher than the trigger frequency. The value of supply voltage at which this normal pulsing ceases is very definite and can be repeated. As the frequency is increased, the maximum possible voltage falls until the useful output is nil. As the frequency is decreased, the maximum voltage rises until at very low frequencies the voltage limit of the tube, set by the operation of Paschen's law, is encountered. The curves of Figure 3 for the

<sup>4</sup> G. N. Glasoe and J. V. Lebacqz, PULSE GENERATORS, McGraw-Hill Book Co., New York, N. Y., 1948, pages 356-359.

<sup>5</sup> M. I. T. Radar School Staff, PRINCIPLES OF RADAR, McGraw-Hill Book Co., 1948, pages 6, 7.

2050, 2D21, and 3D22 show this inverse relationship between trigger frequency and anode supply voltage.

This relationship between frequency and voltage has been found to be very definitely associated with the deionization time of the thyatron. The more the curve of Figure 3 is displaced toward the higher frequencies, the shorter is the deionization time. Deionization time, however, is not to be taken as the reciprocal of the frequency. Its exact nature will be considered later. In order to determine the performance of various standard tubes in radar modulator service and also to obtain a measure of deionization time, additional tests were made with the same circuit. The tests were extended to special tubes with various gases and pressures and, in addition, tests were made to determine the effects of various circuit parameters. In general, these parameters exhibit the same relationship to the curve of maximum anode-voltage versus frequency as they would to deionization time.

THYRATRON GEOMETRY

Types 3D22, 2050, and 2D21 are all shield-grid xenon-filled thyratrons, similar in structure but differing in size. These three types were tested in the same radar modulator circuit with results shown in Figure 3. The smallest type (2D21) gives the best performance because it has the shortest deionization time. A comparison of geometry and frequency for the three types is given in Table III.

Table III

	2D21	2050	3D22	
Spacing:				
Anode-Cathode	1.0	1.5	2.5	relative units
Grid-Cathode	1.0	1.4	3.0	relative units
Maximum Trigger Frequency at 300 volts	2.9	1.6	1.0	relative units

Figure 3 also includes the results on two other types: the 884 and the OA4-G. The 884 has close spacings and, hence, a short deionization time. The OA4-G, on the other hand, is a cold-cathode type. The high pressure (several millimeters) necessary in a cold-cathode tube gives it a very long deionization time. The curves of maximum trigger frequency confirm these statements.

The limitations imposed by Paschen's law may be plainly seen on the curves for the 884 and OA4-G. As the frequency is decreased the shape of the curve changes abruptly from a hyperbola to a straight line with a slope of zero. Because the anode of the 884 does not have the shielding necessary to eliminate long breakdown paths, the break-

down voltage of the 884 is much lower than that of the shield-grid types. In the test circuit above, the peak anode voltage is double the supply voltage. The plateau at 300 volts means, therefore, that the 884 anode voltage is 600 volts peak. The rated maximum peak voltage of the 884 is 350 volts.

### GAS PRESSURE

Because the curve of maximum frequency versus anode-voltage is related to deionization time, frequency should be a function of gas pressure. The effects of pressure variation on frequency are given in the curves of Figures 4 and 5 for types 2D21 and 884, respectively. The effect of lower gas pressure is the same as the effect of shorter deionization time; i.e., better performance. The tests on the 2D21 were made with a 10-ohm line. The tests on the 884 were made at a higher impedance level (600 ohms) in order to keep the average current down. The break in performance when the maximum frequency or voltage is exceeded is so sharp that this method can be used to determine the gas pressure in a given tube. Gas pressure in these tubes has always been difficult to determine, but this method provides a dynamic electrical test that can be used

without special equipment.

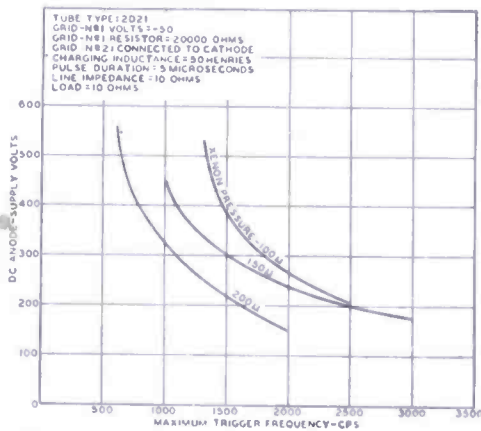


Fig. 4—Effect of pressure variation on performance of type 2D21.

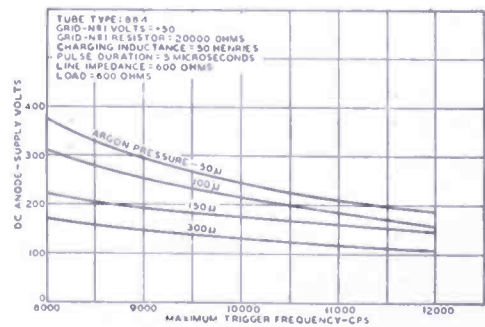


Fig. 5—Effect of pressure variation on performance of type 884.

### GAS-FILLING

The 2D21 thyratron is filled with xenon, a relatively heavy gas. Special 2D21's filled with the lightest of gases, hydrogen, showed a very marked improvement in performance in a radar modulator circuit (see Figure 6). The frequency values for these tubes are in the order of kilocycles. Because these tests are mainly intended to determine differences in initial performance, other important factors, such as length of life, require consideration before selection of a gas filling. Tests with other gases such as helium and argon in the 884 (Figure 7)

confirm the observation that improvement in performance comes with decreasing atomic weight of the gas content.

GRID BIAS

The control grid is a good deionizing agent because it is in the arc path and can sweep out ions in the form of grid current. Figure 8 shows the increase in operating frequency with increasing control grid bias for the 3D22. The increase in frequency is almost proportional to the increase in bias.

It had been reported by some of the laboratories during the war\* that improved pulse operation would result from the use of a bias on the shield grid in addition to that on the control grid. In the case of the small shield-grid thyratrons (3D22, 2050, and 2D21) only a small bias (about 10 volts) can be applied to the shield grid before the 150-

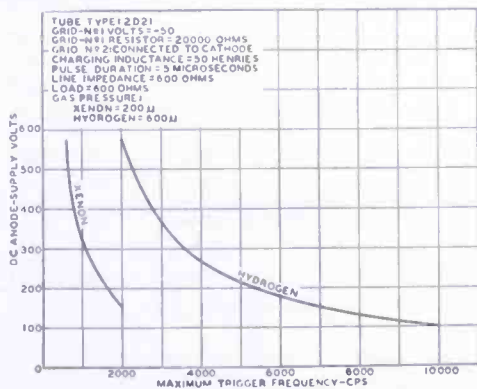


Fig. 6—Effect of gas filling on performance of type 2D21.

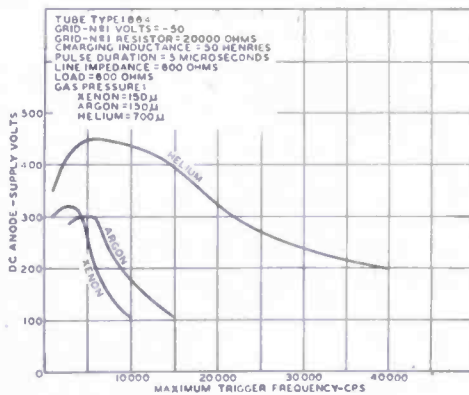


Fig. 7—Effect of gas filling on performance of type 884.

volt trigger signal becomes insufficient to fire the tube. The high control ratio of the shield grid is responsible for this failure to fire. With -50 volts on the control grid, an increase in shield grid bias from 0 to -10 volts shows a negligible improvement in frequency-performance.

Although a grid of a thyatron may have a high control ratio, it may not be a good deionizing agent. This statement is confirmed by frequency runs on the 3D22, first with -100 volts on the control grid and zero on the shield grid, and second with -100 volts on the shield grid and zero on the control grid. In each case the trigger is applied to the grid which has the -100-volt bias. The fact that the second run gives a curve with a slightly lower voltage range indicates that in the 3D22 the shield grid is slightly less effective as a deionizing agent

\* Unpublished communications.

than the control grid. The inefficacy of the shield grid is more pronounced in type 2050 because the shield does not have a sputter partition between cathode and control grid<sup>6</sup>.

### CHARGING INDUCTANCE

It is stated above that a large charging inductance was made standard so that a linear charging waveshape (Figure 3) independent of frequency is obtained. A linear waveshape, however, is not the most satisfactory for efficient deionization. The waveshape of the solid line in Figure 9 has an important advantage. The slower rise immediately after the pulse allows more time for deionization before the reapplication of a given anode voltage. This type of charging is obtained only at one frequency which is twice the resonant frequency of the charging inductance and total line capacitance. Figure 10 shows a comparison of results with these two methods of charging. The 0.5-henry choke

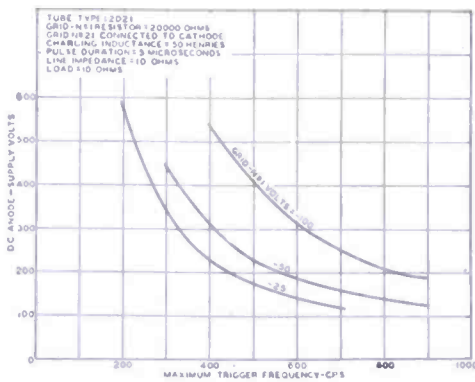


Fig. 8—Effect of grid-bias variations on performance of type 3D22.

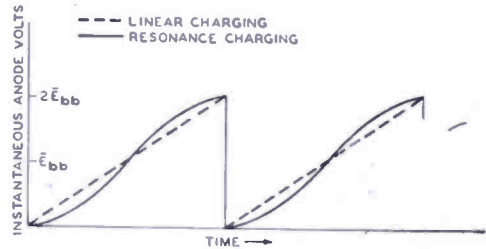


Fig. 9—Waveshapes of charging voltage.

resonates with the 0.25-microfarad capacitance of the line at about 450 cycles per second. At double this frequency, 900 cycles per second, resonance charging should occur. The data show that at 700 cycles per second the improvement over linear charging is considerable. At 800 cycles per second the improvement is slight; above 1000 cycles per second the two curves become identical. The value of 900 cycles per second is a theoretical value; the actual value for resonance may be lower. From these data, one can conclude that the period of time immediately following the discharge is important in determining the performance of the thyatron as a radar modulator.

<sup>6</sup> For cross-sections of these tubes see Hubert H. Wittenberg, "Frequency Performance of Thyratrons", *Elec. Eng.*, Vol. 65, No. 12, page 843, December, 1946.

PULSE DURATION

If a gas tube is conducting for such short periods as in radar service, the amount of ionization within the tube is a function of the length of the conduction period. Although the time required for ionization is quite short (fractions of a microsecond), equilibrium is not established. As proof, one need only to observe that the tube drop is still decreasing as the end of a typical 1-microsecond pulse. Hence, because the amount of ionization is a function of pulse duration, the time required for deionization is also a function of pulse duration. Figure 11 shows the effect of varying the pulse duration on maximum trigger frequency.

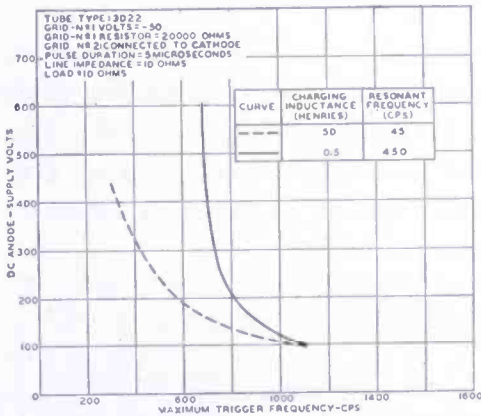


Fig. 10 — Effect of variation of charging method on performance of type 3D22.

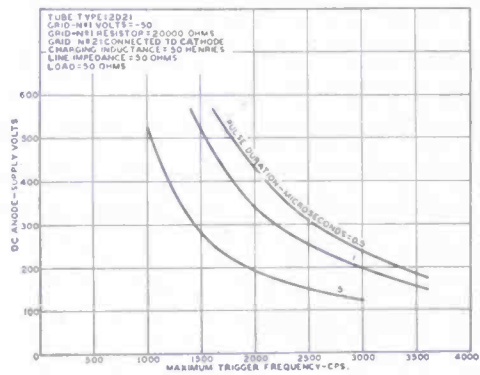


Fig. 11 — Effect of variation of pulse duration on performance of type 2D21.

MISMATCH

In the operation of a line-type thyatron modulator, the short circuit set up by the firing of the thyatron drops the line voltage,  $E$ ,

across the artificial line to the amount  $\frac{Z_n}{Z_n + R_L} E$  volts.

Analysis of this expression shows that there are three possibilities.

- a. If  $R_L = Z_n$  the expression  $\frac{Z_n}{Z_n + R_L}$  is  $\frac{1}{2}$ . The forward wave discharges the line to  $E/2$  and the reflected wave completes the discharge.
- b. If  $R_L > Z_n$  the above expression is less than  $\frac{1}{2}$ . The two passages of the negative wave front do not completely discharge the line and at the end of the pulse and the return of the reflected wave, the line still has a positive charge. The thyatron continues to conduct until the multiple reflections completely discharge the line. Practically, this case is not encountered because the resultant current pulse has undesirable steps.

- c. If  $R_L < Z_n$  the above expression is greater than  $\frac{1}{2}$ . The reflected wave not only completely discharges the line but puts a negative voltage on it. Conduction through the thyatron cannot be maintained with a negative voltage on the line and so the current pulse has just as good waveshape as in case (b) above. Furthermore, this negative voltage is advantageous in that deionization is expedited. This advantage is borne out by the data of Figure 12 which shows that undermatching raises the maximum frequency.

### PEAK CURRENT

Figure 13 shows the results of tests with a matched load in which the line impedance only was varied. Such a variation changed the peak pulse current in an inverse fashion. Although the peak current was changed by a factor of 1:10, the effect was almost negligible on frequency performance. Some undetermined factor is probably counteracting the effect of variations of deionization time.

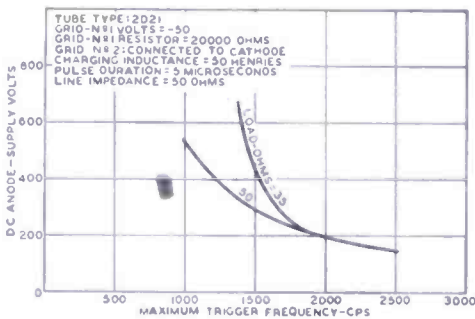


Fig. 12—Effect of mismatch of artificial-line impedance and load on performance of type 2D21.

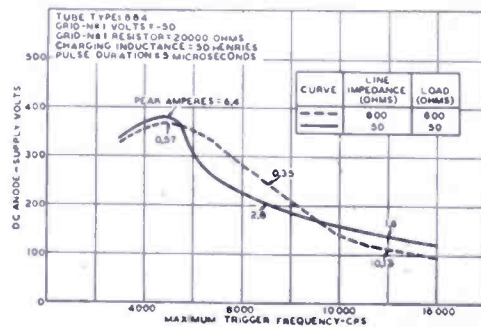


Fig. 13—Effect of varying the matched load and line impedance on performance of type 884.

### THEORETICAL CONSIDERATIONS

#### *The Constancy of Average Anode Current*

It has been observed that when the maximum trigger frequency of a thyatron is measured, the tube always stops pulsing at the same value of average anode current, and this value is independent of dc anode supply voltage and frequency. Because the large charging inductance maintains a constant current over a cycle, the frequency curves are taken with a constant current flow. When the thyatron is not conducting, this current can flow only into the lumped capacitance of the line, the voltage of which necessarily rises at a constant rate. This constancy of rate of rise of line or anode voltage is the basis of the frequency performance of this circuit.

The hyperbolic shape of the curve of dc supply voltage versus frequency must follow as a result of the constancy of average anode current. The relation of the peak anode current to the average anode

current is 
$$I_b = \frac{\bar{I}_b}{t_p f}$$

where  $I_b$  = peak anode current in amperes

$\bar{I}_b$  = average anode current in amperes

$t_p$  = pulse duration in seconds

$f$  = frequency in cycles per second

Because  $\bar{I}_b$  and  $t_p$  are constant during the measurements

$$I_b \propto \frac{1}{f}$$

The peak current,  $I_b$ , is proportional to the peak voltage across the line,  $E_b$ , which is double the average dc anode supply voltage  $\bar{E}_{bb}$ . Hence

$$\bar{E}_{bb} \propto \frac{1}{f}$$

The curve for this expression is, of course, a hyperbola.

#### Anode Voltage "Toe"

When the anode voltage at low frequency is applied to an oscillograph, it appears as a conventional sawtooth wave. If the frequency is raised, a "toe" appears at the beginning of each sawtooth as shown in the photograph of Figure 14. The frequency is 5000 cycles per second, and the period 200 microseconds. The scale used compresses the tube drop during the 5-microsecond pulse to a short almost vertical line. After the pulse, the voltage fails to rise because the thyatron is conducting. After a period of about 60 microseconds, deionization has progressed sufficiently to allow the line voltage to rise, thus forming the toe. During the toe-portion of anode voltage, the thyatron conducts the charging current with a tube drop that is nearly zero. Direct connection of the anode voltage to the deflecting electrodes of the cathode-ray tube indicates that the toe level could not be greater than +5 volts. The drop during the pulse is about 18 volts. The very low drop during the toe might be caused by the presence of a very large number of positive ions created to support the high pulse current, but which are more than enough to support the low charging current.

Superposition was used in Figure 15 to show the current pulse and the tube drop on the same time scale.

During trigger frequency measurements on type 2050, triple exposures of the anode toe were made at three different frequencies along the maximum voltage curve. The resultant photograph, Figure 16, shows that the length of the toe increases with increasing peak current. The parallel lines of voltage rise are due to the constancy of average current.

If the dc supply voltage is kept constant (constant peak current) the anode toe remains constant even though the frequency is varied. Figure 17 is a triple exposure at three different frequencies. The rate of rise of voltage varied because the average current varied, but the anode toe stayed the same.

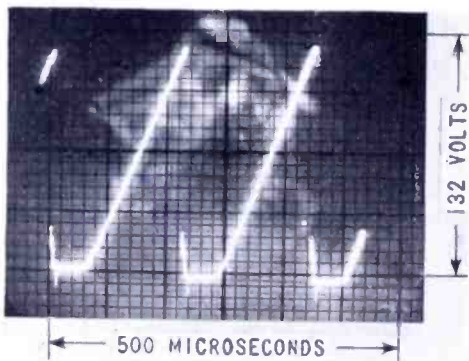


Fig. 14—Voltage waveform at anode illustrating "toe".

Tube Type	2050
Frequency	5000 cps
Pulse Duration	5 $\mu$ s
Line Impedance	50 ohms
Load	50 ohms
Anode Supply Voltage	55 volts

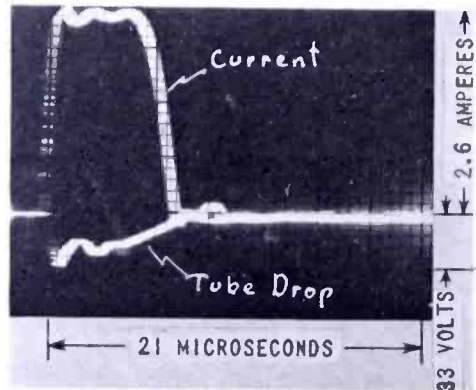


Fig. 15—Waveform of pulse current and tube drop (inverted).

Tube Type	2050
Frequency	2000 cps
Pulse Duration	5 $\mu$ s
Line Impedance	50 ohms
Load	50 ohms
Anode Supply Voltage	142 volts

### Grid Plateau

A phenomenon in the control-grid circuit accompanies that of the anode "toe". The bias supply holds the grid at  $-50$  volts until the trigger appears. The trigger drives the grid far into the conduction region with the result that the grid draws current. At the end of the trigger pulse, when the anode voltage is zero, the grid voltage returns to the bias value although shunt capacitance slightly delays the return. When anode voltage is applied, the grid voltage is held to zero volts for many microseconds after the anode current pulse and trigger pulse are over. Figure 18 is a photograph of this phenomenon. The grid voltage only is shown; superposed are voltages for three different peak pulse currents and their corresponding "grid plateaus". Because

the length of the plateau increases as the anode peak current is increased, the plateau is also a measure of the status of deionization within the tube.

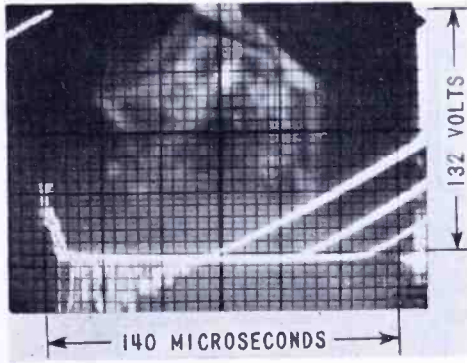


Fig. 16—Waveforms of anode voltage at three peak currents (average current constant).

Tube Type	2050	2050	2050
Frequencies	4000	2000	1000 cps
Average Current	35	35	35 ma.
Anode Supply	63	135	284 volts
Peak Current	1.2	2.7	5.7 amps.
Pulse Duration	5	5	5 $\mu$ s
Line Impedance	50	50	50 ohms
Load	50	50	50 ohms

cent of the period.

The length of the grid plateau is a function of grid resistance, the higher the resistance the longer the plateau. The figures shown are for the standard grid resistance of 20,000 ohms.

*“Shoot Through”*

During the course of these experiments another phenomenon was observed which is worthy of mention. If the positive anode voltage was applied too soon after the anode current pulse, the thyatron fired automatically without a grid trigger pulse. This phenomenon is

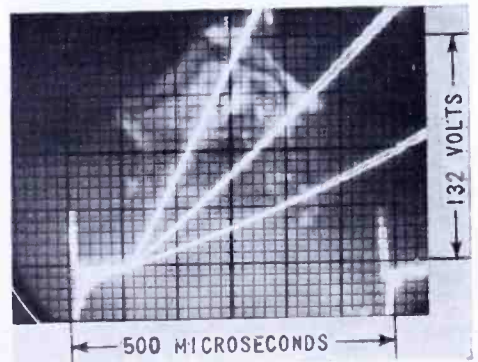


Fig. 17—Waveform of anode voltage at three average currents (peak current constant).

Tube Type	2050	2050	2050
Frequencies	2000	1000	500 cps
Average Current	35	15	7 ma.
Anode Supply	130	130	130 volts
Peak Current	2.6	2.6	2.6 amps.
Pulse Duration	5	5	5 $\mu$ s
Line Impedance	50	50	50 ohms
Load	50	50	50 ohms

Figure 19 is a photograph of the anode toe and grid plateau on the same time scale. In general, the anode toe is much longer than the plateau. Figure 20 compares the anode toe and grid plateau with the minimum period, which is the reciprocal of the maximum frequency. Note that these deionization processes occupy 5 to 20 per

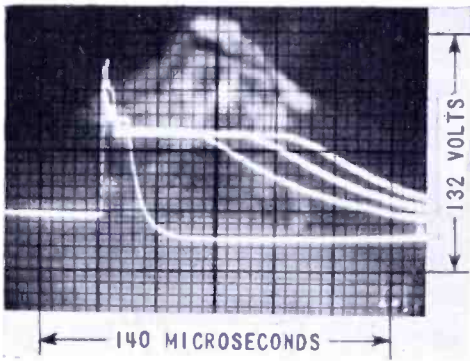


Fig. 18—Waveform of grid voltage showing grid plateau at different operating conditions.

Tube Type	2050	2050	2050	2050
Frequencies	—	2000	1000	600 cps
Average Current	0	36	34	33 ma.
Anode Supply	0	132	280	500 volts
Peak Current	0	2.6	5.6	10 amps.
Pulse Duration	5	5	5	5 $\mu$ s
Line Impedance	50	50	50	50 ohms
Load	50	50	50	50 ohms

occurrence of the main pulse. The second firing consists of a pulse of small amplitude followed by a normal cycle of operation and then a repetition of the "shoot through". The British reported observing the same phenomenon in the use of mercury-vapor thyratrons in radar modulators. In their case, however, the thyatron remained conducting for an entire cycle before recovery. The length of conduction after misfiring is probably a function of the charging circuit.

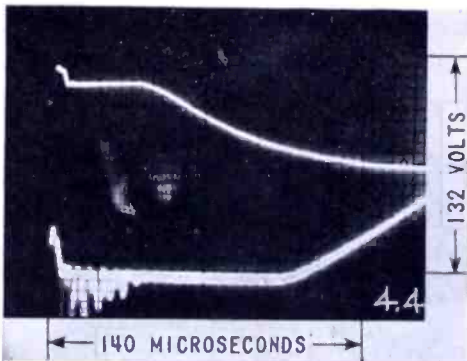


Fig. 19—Waveform of grid plateau and anode toe on same time scale.

Tube Type	2050
Frequency	1500 cps
Average Current	35 ma.
Anode Supply	180 volts
Peak Current	3.6 amps.
Pulse Duration	5 $\mu$ s
Line Impedance	50 ohms
Load	50 ohms

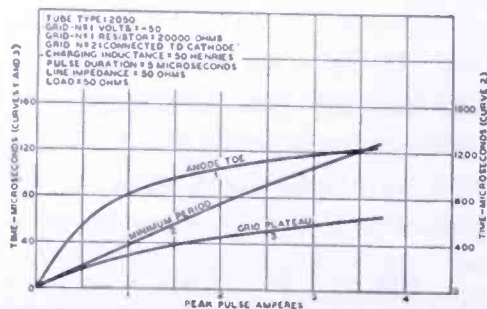


Fig. 20—Comparison of anode toe and grid plateau with minimum period.

<sup>7</sup> H. de B. Knight and L. Herbert, "The Development of Mercury-Vapour Thyratrons for Radar Modulator Service", *Jour. Inst. Elec. Eng.* (Brit.), Vol. 93, Part IIIA, No. 5, page 949, March-May, 1946.

“Shoot through” has been observed only with low impedance lines indicating that high current is a possible cause. The circuit of Figure 21 used a 10-ohm line. The effect of “shoot through” may be observed on the grid voltage wave, a photograph of which is shown in Figure 22; the upper curve is the

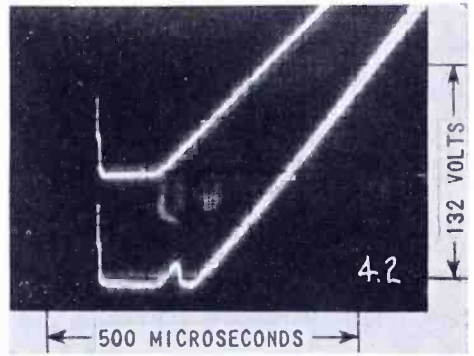


Fig. 21—Waveforms of anode voltage before and after misfiring action (“shoot through”).

Tube Type	2050	2050
Frequency	1500	1500 cps
Average Current	96	114 ma.
Anode Supply	104	105 volts
Peak Current	10	10 amps.
Pulse Duration	5	5 $\mu$ s
Line Impedance	10	10 ohms
Load	10	10 ohms

grid voltage, whereas the lower is the anode voltage.

#### Avoidance of Anode Toe

It is obvious from the data collected on the anode toe that if the toe could be avoided as the anode voltage wave rises, the thyratron can be operated at much higher peak voltages. Such behavior is obtained by suitable undermatching of the line. If the load-to-line ratio is 0.7, a

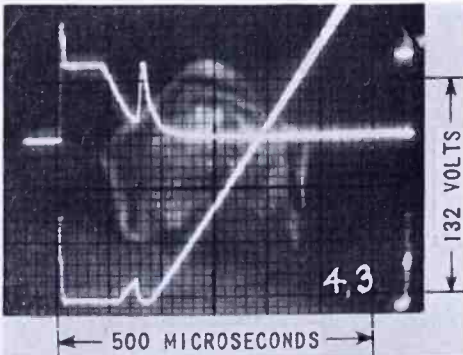


Fig. 22—Effect of “shoot through” on grid voltage.

Tube Type	2050
Frequency	1500 cps
Average Current	140 ma.
Anode Supply	134 volts
Peak Current	13 amps.
Pulse Duration	5 $\mu$ s
Line Impedance	10 ohms
Load	10 ohms

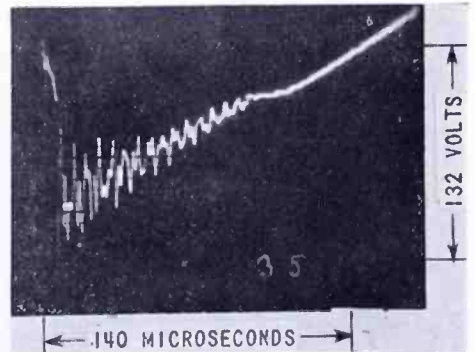


Fig. 23—Negative swing of anode voltage due to mismatch of line and load.

Tube Type	2050
Frequency	2000 cps
Average Current	40 ma.
Anode Supply	147 volts
Peak Current	3 amps.
Pulse Duration	5 $\mu$ s
Line Impedance	50 ohms
Load	30 ohms

small improvement in performance is noted (Figure 12). This reduction, however, is not enough to eliminate the anode toe as Figure 23 shows. But if the ratio is reduced to 0.4, the rising voltage wave misses the toe completely (see Figure 24), with the result that the peak voltage which the thyatron can take rises suddenly from 340 volts to 730 volts.

### The Deionization Process

The data and analysis thus far lead to the basic characteristic of the deionization process in a gas tube. As Berkey and Haller<sup>8</sup> reported several years ago, the curve for reignition voltage of a gas tube versus time is given in Figure 25. Reignition voltage is the voltage required to cause anode current to flow at a given time after cessation of current flow. In Figure 25 the current ceases to flow at  $t_1$  by action of the circuit. After time  $t_1$ , the reignition voltage rises slowly at first, then faster, then asymptotically until the steady-state igni-

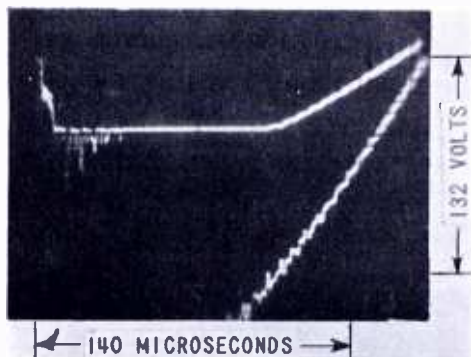


Fig. 24—Elimination of anode toe by load-to-line mismatch ratio of 0.4.

	Upper Trace	Lower Trace
Tube Type	2050	2050
Frequency	2000	2000 cps
Anode Current	37	89 ma.
Anode Supply	143	247 volts
Peak Anode Voltage	340	730 volts
Peak Current	3.4	7.3 amps.
Pulse Duration	5	5 $\mu$ s
Line Impedance	50	50 ohms
Load	50	20 ohms

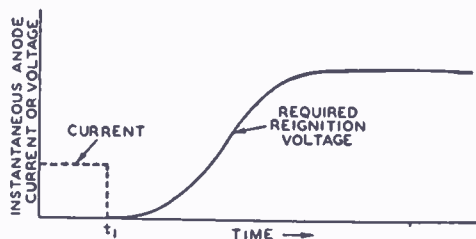


Fig. 25—Reignition voltage of gas tube.

tion or breakdown value is reached. The curve is a function of geometry, gas content, gas pressure, pulse current, grid voltage, and grid resistance. Frequency limitations will be encountered in gas tubes whenever the applied voltage wave crosses this reignition voltage curve.

<sup>8</sup> W. E. Berkey and C. E. Haller, "Reignition Potential of Hot-Cathode Grid-Glow Tubes", *Electrical Journal*, Vol. 31, page 483, December, 1934.

As this paper was being written, a paper<sup>9</sup> appeared which further substantiates this theory of the mechanism of the deionization process.

#### ACKNOWLEDGMENT

Credit is due Mr. B. W. Squier, formerly of this laboratory, who took the data on which many of the curves of this paper are based.

---

<sup>9</sup> M. Birnbaum, "A Method For The Measurement of Ionization and Deionization Times of Thyatron Tubes", A.I.E.E. Technical Paper 48-33, December, 1947.

# SOME CHARACTERISTICS OF DIODES WITH OXIDE-COATED CATHODES\*

BY

W. R. FERRIS

Research Department, RCA Laboratories Division,  
Princeton, N. J.

*Summary*—The behavior of diodes with oxide-coated cathodes is investigated theoretically and experimentally. By plotting the Epstein-Fry-Langmuir solution for the space charge current and the Boltzmann equation for the retarding-field current as continuous curves with  $V \cdot |e/kT|$  as abscissa, a universal set of characteristic curves is obtained. A series resistance was found to exist in the cathode coating of many tubes. When allowance is made for this resistance, excellent correlation is obtained between the theoretical and measured tube characteristics. The solution for the incremental conductance is also obtained and plotted on the universal characteristic curve sheet.

ALTHOUGH the general solution for the static plate-current versus plate-voltage relation of diodes with equipotential cathodes and parallel plane construction has been known since 1923, the form in which it has been presented is such that a large amount of labor is necessary to fit the solution to a particular tube. In this paper a new set of coordinates is used which presents the solution in a form immediately applicable to a given diode. In addition, a solution for the incremental conductance is presented. Both characteristics are given in graphical form in a convenient chart, Figure 2, which covers a sufficient range of values to include most practical cases. The mathematical basis for the construction of the chart is given in outline form in the text though, for details of the solution, reference is made to a previous paper of Langmuir and to a new tabulation of functions at the end of this paper.

The work which prompted this investigation was the development of some small diodes for use as ultra-high-frequency detectors and converters. Certain anomalies in the performance of the available tubes were found, and the analysis explained them most satisfactorily. One effect, the low conductance-to-current ratio of all diodes except those with extremely close spacings or low currents, was shown to be fully consistent with the theory.†

\* Decimal Classification: R131.

† An unfortunate typographical error, a misplaced decimal, in an equation given by Langmuir (see reference 4) formula 313 and the example in the next two lines, has caused considerable trouble to many investigators and has produced a general lack of appreciation for the magnitude of the effect of initial velocity distribution on tube characteristics.

The original attempt at the derivation of the formula for the potential distribution in diodes was made by Epstein<sup>1</sup>. This work was extended and presented in correct form by Fry<sup>2</sup>, so far as the solution was concerned, but, as the confirmation of the applicability of the Maxwell-Boltzmann distribution for electrons outside of a cathode had

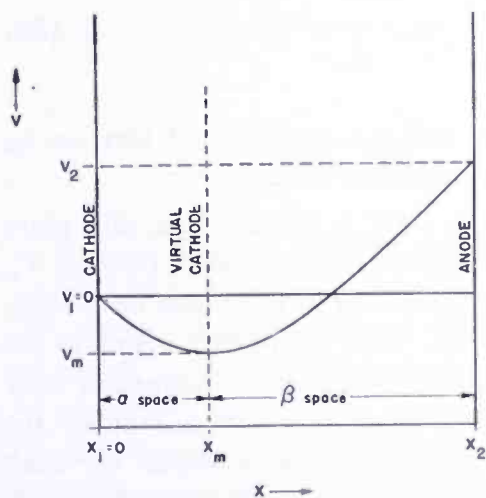


Fig. 1—Schematic potential diagram of a diode.

$$\eta = \frac{11606}{T} (V - V_m) \quad (1) \quad \xi = 9.174 \cdot 10^5 T^{-3/2} (I/A)^{1/2} (x - x_m) \quad (2)$$

In these expressions  $T$  is the cathode temperature in degrees Kelvin,  $A$  is the area,  $V_m$  and  $x_m$  are respectively the potential and position of the potential minimum which exists whenever the anode current  $I$  exceeds a certain critical value  $I_1$ , later defined, and does not exceed the total emission current,  $I_0$ . Likewise  $V$  is the potential of the variable point  $x$ . Note in Figure 1 that  $x$  is not a single-valued function of  $V$ , there being separate values of  $\xi$  for the  $\alpha$  and  $\beta$  spaces. The value of the plate voltage,  $V_2 - V_1$ , of Figure 1 may be either negative or positive. Since  $V_m$  and  $x_m$  are functions of the current,  $I$  is not given explicitly by (2) but the analysis below enables one to obtain an explicit solution by making use of Langmuir's tabulated values of  $\xi$  as a function of  $\eta$ .<sup>‡</sup>

<sup>1</sup> P. S. Epstein, *Verhandlungen Deutsche Physikalische Gesellschaft*, pp. 21, 85—1919.

<sup>2</sup> T. C. Fry, "The Thermionic Current between Parallel-Plane Electrodes; Velocities of Emission Distributed According to Maxwell's Law". *Phys. Rev.*, Vol. 17, No. 4, p. 441, April, 1921.

<sup>3</sup> I. Langmuir, "The Effect of Space Charge and Initial Velocities on Potential Distribution and Thermionic Current between Parallel-Plane Electrodes". *Phys. Rev.*, Vol. 21, No. 4, p. 419, April, 1923.

<sup>‡</sup> Tables of the various functions mentioned in this paper are presented on page 147 et seq.

not been made at that time, he employed the old Maxwell distribution in his examples. Langmuir<sup>3</sup> amended Fry's solution to include the new distribution and calculated the values of the dimensionless functions  $\eta$  and  $\xi$ , described below, to five significant figures, thereby formally completing the problem.

To put Langmuir's solution in a more readily useful form we take his definitions for  $\eta$  and  $\xi$  which, after substitution of the numerical values of the physical constants, are:

Reference to Langmuir's table shows that, for all values of  $\eta$  greater than about 25,  $\xi_\alpha$  has a constant value of  $-2.5539$ , and it can be rigorously shown that this is the value of the function for  $\eta = \infty$  to the required number of decimal places. If we rewrite equation (2) as

$$I = \left( \frac{\xi_\alpha}{9.174 \times 10^5} \right)^2 \frac{T^{3/2}}{(x - x_m)^2} A \quad (2a)$$

and set  $\xi_\alpha = -2.5539$ , the equation is still not explicit in  $I$  because  $x_m$  is still a function of  $I$ . This may be remedied as follows:

There is a certain value of current  $I$  for a diode which will place the potential minimum at the anode surface, and for this current  $V_m$  is the applied anode voltage and  $x_1 - x_2 = -s$ , is the value of  $x - x_m$ , where  $s$  is the cathode to anode spacing. This value of current is the critical current,  $I_1$ , mentioned above. If the emission current is very much greater than this value, then  $I_1$  is nearly independent of the emission, that is, it approaches an asymptotic value which we shall designate as  $I_\infty$ , the subscript  $\infty$  indicating that  $I_\infty$  is the value of  $I_1$  for a tube whose emission is infinitely greater than  $I_1$ . The value of  $I_\infty$  is a function only of the geometry and temperature of the tube and may be obtained explicitly from (2a) by setting  $\xi_\alpha = -2.5539$  and  $x - x_m = s$ , the cathode to anode spacing. The substitution gives

$$I_\infty = \left( \frac{2.5539}{9.174 \times 10^5} \right)^2 \frac{T^{3/2}}{s^2} A \quad \text{amperes.} \quad (3)$$

The above equation may be improved somewhat by expressing  $T$  in thousands of degrees Kelvin giving

$$I_\infty = 0.2451 \times 10^{-6} \left( \frac{T}{1000} \right)^{3/2} \frac{A}{s^2} \quad \text{amperes.} \quad (4)$$

Since the dimensions of the tube enter only in the combination  $A/s^2$ , it is immaterial in what units the dimensions are expressed. In most of what follows, only ratios of currents will be used, so it will be immaterial whether current density or total current is used.

To recapitulate,  $I_\infty$  is the limiting value of current,  $I_1$ , which would give a potential minimum at the anode, if the cathode emission were infinite. The value of  $I_1$  is always less than  $I_\infty$ , reaching only about 96.5 per cent of  $I_\infty$  when  $I_s$  is 11,000 times  $I_1$ . To find  $I_1$ , having com-

puted  $I_\infty$  and knowing  $I_s$ , we first divide the expression for  $I_\infty$  by that for  $I_1$  obtaining

$$\frac{I_\infty}{I_1} = \left( \frac{2.5539}{(\xi_\alpha)_1} \right)^2 \quad (5)$$

or after multiplying by  $I_s$  and arranging,

$$\frac{I_s}{I_\infty} = \frac{I_s}{I_1} \left( \frac{(\xi_\alpha)_1}{2.5539} \right)^2 \quad (5a)$$

This is still an implicit expression of  $I_1$  since  $(\xi_\alpha)_1$  is a function of  $I_s/I_1$ , and it is necessary to assume values of  $I_s/I_1$ , calculate the value of  $\eta$  at the cathode surface from the expression  $\eta_1 = \ln(I_s/I_1)$ , and then look up the corresponding value of  $-(\xi_\alpha)_1$  in Langmuir's table. In this way a plot of  $I_s/I_\infty$  versus  $I_s/I_1$  may be prepared and (5a) may be solved completely in terms of the two quantities  $I_s$  and  $I_\infty$ , one of which is measurable and the other is calculable from (4).

It is desirable to use dimensionless quantities for plotting the characteristics and a convenient pair is  $I/I_\infty$  versus  $eV/kT$ , the reasons for this choice being apparent later. Also it is desirable to use semi-logarithmic paper for the following reasons:

If the anode voltage is less than  $V_m$ ,  $I$  is less than  $I_1$ , and is given by the Boltzmann equation

$$I = I_s \epsilon^{\frac{v\sigma}{kT}} \quad (6)$$

or after dividing both sides by  $I_\infty$

$$\frac{I}{I_\infty} = \frac{I_s}{I_\infty} \epsilon^{\frac{v\sigma}{kT}} \quad (6a)$$

If this equation is plotted on semi-logarithmic paper with  $eV/kT$  as abscissa and  $I/I_\infty$  as ordinate with  $I_s/I_\infty$  as a parameter, it is represented by a family of parallel straight lines. Since the Boltzmann equation holds only for values of current so low that no virtual cathode exists and  $I_1$  is the current for which the virtual cathode just appears, each of the straight lines must be stopped at the value  $I/I_\infty = I_1/I_\infty$  and the rest of the characteristic will be one of a family of curved lines each merging into a horizontal straight line at the point where  $I/I_\infty = I_s/I_\infty$ .

The next part of the plotting is concerned with filling in the curved portions of the family of curves between the inclined portion representing the Boltzmann equation and the horizontal part representing the saturation region indicating temperature limitation of emission.

To do this set  $I_N = NI_1$  for each curve in turn.

$$\text{Thus for } N = 1, I_1 = \left[ \frac{(\xi_\alpha)_1}{9.174 \times 10^5} \right]^2 \frac{T^{3/2} A}{s^2} \quad (7)$$

and for  $N > 1$

$$\begin{aligned} I_N = NI_1 &= \left[ \frac{(\xi_\alpha)_N}{9.174 \times 10^5} \right]^2 \frac{T^{3/2} A}{(x_1 - x_m)^2} \\ &= \left[ \frac{(\xi_\beta)_N}{9.174 \times 10^5} \right]^2 \frac{T^{3/2} A}{(x_2 - x_m)^2} \end{aligned} \quad (8)$$

Dividing (8) by (7) we have

$$N = \frac{s^2}{(x_1 - x_m)^2} \left[ \frac{(\xi_\alpha)_N}{(\xi_\alpha)_1} \right]^2 \quad \text{or } (x_1 - x_m) = \frac{-s}{\sqrt{N}} \left[ \frac{(\xi_\alpha)_N}{(\xi_\alpha)_1} \right] \quad (9)$$

the negative sign of the square root being chosen because all distances are measured from the actual cathode surface and  $x < x_m$  for the  $\alpha$  space.

$$\text{so } (x_2 - x_m) = (x_2 - x_1) + (x_1 - x_m) = s \left[ 1 - \frac{1}{\sqrt{N}} \frac{(\xi_\alpha)_N}{(\xi_\alpha)_1} \right] \quad (10)$$

$$\begin{aligned} \text{and } (\xi_\beta)_N &= \left( \frac{x_2 - x_m}{x_1 - x_m} \right) \cdot (\xi_\alpha)_N = \frac{s \left[ 1 - \frac{1}{\sqrt{N}} \frac{(\xi_\alpha)_N}{(\xi_\alpha)_1} \right]}{-\frac{s}{\sqrt{N}} \left[ \frac{(\xi_\alpha)_N}{(\xi_\alpha)_1} \right]} \cdot (\xi_\alpha)_N \\ &= (\xi_\alpha)_N - \sqrt{N} (\xi_\alpha)_1 \end{aligned} \quad (11a)$$

Now  $(\xi_\alpha)_1$  is a function of  $\eta_1$ , and  $(\xi_\beta)_1$  is a function of some  $\eta_2$ , but  $(\xi_\beta)_1 = 0$ , so  $\eta_2 = 0$ . Likewise,  $(\xi_\alpha)_N$  is a function of some  $(\eta_1)_N$ , and  $(\xi_\beta)_N$  is a function of some  $(\eta_2)_N$ , but  $\eta_1 = \ln I_s/I_1$  and  $(\eta_1)_N$

$$= \ln I_s/N I_1 = \eta_1 - \ln N. \tag{11b}$$

From (11a) we may obtain  $(\xi_\beta)_N$  and look up the corresponding value of  $(\eta_2)_N$  in Langmuir's table.

$$\text{Since } (\eta_1)_N = \frac{e}{kT} [(V_1)_N - (V_m)_N]$$

$$\text{and } (\eta_2)_N = \frac{e}{kT} [(V_2)_N - (V_m)_N]$$

$$(\eta_1)_N - (\eta_2)_N = \frac{e}{kT} [(V_1)_N - (V_2)_N]$$

where  $(V_1)_N$  and  $(V_2)_N$  are respectively the cathode and anode potentials.

Referring all potentials to the cathode for which  $V_1 = 0$

$$\frac{e \cdot (V_2)_N}{kT} = (\eta_2)_N - (\eta_1)_N \tag{12}$$

The solution for the current versus voltage is now complete, and as many points as desired may be found by assigning different values to  $N$  from  $N = 1$  to  $N = I_s/I_1$ . In this way Figure 2 was drawn. To use this curve, it is only necessary to calculate the value of  $I_\infty$  and to know the total emission and the cathode temperature. Then the curve for the appropriate value of  $I_s/I_\infty$  is the complete voltage versus current characteristic. If the temperature is not known, it is theoretically possible to obtain it from the slope of the linear portion of the curve obtained by direct measurement of the current versus voltage. Usually this method seems to give a value of temperature higher than the value obtained by the use of an optical pyrometer, as mentioned in the section on experimental results, but it may be the actual temperature of the seat of the electron emission.

An interesting case is that for which  $I_s/I_\infty \rightarrow \infty$  for which  $I_1 \rightarrow I_\infty$ . From (11b)  $(\eta_1)_N = \ln (I_s/I_1) - \ln N$  and  $(\eta_1)_N/(\eta_1)_1 \rightarrow 1$ , so  $(\xi_\alpha)_1 \doteq (\xi_\alpha)_N \doteq 2.5539$ . Now  $(\xi_\beta)_N = (\xi_\alpha)_N - \sqrt{N} (\xi_\alpha)_N = (\xi_\alpha)_1 (1 - \sqrt{N}) = 2.5539 (1 - \sqrt{N})$  and  $(\eta_1)_N = \ln (I_s/I_1) - \ln N$ .  $(\eta_2)_N$  may be found from Langmuir's table for  $\xi_\beta = 2.5539 (1 - \sqrt{N})$

$$\text{Then } Ve/kT = (\eta_2)_N - (\eta_1)_N = (\eta_2)_N + \ln N - \ln (I_s/I_1) \tag{13}$$

if  $I_s \gg I_1$ ,  $I_1 \rightarrow I_\infty$  and  $\ln (I_s/I_1) = \ln (I_s/I_\infty)$  which is constant.

Thus when  $I_s \gg I_1$ , the shape of the curves is the same whatever the value of  $I_s/I_1$ , the effect of any difference in  $I_s/I_1$  being simply a translation along the  $eV/kT$  axis. Since  $I_s/I_\infty$  is actually very much greater than 1000 for all but close-spaced tubes operating at high current densities, this case is of considerable practical interest.

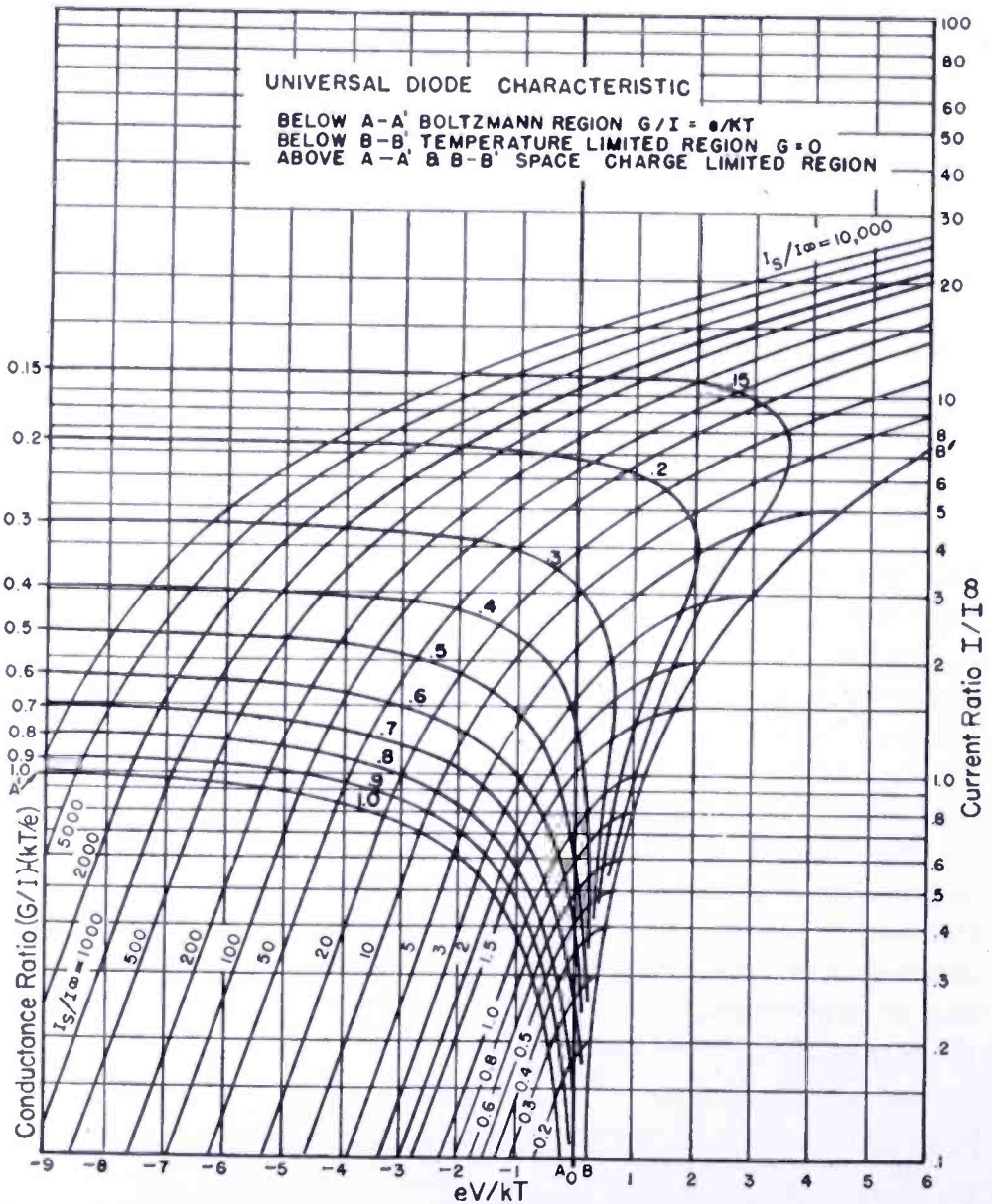


Fig. 2—Universal diode characteristic where  $I_s$  is the emission current,  $I_\infty = 0.245 \times 10^{-6} (T/1000)^{3/2} (A/s^2)$ ,  $T$  is the cathode temperature in degrees Kelvin,  $A$  is the cathode area, and  $s$  the cathode-anode distance. The value of  $e/k$  is 11,606 degrees per volt. Steps for calculation. (a) compute  $I_\infty$ ; (b) compute  $I_s/I_\infty$ ; (c) compute  $(11,606/T)V$  (abscissa); (d) Intersection of  $I_s/I_\infty$  curve and abscissa gives current and conductance ratio. For  $I_s/I_\infty > 10,000$  use Figure 3.

Letting  $\ln (I_s/I) = -V_o e/kT$  we have

$$(V - V_o) e/kT = (\eta_2)_N + \ln N \tag{14}$$

This quantity is used as the abscissa in Figure 3.

To see how well the equation  $I \propto (V - V')^{3/2}$  can be made to fit this ideal curve we may plot  $(I/I_\infty)$  versus  $eV/kT$  (Figure 4). It is seen that the fit is good only when  $I/I_\infty$  is very large. Note that the equation given by Langmuir<sup>4</sup> is not of exactly of this form as he introduces the term  $(x - x_m)$  in the denominator which renders the solution implicit but produces a better fit than the simple three halves power equation.

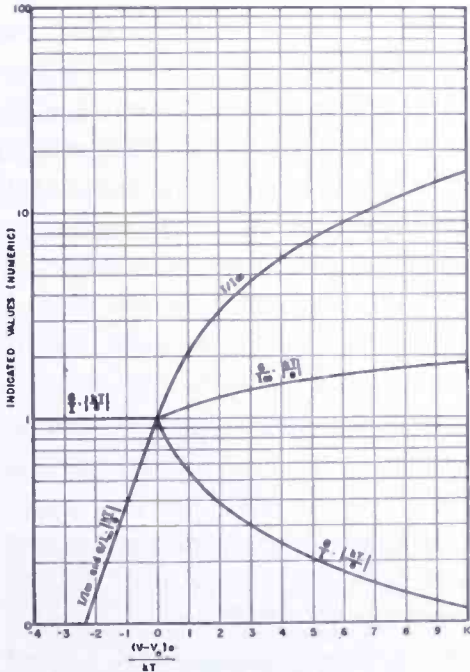


Fig. 3—Universal diode characteristic for very high emission cathodes ( $I_s \gg I_\infty$ ). Symbols similar to Figure 2 except for  $V_o = (kT/e) \ln (I_s/I_\infty)$ .

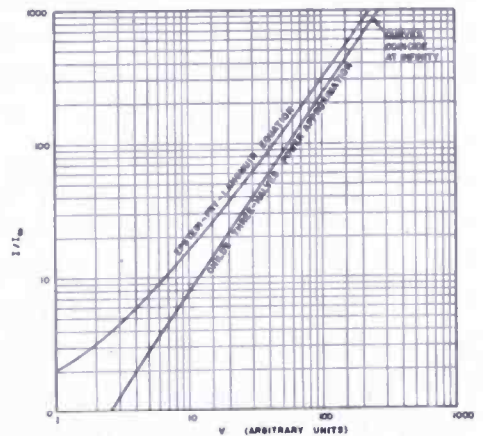


Fig. 4—Correlation between Child's three-halves power equation and the Epstein-Fry-Langmuir Equation for a diode with very high emission.

The incremental conductance may be obtained by differentiation of the expression for the current. Since the universal curves give the plate current under all conditions, it is most convenient to plot the values of conductance on the same chart. This may be done as follows:

In the region for which the Boltzmann equation holds the current is simply expressed by (6). Since the conductance,  $G$ , is defined by  $G = dI/dV$ , the ratio of conductance to plate current throughout this

<sup>4</sup> I. Langmuir and K. T. Compton, "Electrical Discharges in Gases". *Rev. Mod. Phys.*, Vol. 3, No. 2, pp. 241, April, 1931. Note: The value 0.0016 should be 0.016 in formula 313.

entire region is

$$G/I = e/kT. \tag{15}$$

It is convenient to show the conductance on the rest of the chart by plotting the locus of points where the value of  $G/I$  is a certain fraction of  $e/kT$ . The locus of the points for which  $I/I_\infty = I_1/I_\infty$ , that is the upper limit of the Boltzmann region, is then also the locus of the points for which  $G/I = e/kT$ , and the region where, say,  $G/I$  is  $0.9e/kT$  will be a curve lying slightly above this and so on. The loci which represent these  $G/I$  values are curves with a left-hand portion which is nearly horizontal on the chart (Figure 2), obtained by the derivation in Appendix I.

EXAMPLE SHOWING THE USE OF THE UNIVERSAL CHARACTERISTICS

Consider a tube with a disc cathode 0.100 inch in diameter having an anode to cathode spacing of 0.0032 inch and a cathode temperature of 1190 degrees Kelvin. Assume a cathode emission of approximately 5 amperes per square centimeter. The measured static characteristic is shown in Figure 5. Plot the theoretical current-versus-voltage and conductance-versus-voltage characteristics.

From (4)

$$I_\infty = 0.2451 \times 10^{-6} \left( \frac{T}{1000} \right)^{3/2} \frac{A}{S^2} = 245 \times 10^{-6} \text{ ampere}$$

$$I_s = 5\pi (.050 \times 2.54)^2 = 0.253 \text{ ampere approximately } I_s/I_\infty = 968.$$

From the universal curve  $I_1/I_\infty = 0.97$  so that  $I_1 = 235 \times 10^{-6}$  ampere and, from the same curve  $eV/kT = -6.9$  so that  $V = -0.71$  volt.

Thus, except for contact potential, an applied retarding potential of 0.71 volt should permit  $235 \times 10^{-6}$  amperes to flow. Reference to the static characteristic for a sample tube of this construction showed that the voltage for this current was actually nearly 0.19 volt positive. This would indicate a positive contact potential of 0.90 volt. To find the rest of the theoretical characteristic for this tube we must

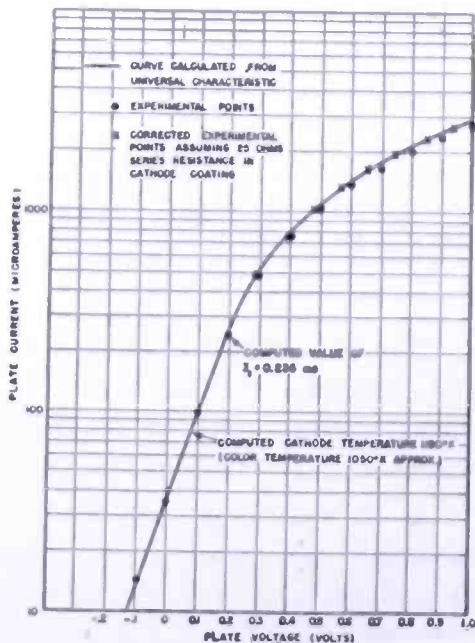


Fig. 5—Plate current characteristic of small parallel plane diode with very thin cathode coating.

multiply the values of  $eV/kT$  for the  $I_s/I_\infty = 1000$  curve by  $T/11600 = 0.1025$  and add 0.90 and then multiply the ordinate values by  $I_\infty = 245 \times 10^{-6}$ . The solid curve of Figure 5 is the theoretical characteristic while the circled points are the measured values on the actual diode. The fit is excellent up to a value of plate current several times  $I_1$  and can be improved still more by correcting for the series resistance of the cathode coating (as explained in the next section) which is of the order of 25 ohms for this tube. To obtain the theoretical values of conductance, first find the value of  $e/kT$ , which is 9.75 for this temperature. The conductance for the linear portion of the curve is then simply 9.75 times the current; for the curved region this value of conductance must be multiplied by an additional factor given by the conductance curves crossing the universal characteristics. Thus for a plate current of 1.0 milliamperes  $I/I_\infty = 4.1$  and the conductance is  $1000 \times 9.75 \times 0.35 = 3400$  micromhos.

#### EXPERIMENTAL RESULTS

The static characteristics of some early experimental "lighthouse" diodes were measured and found to depart substantially from the theoretical curves of the preceding section. The conductance at plate current values of a few hundred microamperes was only a small fraction of what would be predicted from the known dimensions of the tubes, and the slope of the "Boltzmann" curves was not even constant. This effect could, of course, be caused by series resistance in the test circuit, but after elimination of all possibility of such error, the anomaly still existed. It was tentatively assumed that the oxide coating of the cathodes had a series resistance of either the ordinary semiconductor type or perhaps that of a blocking layer. The possibility of a blocking layer on the anode was also recognized. Different values were assumed for this resistance, and the voltage-current characteristics were plotted, making allowance for the voltage drop which such values of resistance would cause. For each tube there was a fixed value of resistance which would make the corrected characteristic agree with the calculated value within experimental error both for the retarding field (Boltzmann) region and for the space-charge limited region of the curves up to a value of plate current approaching the total emission of the tubes in some cases. Typical curves are shown in Figures 5 to 7. Lighthouse diodes made after the early production difficulties had been overcome, were measured and showed almost no series resistance, that is, less than 10 ohms. A possible explanation for the difference is in the relatively poorer cathode activation which

is often found in early experimental samples as compared with the more uniform and higher performance tubes which can be made by careful attention to achieve optimum cathode coating and processing.

Another interesting point observed was that the radio-frequency loss was the most severe for the tubes showing the highest series resistance.

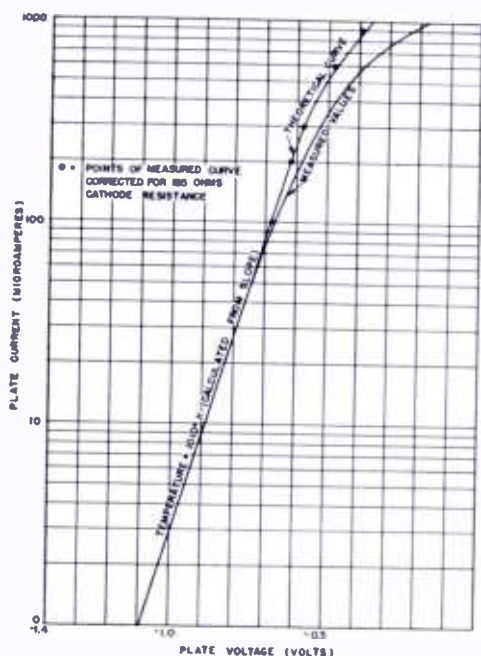


Fig. 6—Plate current characteristics of early experimental type 559 diode.

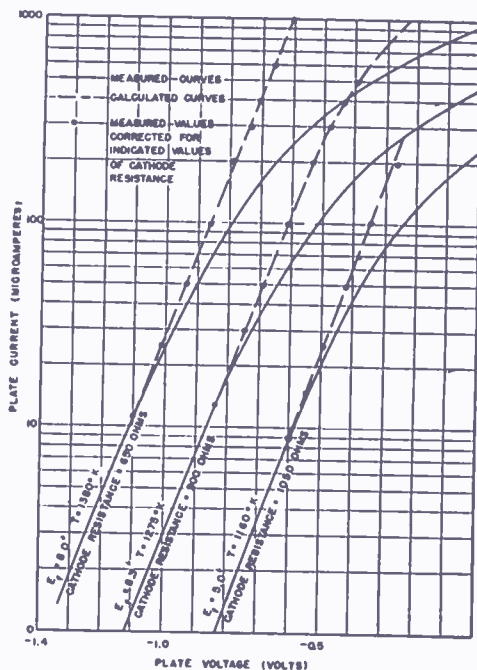


Fig. 7—Plate current characteristic of another early sample type 559 diode.

The slope of the Boltzmann curves should be inversely proportional to the absolute temperature of the emitter. In every case the temperature so obtained was higher than that obtained with an optical pyrometer, a result not unexpected since it is the color temperature which is measured with the pyrometer and the emission is governed by the true "black body" temperature of the electron source. No attempt was made to find this temperature because of the uncertainty of the source of the electrons, that is, whether the temperature of the surface of the cathode or that of an underlying layer is significant.

The series resistance of the coating versus temperature was determined in one case as shown in Figure 7. Since the resistance decreases with increasing temperature, it apparently obeys the same law as the resistance of a semi-conductor and does not seem to be of the nature of a blocking layer. It differs in this respect from the large resistance of cathodes operating at extremely high current density, which is unquestionably produced by a blocking layer.

In some filament-type tubes using very fine wire it has been found that the passage of plate current may produce enough heat to maintain the emission after the filament voltage is removed. The  $I^2R$  loss in the core wire could not possibly produce sufficient heat to maintain the emission or the observed red heat, but the assumption of a series resistance of about 300 ohms for the oxide coating would suffice. This value is entirely possible in view of the results above. In general, thin coatings show less series resistance than thicker ones and "hot exhausted" tubes, that is, those which permit radio frequency heating on exhaust are easier to make with low coating resistance than tubes like the "lighthouse" types which cannot be so treated.

## APPENDIX I

### DERIVATION OF THE DIODE CONDUCTANCE FORMULA

The parametric equations of the space-charge relations provide a convenient starting point for obtaining the conductance. These equations are equations (1) and (2a), together with the equation for the value of  $\eta$  at the cathode, that is,

$$\eta_1 = \ln \frac{I_s}{I}$$

The quantity sought is  $G/I = dI/IdV$ . An additional relation to be used is the differential equation giving the relation between  $\eta$  and  $\xi$ , that is

$$\frac{d\xi}{d\eta} = \varphi^{-\frac{1}{2}}$$

where

$$\varphi_{\beta} = \epsilon^{\eta} - 1 \mp \frac{2}{\sqrt{\pi}} \left( \eta^{\frac{1}{2}} - \epsilon^{\eta} \int_0^{\eta^{\frac{1}{2}}} \epsilon^{-x^2} dx \right)$$

The derivation is simple, but the manipulation to obtain the final form is not immediately obvious and is therefore given here. We have

$$\eta = (V_m - V) \cdot e/kT = 11606 (V_m - V)/T$$

$$\xi = 9.174 \times 10^5 T^{-\frac{1}{2}} (I/A)^{\frac{1}{2}} (x - x_m)$$

$$\frac{d\xi}{d\eta} = \varphi^{-\frac{1}{2}}$$

$$\xi_{\beta} - \xi_{\alpha} = 9.174 \times 10^5 T^{-\frac{1}{2}} (I/A)^{\frac{1}{2}} (x_2 - x_1) = C (I/A)^{\frac{1}{2}}$$

$$\ln (\xi_{\beta} - \xi_{\alpha}) = \frac{1}{2} \ln (I/A) + \ln C$$

$$d\xi_{\alpha} = d\eta_1 / \sqrt{\varphi_{\alpha}} \quad d\xi_{\beta} = d\eta_2 / \sqrt{\varphi_{\beta}}$$

$$\eta_2 - \eta_1 = eV/kT \quad \eta_1 = \ln I_s/I$$

$$\frac{d\xi_{\beta} - d\xi_{\alpha}}{\xi_{\beta} - \xi_{\alpha}} = \left(\frac{1}{2}\right) dI/I$$

so

$$\frac{dI}{I} = \left( \frac{d\eta_2}{\sqrt{\varphi_{\beta}}} - \frac{d\eta_1}{\sqrt{\varphi_{\alpha}}} \right) / \frac{1}{2} (\xi_{\beta} - \xi_{\alpha})$$

$$= \frac{\sqrt{\varphi_{\alpha}} (d\eta_2 - d\eta_1)}{\frac{1}{2} (\xi_{\beta} - \xi_{\alpha}) \sqrt{\varphi_{\alpha} \varphi_{\beta}}} - \frac{\sqrt{\varphi_{\alpha}} - \sqrt{\varphi_{\beta}}}{\frac{1}{2} (\xi_{\beta} - \xi_{\alpha}) \sqrt{\varphi_{\alpha} \varphi_{\beta}}} \left( \frac{dI}{I} \right) \text{ since } \eta_1 = \ln I_s/I$$

$$\therefore \frac{dI}{I} = \frac{(d\eta_2 - d\eta_1) \sqrt{\varphi_{\alpha}}}{\sqrt{\varphi_{\alpha}} + \frac{1}{2} (\xi_{\beta} - \xi_{\alpha}) \sqrt{\varphi_{\alpha} \varphi_{\beta}} - \sqrt{\varphi_{\beta}}}$$

and since  $\eta_2 - \eta_1 = eV/kT$ ,  $dV = (d\eta_2 - d\eta_1) kT/e$

$$\frac{1}{I} \frac{dI}{dV} = \frac{e \sqrt{\varphi_{\alpha}}}{kT} \frac{1}{\sqrt{\varphi_{\alpha}} + \frac{1}{2} (\xi_{\beta} - \xi_{\alpha}) \sqrt{\varphi_{\alpha} \varphi_{\beta}} - \sqrt{\varphi_{\beta}}}$$

the values of  $\xi_{\alpha}$ ,  $\xi_{\beta}$ ,  $\varphi_{\alpha}$  and  $\varphi_{\beta}$  are found for the same values of  $\eta_1$  and  $\eta_2$  used in plotting the plate current. The limiting values of  $dI/dV$  is given by the Child's equation  $I = KV^{3/2}$ , which when differentiated and divided by itself gives

$$G/I = \frac{1}{I} \frac{dI}{dV} = (3/2) V^{-1}$$

This approaches zero with increasing plate current for the infinite emission condition as can be seen on the universal chart for the curves with a large ratio of  $I_s/I_{\infty}$  and it also approaches zero at an even faster rate if the emission is limited.

Table I

$\eta$	$-\xi_a$	$\xi_\beta$	$\varphi_a$	$\varphi_\beta$	$\sqrt{\varphi_a}$	$\sqrt{\varphi_\beta}$
0.00	0.0000	0.0000	0.0000	0.0000	0.0000	0.0000
0.01	0.1962	0.2037	0.0108	0.0093	0.1041	0.0963
0.02	0.2751	0.2904	0.0224	0.0180	0.1495	0.1344
0.03	0.3350	0.3576	0.0345	0.0265	0.1855	0.1628
0.04	0.3848	0.4148	0.0469	0.0347	0.2166	0.1863
0.05	0.4281	0.4657	0.0599	0.0427	0.2447	0.2066
0.06	0.4670	0.5121	0.0731	0.0505	0.2704	0.2247
0.07	0.5024	0.5550	0.0867	0.0583	0.2945	0.2415
0.08	0.5350	0.5952	0.1009	0.0657	0.3177	0.2563
0.09	0.5655	0.6332	0.1153	0.0731	0.3396	0.2704
0.10	0.5941	0.6693	0.1300	0.0804	0.3606	0.2836
0.15	0.7167	0.8296	0.2082	0.1154	0.4563	0.3397
0.20	0.8170	0.9674	0.2944	0.1484	0.5426	0.3852
0.25	0.9028	1.0909	0.3881	0.1799	0.6230	0.4242
0.30	0.9785	1.2042	0.4897	0.2101	0.6998	0.4584
0.35	1.0464	1.3098	0.5993	0.2389	0.7741	0.4888
0.40	1.1081	1.4092	0.7164	0.2672	0.8464	0.5169
0.45	1.1648	1.5035	0.8421	0.2945	0.9177	0.5427
0.50	1.2173	1.5936	0.9764	0.3210	0.9881	0.5666
0.60	1.3120	1.7636	1.2722	0.3720	1.1279	0.6099
0.70	1.3956	1.9224	1.6068	0.4208	1.2676	0.6487
0.80	1.4704	2.0725	1.9836	0.4674	1.4083	0.6833
0.90	1.5380	2.2154	2.4067	0.5125	1.5513	0.7159
1.00	1.5996	2.3522	2.8806	0.5560	1.6972	0.7457
1.10	1.6561	2.4839	3.4103	0.5981	1.8467	0.7733
1.20	1.7081	2.6110	4.0013	0.6389	2.0003	0.7993
1.40	1.8009	2.8539	5.3930	0.7174	2.3223	0.8470
1.60	1.8813	3.0842	7.1140	0.7920	2.6672	0.8900
1.80	1.9515	3.3040	9.2359	0.8634	3.0391	0.9292
2.00	2.0134	3.5151	11.846	0.9320	3.4418	0.9654
2.20	2.0681	3.7187	15.052	0.9980	3.8797	0.9940
2.40	2.1168	3.9158	18.985	1.0618	4.3571	1.0304
2.60	2.1602	4.1071	23.804	1.1236	4.8789	1.0600
2.80	2.1990	4.2934	29.706	1.1835	5.4503	1.0879
3.00	2.2338	4.4750	36.929	1.2418	6.0769	1.1143
3.20	2.2650	4.6524	45.767	1.2985	6.7651	1.1395
3.40	2.2930	4.8261	56.574	1.3506	7.5216	1.1621
3.60	2.3183	4.9963	69.789	1.4077	8.3540	1.1864
3.80	2.3410	5.1634	85.943	1.4605	9.2705	1.2085
4.00	2.3615	5.3274	105.68	1.5122	10.280	1.2297
4.50	2.4044	5.7259	176.40	1.6367	13.282	1.2793
5.00	2.4376	6.1089	293.07	1.7555	17.119	1.3249
5.50	2.4634	6.4811	485.52	1.8692	22.026	1.3672
6.00	2.4834	6.8416	802.88	1.9786	28.335	1.4066
6.50	2.4990	7.1924	1328.20	2.0852	36.444	1.4440
7.00	2.5112	7.5345	2189.1	2.1859	46.795	1.4785
7.50	2.5206	7.8690	3611.8	2.2846	60.098	1.5115
8.00	2.5280	8.1963	5957.5	2.3804	77.185	1.5429
9.00	2.5382	8.8323	16202.0	2.5641	127.30	1.6013

Table I (continued)

$\eta$	$-\xi_a$	$\xi_b$	$\varphi_a$	$\varphi_b$	$\sqrt{\varphi_a}$	$\sqrt{\varphi_b}$
10.0	2.5444	9.4465	$2\epsilon\eta$	2.7388	$\sqrt{2\epsilon\eta}$	1.6549
11.0	2.5481	10.0417	$2\epsilon\eta$	2.9056	$\sqrt{2\epsilon\eta}$	1.7046
12.0	2.5504	10.6204	$2\epsilon\eta$	3.0656	$\sqrt{2\epsilon\eta}$	1.7509
13.0	2.5518	11.1845	$2\epsilon\eta$	3.2195	$\sqrt{2\epsilon\eta}$	1.7943
14.0	2.5526	11.7355	$2\epsilon\eta$	3.3679	$\sqrt{2\epsilon\eta}$	1.8352
15.0	2.5531	12.2747	$2\epsilon\eta$	3.5114	$\sqrt{2\epsilon\eta}$	1.8739
16.0	2.5534	12.8032	$2\epsilon\eta$	3.6505	$\sqrt{2\epsilon\eta}$	1.9106
18.0	2.5537	13.8313	$2\epsilon\eta$	3.9121	$\sqrt{2\epsilon\eta}$	1.9779
20.0	2.5538	14.8260	$2\epsilon\eta$	4.1695	$\sqrt{2\epsilon\eta}$	2.0419
25.0	2.5539	17.1931	$2\epsilon\eta$	4.7526	$\sqrt{2\epsilon\eta}$	2.1800
30.0	2.5539	19.4253	$2\epsilon\eta$	5.2818	$\sqrt{2\epsilon\eta}$	2.2982
35.0	2.5539	21.5522	$2\epsilon\eta$	5.7696	$\sqrt{2\epsilon\eta}$	2.4020
40.0	2.5539	23.5939	$2\epsilon\eta$	6.2246	$\sqrt{2\epsilon\eta}$	2.4949
45.0	2.5539	25.5643	$2\epsilon\eta$	6.6526	$\sqrt{2\epsilon\eta}$	2.5792
50.0	2.5539	27.4740	$2\epsilon\eta$	7.0579	$\sqrt{2\epsilon\eta}$	2.6567
60.0	2.5539	31.141	$2\epsilon\eta$	7.8126	$\sqrt{2\epsilon\eta}$	2.7951
70.0	2.5539	34.642	$2\epsilon\eta$	8.5077	$\sqrt{2\epsilon\eta}$	2.9168
80.0	2.5539	38.007	$2\epsilon\eta$	9.1552	$\sqrt{2\epsilon\eta}$	3.0253
90.0	2.5539	41.258	$2\epsilon\eta$	9.7639	$\sqrt{2\epsilon\eta}$	3.1247
100.0	2.5539	44.412	$2\epsilon\eta$	10.3399	$\sqrt{2\epsilon\eta}$	3.2156
150.0	2.5539	59.086	$2\epsilon\eta$	12.8657	$\sqrt{2\epsilon\eta}$	3.5869
200.0	2.5539	72.479	$2\epsilon\eta$	14.9975	$\sqrt{2\epsilon\eta}$	3.8727
300.0	2.5539	96.877	$2\epsilon\eta$	19.5766	$\sqrt{2\epsilon\eta}$	4.4245
400.0	2.5539	119.185	$2\epsilon\eta$	21.5958	$\sqrt{2\epsilon\eta}$	4.6471
500.0	2.5539	140.068	$2\epsilon\eta$	24.2565	$\sqrt{2\epsilon\eta}$	4.9251
600.0	2.5539	159.885	$2\epsilon\eta$	26.6626	$\sqrt{2\epsilon\eta}$	5.1636
700.0	2.5539	178.861	$2\epsilon\eta$	28.8754	$\sqrt{2\epsilon\eta}$	5.3736
800.0	2.5539	197.146	$2\epsilon\eta$	30.9353	$\sqrt{2\epsilon\eta}$	5.5619
900.0	2.5539	214.850	$2\epsilon\eta$	32.8702	$\sqrt{2\epsilon\eta}$	5.7333
1000.0	2.5539	232.054	$2\epsilon\eta$	34.7003	$\sqrt{2\epsilon\eta}$	5.8907

Table II

$I_s/I_\infty$	$I_s/I_1$	$\eta_1$	$-(\xi_a)_1$	$[(\xi_a)_1/\xi_\infty]^2$
0.00	1.000	0.0000	0.0000	0.0000
0.10	1.178	0.1638	0.7445	0.0850
0.15	1.265	0.2351	0.8775	0.1181
0.20	1.353	0.3025	0.9819	0.1478
0.25	1.440	0.3643	1.0640	0.1736
0.30	1.525	0.4220	1.1329	0.1968
0.40	1.692	0.5260	1.2418	0.2365
0.50	1.853	0.6168	1.3260	0.2696
0.60	2.012	0.6992	1.3950	0.2984
0.70	2.169	0.7744	1.4505	0.3226
0.80	2.322	0.8424	1.4989	0.3445
0.90	2.472	0.9050	1.5411	0.3641
1.00	2.621	0.9634	1.5776	0.3816
1.50	3.342	1.2066	1.7111	0.4489
2.00	4.034	1.3948	1.7991	0.4963
2.50	4.712	1.5501	1.8604	0.5306
3.00	5.367	1.6803	1.9093	0.5589
4.00	6.654	1.8952	1.9798	0.6010
5.00	7.901	2.0670	2.0315	0.6329
6.00	9.125	2.2111	2.0708	0.6575
7.00	10.34	2.3360	2.1013	0.6770
8.00	11.53	2.4450	2.1265	0.6933
9.00	12.72	2.5422	2.1474	0.7070
10.00	13.90	2.6319	2.1665	0.7196
15.0	19.65	2.9781	2.2300	0.7624
20.0	25.3	3.231	2.2693	0.7895
25.0	30.9	3.431	2.2976	0.8094
30.0	36.4	3.595	2.3176	0.8235
40.0	47.4	3.859	2.3470	0.8446
50.0	58.2	4.064	2.3669	0.8589
60.0	69.0	4.224	2.3815	0.8695
70.0	79.3	4.323	2.3990	0.8824
80.0	90.2	4.502	2.4057	0.8873
90.0	100.9	4.614	2.4119	0.8919
100.0	111.5	4.714	2.4186	0.8969
150.0	164.0	5.100	2.4381	0.9114
200.0	217.5	5.382	2.4573	0.9258
300.0	320.0	5.768	2.4739	0.9383
400.0	422.0	6.046	2.4846	0.9465
500.0	525.5	6.264	2.4916	0.9518
600.0	627.5	6.442	2.4972	0.9561
700.0	730.0	6.593	2.5013	0.9592
800.0	832.0	6.724	2.5045	0.9617
900.0	934.0	6.839	2.5072	0.9638
1000.0	1035.0	6.942	2.5098	0.9658

# RCA TECHNICAL PAPERS†

## Fourth Quarter, 1948

Any request for copies of papers listed herein should be addressed to the publication to which credited.

- "An A.C.-D.C. Receiver for AM and FM", W. A. Harris and R. F. Dunn, *Radio News* (November) ..... 1948
- "Aircraft Antennas. Part II—How to Use Charts to Find Reactance and Resistance of Fore and Aft, Trailing, Vertical, Center-Fed V and Off-Center-Fed V Aircraft Antennas", S. Wald, *Communications* (November) ..... 1948
- "Analysis of a Simple Model of Two-Beam Growing-Wave Tube", L. S. Nergaard, *RCA Review* (December) ..... 1948
- "The Chemistry of High-Speed Electrolytic Facsimile Recording", by H. G. Greig, *Proc. I.R.E.* (October) ..... 1948
- "Colorimetry in Television", W. H. Cherry, *Jour. Soc. Mot. Pic. Eng.* (December) ..... 1948
- "Custom-Built Dual-Recording Console", A. S. Karker, *Broadcast News* (October) ..... 1948  
*Communications* (November) ..... 1948
- "Developmental Television Transmitter for 500-900 Megacycles", R. R. Law, W. B. Whalley, and R. P. Stone, *RCA Review* (December) ..... 1948
- "The Dilemma of Specialization", G. M. K. Baker, *Proc. I.R.E.* (Editorial) (October) ..... 1948
- "Duplex Tetrode UHF Power Tubes", by P. T. Smith, H. R. Hegbar, *Proc. I.R.E.* (November) ..... 1948
- "Electron Micrograph Studies of Two Strains of Pleuropneumonia-like (L) Organisms of Human Derivation", J. Hillier (Coauthor), *Journal of Bacteriology* (November) ..... 1948
- "Electro-Optical Characteristics of Television Systems; Part IV—Correlation and Evaluation of Electro-Optical Characteristics of Imaging Systems", O. H. Schade, *RCA Review* (December) ..... 1948
- "Field Test of Ultra-High-Frequency Television in the Washington Area", G. H. Brown, *RCA Review* (December) .... 1948
- "Flying Spot Scanner for Television", Donald Pike, *Broad. Eng. Jour.* (December) ..... 1948
- "Homing and Navigational Courses of Automatic Target-Seeking Devices", Luke Chia-Liu Yuan, *Jour. Appl. Phys.* (December) ..... 1948
- "The Impedance of Aircraft Antennas", Sidney Wald, *Communications* (November) ..... 1948

† Report all corrections or additions to RCA Review, Radio Corporation of America, RCA Laboratories Division, Princeton, N. J.

- "Improved Optical Reduction Sound Printer", J. L. Pettus, *Jour. Soc. Mot. Pic. Eng.* (December) ..... 1948
- "Intermodulation and Harmonic Distortion Measurements", J. Avins, *Audio Eng.* (October) ..... 1948
- "L-Type Variation and Bacterial Reproduction by Large Bodies as Seen in Electron Micrographic Studies of Bacteriodes Funduliformis", J. Hillier (Coauthor), *Journal of Bacteriology* (November) ..... 1948
- "Magnetic Recording for the Technician", Dorothy O'Dea, *Jour. Soc. Mot. Pic. Eng.* (November) ..... 1948
- "Microwave Optics Between Parallel Conducting Sheets", H. B. DeVore and Harley Iams, *RCA Review* (December) ..... 1948
- "Multi-Channel Radio-Telegraph System for High-Frequency Circuits", T. E. Jacobi, *RCA Review* (December) ..... 1948
- "New, Lightweight Remote Amplifier", R. C. Abbett, *Broadcast News* (October) ..... 1948
- "New Preparation Techniques for the Electron Microscopy of Bacteria", J. Hillier (Coauthor), *Journal of Bacteriology* (November) ..... 1948
- "A New 100-Watt Triode for 1000 Megacycles", by W. P. Bennett, E. A. Eschbach, C. E. Haller, W. R. Keye, *Proc. I.R.E.* (October) ..... 1948
- "A Novel Ten-Inch Television Receiver", W. J. Stolze and E. I. Anderson, *RCA Licensee Bulletin LB-761* (October 1) .... 1948
- "Oil-Filled Miniature Tuning Capacitors", S. Wald, *Tele-Tech* (October) ..... 1948
- "Optimum High-Frequency Bias in Magnetic Recording", G. L. Dimmick and S. W. Johnson, *Jour. Soc. Mot. Pic. Eng.* (November) ..... 1948
- "Performance of 931-A Type Multiplier in a Scintillation Counter", G. A. Morton and J. A. Mitchell, *RCA Review* (December) ..... 1948
- "Planning Radio and Television Studios", G. M. Nixon, *Broadcast News* (December) ..... 1948
- "Practical Equipment Layouts for Television Stations", *Broadcast News* (December) ..... 1948
- "Precision Interval Timer", Sidney Wald, *Electronics* (December) ..... 1948
- "Radio — Scientific Developments Television — U.S.A.", G. L. Beers, SECTION OF ENCYCLOPAEDIA BRITANNICA YEAR BOOK (Spring) ..... 1948
- "RCA-NBC Views on TV Expansion", E. W. Engstrom, *FM & Tele.* (October) ..... 1948
- "Relation Between Amplitude and Phase in Electrical Networks", T. Murakami and M. S. Corrington, *RCA Review* (December) ..... 1948
- "Remote Control for Radio Tuning", S. Wald, *Electronics* (December) ..... 1948

- "Scale Models Made from Paper Cutouts Aid TV Station Planning", M. L. Gaskill, *Broadcast News* (December) ..... 1948
- "Sensitometric Aspect of Television Monitor-Tube Photography", F. G. Albin, *Jour. Soc. Mot. Pic. Eng.* (December) ..... 1948
- "Single-Sideband Crystal Filters", P. K. Taylor, *Electronics* (October) ..... 1948
- "Spurious Multiple Responses in FM Receivers", Frank Mural, *RCA Licensee Bulletin LB-762* (October 20) ..... 1948
- "Stability versus Chaos", A. N. Goldsmith, *Television* (November) ..... 1948
- "A Technique for the Making and Mounting of Fine Mesh Screens", H. B. Law, *Rev. Sci. Instr.* (December) ..... 1948
- "Television Antennas and Transmission Lines", J. R. Meagher, *RCA Rad. Serv. News* (November-December) ..... 1948
- "The Transitrol, An Experimental Automatic-Frequency-Control Tube", J. Kurshan, *RCA Review* (December) ..... 1948
- UNDERSTANDING TELEVISION, Orrin E. Dunlap, Jr., Greenberg: Publisher, New York, N. Y. .... 1948
- "Using TV Test Patterns", John R. Meagher, *Radio-Electronics* (November) ..... 1948
- "Vapor Pressure Data for Various Substances (A Graphical Presentation)", R. R. Law, *Rev. Sci. Instr.* (December) ... 1948
- "Wide-Band I-F Alignment by Alternate Loading", R. G. Middleton, *RCA Rad. Serv. News* (November-December) ..... 1948
- "35-Mm. Magnetic Recording System", E. Masterson, *Jour. Soc. Mot. Pic. Eng.* (November) ..... 1948
- "500 Watt TV Transmitter", M. L. Gaskill, *Tele-Tech* (November) ..... 1948

---

NOTE—Omissions or errors in these listings will be corrected in the yearly index.

## AUTHORS



LOY E. BARTON received the B.E.E. degree in 1921 and the E.E. degree in 1925 from the University of Arkansas. From 1921 to 1925 he was an instructor in mechanical engineering at the University of Arkansas; from 1925 to 1927 he was a Radio Test Engineer with the General Electric Company. He returned to the University of Arkansas and from 1927 to 1929 was Associate Professor in Electrical Engineering. Since that time he has been with RCA, except for a three-year period with Philco. He directed the development and design of Sonar equipment at RCA in Camden early in World War II and

spent the last two years of the war on a special Radar assignment at the Naval Research Laboratory in Washington. Mr. Barton is a member of Sigma XI, Tau Beta Pi and a Senior Member of the Institute of Radio Engineers.

DONALD S. BOND is a graduate of the University of Chicago, where he received a bachelor's degree in 1929 and a master's degree in physics in 1931. Subsequently he held a graduate fellowship and was a research assistant in physics at Chicago. In 1929 he joined Bell Telephone Laboratories, where he was engaged in vacuum tube research. Work in this field and in broadcast receiver development continued at Grigsby-Grunow Company during the period from 1931 to 1934. In the following year he joined the Radio Corporation of America. His work has included development and research in receivers, navigation aids, and communication systems. He is at present a research engineer in the RCA Laboratories Division. Mr. Bond is a member of Phi Beta Kappa, Sigma Xi, and the American Physical Society, a senior member of the Institute of Radio Engineers, and a fellow of the American Association for the Advancement of Science.



C. LOUIS CUCCIA received the B.S. degree in E.E. in 1941 and the M.S. degree in 1942 from the University of Michigan. From 1941 to 1942 he was affiliated with the department of engineering research of the University of Michigan for Fisher Body Division of the General Motors Corporation. In June 1942, he joined the research department of the RCA Manufacturing Company in Harrison, N. J. In November 1942, he transferred to the research staff of RCA Laboratories Division in Princeton, N. J. Mr. Cuccia is an Associate Member of the Institute of Radio Engineers and a member of Sigma Xi.

VERNON J. DUKE received the degree of B.S. in Electrical Engineering from the University of Colorado in 1928. During 1928 and 1929 he was with the General Electric Company in Fort Wayne, Indiana, and later in Schenectady. From 1929 to 1937 he was with the National Broadcasting Company at Denver. In 1937 he in 1941 to the Development Laboratory. From early 1942 until the spring of 1945 he was engaged on war projects for the Office of Scientific Research and Development. Since 1945, as a Staff Engineer of NBC, he has been designing equipment and circuits which are now in use in television studios at NBC. During the past two years he has been engaged in the development of Ultrafax. Mr. Duke is a member of the Institute of Radio Engineers.





EVERETT EBERHARD received his B.S. degree in Electrical Engineering from the University of Kansas in 1936. From 1936 to 1938 he was an assistant in the Electrical Engineering Department at Yale University where he received an M.S. degree in Electrical Engineering in 1938. From 1938 to 1940 he was employed as an Instructor in the electrical engineering department at South Dakota State College. From 1940 through 1945 he worked for the U.S. Air Force first as a civilian instructor in radio and radar and later as a radar officer. He joined RCA Victor Division, Camden, in 1946 and since

that time has worked in the Advanced Development Section of the Engineering Products Department. Mr. Eberhard is a member of Tau Beta Pi, Sigma Tau, the American Institute of Electrical Engineering and the Institute of Radio Engineers.

RICHARD D. FAULKNER received his B.S. degree in Glass Technology from Alfred University in 1944. He joined the Tube Department of RCA Victor Division at Lancaster, Pa. the same year and is working on glass problems in the Tube Development Shop. Mr. Faulkner is a member of Karmos and of the American Ceramic Society.



WARREN R. FERRIS received the B.S. degree in electrical engineering from Rose Polytechnic Institute in 1927, the M.S. degree in electrical engineering from Union College in 1932, and the D.E.E. degree from the Polytechnic Institute of Brooklyn in 1946. From 1927 to 1930 he was employed by the General Electric Company at the Research Laboratory at Schenectady, New York. In 1930 he joined the Research and Development Laboratory of the RCA Manufacturing Company at Harrison, N. J. In 1942 he transferred to RCA Laboratories Division at Princeton. Since 1946 he has been with the Naval Re-

search Laboratory, Washington, D. C. Mr. Ferris is a member of Sigma Xi and a Senior Member of the Institute of Radio Engineers.

GORDON L. FREDENDALL received the Ph.D. degree from the University of Wisconsin. From 1931 to 1936 he taught electrical engineering and mathematics, and engaged in research work in mercury-arc phenomena at the University of Wisconsin. Since 1936 he has been with Radio Corporation of America, working on television research. He is at present located in Princeton, N. J., at RCA Laboratories Division. Dr. Fredendall is an Associate Member of the Institute of Radio Engineers.





E. DUDLEY GOODALE received the B.S. degree in Electrical Engineering from Union College in 1928 and the B.S. and M.S. degrees in Electrical Engineering from the Massachusetts Institute of Technology in 1930 and 1931. From 1932 to 1937 he was engaged in vacuum tube engineering work with the RCA Manufacturing Company at Harrison, New Jersey. In 1937 he transferred to the Development Group of the National Broadcasting Company in New York where he has been directly associated with television development activities since that time. Mr. Goodale is a member of Eta Kappa Nu, Sigma Xi, the Institute of Radio Engineers and is a licensed Professional Engineer in New York State.

JOSEPH KELAR received his B.S. degree in Electrical Engineering from the University of Wisconsin in 1942. From 1934 to 1939 he was supervisor of assembly and testing for Cutler-Hammer, Inc. Early in 1943 he joined the Tube Department of RCA Victor Division, at Harrison, N. J. as a cathode-ray-tube development engineer. Later in 1943 he was transferred to the Lancaster plant. From 1947 to 1948, when he left the company, he was engineering leader in charge of the development of directly viewed kinescopes. He is mainly responsible for the development of the tilted-lens ion trap and for many contributions to the development of the 16-inch kinescope.

RAY D. KELL received his B.S. degree in electrical engineering from the University of Illinois in 1926. From 1927 to 1930 he was engaged in television research in the radio consulting laboratory of the General Electric Company. From 1930 to 1941 he was a member of the research division of RCA Manufacturing Company, and since 1941 he has been with RCA Laboratories Division. He received the "Modern Pioneer" Award from the National Association of Manufacturers in February 1940, and the Stuart Ballantine Medal of the Franklin Institute in 1948 for his work in television. Mr. Kell is a member of Sigma Xi and a Fellow of the Institute of Radio Engineers.



RALPH C. KENNEDY received the B.A. degree from San Jose State College in 1943 and the M.A. and E.E. degrees in Electrical Engineering from Stanford University in 1945 and 1946 respectively. In 1938 he became Chief Engineer at KRE. After serving as transmitter engineer at KROY and KQW he joined the Hewlett-Packard Company as a development engineer in 1943. In 1944 he became a transmitter engineer at KPO, the National Broadcasting Company transmitter in San Francisco. In 1946 he was transferred to the sound broadcasting development group of the National Broadcasting Company. For the past year Mr. Kennedy has been engaged in various phases of television development. Mr. Kennedy is a member of the American Mathematical Society and the Institute of Radio Engineers.



**CHARLES T. LATTIMER** received his B.S. degree in Chemical Engineering from the University of Notre Dame in 1941. From 1941 to 1943 he was employed by the Marathon Corporation in Rothschild, Wisconsin, engaged in lignin chemistry research. In 1943 he was commissioned in the Navy and served as a night-fighter radar officer aboard an aircraft carrier in the Third Fleet. In 1946 he joined the Tube Department, of RCA Victor Division, at Lancaster, Pa., and is associated with work on cathode-ray-tube screen application and general chemical problems in the Tube Development Shop. Mr. Lattimer is a

member of the American Chemical Society.

**LOUIS PENSAK** received a B.S. degree from Long Island University in 1932 and spent the next year as a graduate assistant at the University of Pittsburgh. In 1936 he received an M.S. degree from New York University. He was employed by the Radio Corporation of America in 1937 in the cathode-ray-tube development section and in 1940 was transferred to the Research Department of RCA Victor Division. Since 1941, he has been with RCA Laboratories Division. Mr. Pensak is a member of Sigma Xi and an Associate Member of the Institute of Radio Engineers.



**HENRY P. STEIER** studied mechanical engineering at the University of Pittsburgh from 1932 to 1935 and electrical engineering at Columbia University from 1940 to 1941 where he received his B.S. degree in Electrical Engineering. He joined the National Union Radio Corporation in 1943 as electrical measurements engineer. Later in the same year he came to the Tube Department of the RCA Victor Division at Harrison, N. J. as a cathode-ray-tube factory engineer. From there he moved in the same capacity to the tube plant at Lancaster, Pa. In 1945 he transferred to the Engineering Section as a

cathode-ray-tube development engineer.

**WILLIAM M. WEBSTER** studied physics at Rensselaer Polytechnic Institute and at Union College as a Navy V-12 student. He received a B.S. degree in physics in 1945. He was released from active duty in 1946 and joined the RCA Laboratories Division, Princeton, in October of that year. He is currently enrolled in the Graduate School of Princeton University on a part-time basis. Mr. Webster is an associate member of the Institute of Radio Engineers.





HUBERT H. WITTENBERG received the B.E.E. degree from the Rose Polytechnic Institute in 1937. In the same year he joined the Tube Research and Engineering Department of RCA Manufacturing Company in Harrison, N. J., where he was engaged in the development of thyratrons and related gas type tubes. In 1943 he was transferred to the Plant in Lancaster, Pa. During the war he was engaged in the application of thyratrons to radar and since has specialized in application engineering for the industrial field. Mr. Wittenberg is a member of American Institute of Electrical Engineers.

